Studies on Thermal Storage Integrated Micro-Trigeneration System

by

DHEERAJ KISHOR JOHAR

(2012RME9035)

Department of Mechanical Engineering

MALAVIYA NATIONAL INSTITUTE OF TECHNOLOGY, JAIPUR

INDIA

March, 2018

Studies on Thermal Storage Integrated Micro-Trigeneration System

by

DHEERAJ KISHOR JOHAR

(2012RME9035)

Department of Mechanical Engineering

Submitted in fulfillment of the requirements for the degree of

DOCTOR OF PHILOSOPHY

to

MALAVIYA NATIONAL INSTITUTE OF TECHNOLOGY, JAIPUR
INDIA

March, 2018

I dedicate this Thesis to my beloved parents who sacrificed their comforts for the education of their children.

DEPARTMENT OF MECHANICAL ENGINEERING

MALAVIYA NATIONAL INSTITUTE OF TECHNOLOGY JAIPUR

CERTIFICATE

This is to certify that the thesis entitled **'Studies on Thermal Storage Integrated Micro-Trigeneration System'** submitted by **Mr. Dheeraj Kishor Johar (2012RME9035)**, to the Malaviya National Institute of Technology, Jaipur for the award for the degree of **Doctor of Philosophy** is a bonafide record of original research work carried out by him. He has worked under our guidance and supervision and has fulfilled the requirement for the submission of this thesis.

The results contained in thesis have not been submitted in part or full, to any other University or Institute for the award of any degree or diploma.

(Prof. Dilip Sharma)
Professor
Department of Mechanical Engineering
Malaviya National Institute of Technology
Jaipur

(Prof. S.L.Soni)
Professor
Department of Mechanical Engineering
Malaviya National Institute of Technology
Jaipur

Date: March 04, 2018

DECLARATION

I, **Dheeraj Kishor Johar**, declare that this thesis titled, "**Studies on Thermal Storage Integrated Micro-Trigeneration System**" and the work presented in it are my own. I confirm that:

- This work was done wholly or mainly while in candidature for a research degree at this institute.

- Where any part of this thesis has previously been submitted for a degree or any other qualification at this institute or any other institution, this has been clearly stated.

- Where I have consulted the published work of others, this is always clearly attributed.

- Where I have quoted from the work of others, the source is always given. With the exception of such quotations, this thesis is entirely my own work.

- I have acknowledged all main sources of help.

- Where the thesis is based on work done by myself, jointly with others, I have made clear exactly what was done by others and what I have contributed myself.

Date: March 04, 2018

Dheeraj Kishor Johar
(2012RME9035)

ACKNOWLEDGEMENT

I wish to express my deep regards and profound sense of gratitude to my revered and learned supervisors **Prof. Dilip Sharma** and **Prof. S. L. Soni** of Department of Mechanical Engineering, Malaviya National Institute of Technology Jaipur, who through their excellent guidance have enabled me to accomplish this work. They have been a great source of inspiration to me, all through. I am very grateful to them for guiding me on how to conduct the research and how to effectively present the work in a well-articulated manner.

I am grateful to **Prof. Udaykumar R. Yaragatti**, Director, MNIT Jaipur, **Prof. I.K. Bhat**, ex-Director, MNIT Jaipur and **Prof. G. S. Dangayach**, HOD, Mechanical Engineering Department, MNIT Jaipur for granting permission to do this research and for various approvals and funding for the same. I extend my sincere thanks to my Departmental Research Evaluation Committee (DREC) members, **Prof. J. Mathur, Dr. G. D. Agarwal and Dr. N. Rohatgi**, for their valuable suggestions and encouragement throughout the course of study.

I would like to thank **Mr. Pradeep Gupta** and **Dr. Rahul Goyal** from the deep of my heart, for their continuous help during the experimental work, for writing research papers and for the preparation of this report. Without their help, this work could not have been completed.

I am also grateful to **Mr. Sumit Sharma, Mr. Umardaraj, Mr. Manish Arya, Mr. Dharmendra Kumawat, Mr. Narayan Lal Jain, Mr. Pushpendra Kumar Sharma, Mr. Deepanshu Arora, Mr. Anmesh Kumar Srivastava, Mr. Jitendra Singh, Dr. Vinod Sigh, Mr. Amit Jhalani, Mr. Hemant Raj, Mr. Swaraj Das, Mr. Arun Johar** and **Mr. Vaibhav Rai Khare** for their assistance during the experimental work and, Research Scholars at MNIT Jaipur for their useful support from time to time during this research.

I am also thankful to **Mr. Ramesh Meena, Mr. Jitendra Arya, Mr. Bahadur Ram Nayak, Kailash Chand** Sr. Technician for helping me in conducting the experiments and would like to thank **Mr. Sanjay Kumar Tailor**, Sr. Technical Assistant, **Mr. Mahavir Singh**, Technician, **Mr. Kolahal Prashad**, Lab Attendant, Mechanical

Engineering Department, MNIT Jaipur for their help in documentations, procurement of equipment, experimental work, etc.

I thank **Prof. B.L. Swani**, Dean, **Dr. Lava Bhargava**, Associate Dean, **Mr. Suraj BhanMeena**, **Mr. Jasbir Singh** and the entire Department of Academic Affairs for their timely and appropriate help from time to time for all administrative activities for the successful completion of this research work.

Words will never be adequate to express the sense of reverence, veneration and gratitude to my beloved parents, **Shri Om Prakash Johar** and **Smt. Nishi Bala Johar**, who always wished to see me completing my doctorate. My sincere thanks to my wife, **Mrs. Ambika Johar** for her sacrifice, understanding, cooperation and patience during my busy years on this research. I would like to thank my loving daughter **Divyanshi Johar** who is in toddler stage. I would also like to thank **friends and relatives** for their blessings and constant encouragement.

I would like to thank with apology all those, whose names I missed mentioning above inadvertently.

Last but not the least; I would like to say a big thanks to **God, The Almighty**, for making me capable of accomplishing this task.

Place: Jaipur

Date: March 04, 2018 **(Dheeraj Kishor Johar)**

ABSTRACT

Increasing demand of energy has raised the prices of conventional energy sources, and environmental awareness has led to increase in use of renewable energy sources and focus on increased energy efficiency. In context of increased energy efficiency, thermal energy storage and waste heat recovery play an important role as these systems improve overall efficiency of systems.

Among several options available for waste heat recovery, micro-cogeneration and micro-trigeneration are emerging as the fast growing techniques to increase energy efficiency and reduce overall emissions in domestic and small-scale applications.

The major technical constraint that prevents successful implementation of waste heat recovery is its intermittent and time mismatched demand and availability. Thermal energy storage (TES) technology plays an important role to overcome this problem as it allows excess thermal energy to be stored for later use.

This study aimed initially to design and develop a thermal energy storage system for small capacity stationary CI engine and further to integrate the developed system with micro-trigeneration system (also developed in the lab) for feasibility study and performance investigation of TES coupled micro-trigeneration system for on power and off power mode. Thermal energy storage system comprising of shell and tube type construction was developed and erythritol was used as a storage medium. This thermal energy storage system was also coupled to engine to achieve thermal storage integrated trigeneration system. In this study a 4.4 kW stationary compression ignition engine was coupled with a double pipe heat exchanger, vapour absorption refrigeration system to achieve trigeneration i.e. power, heating and cooling. Various combinations of thermal energy storage system integrated micro-trigeneration were investigated.

Engine performance and emission characteristics for various modes like single generation, single generation with thermal energy storage, cogeneration, cogeneration with thermal energy storage and trigeneration with thermal energy storage were determined. Performance parameters related to thermal energy storage system (charging efficiency, discharging efficiency, and temperature profiles), double pipe heat exchanger (effectiveness) and vapour absorption system (Coefficient of performance) were also determined.

Test results showed that it was feasible to realize a thermal storage integrated micro-trigeneration system using a small stationary diesel engine. There was slight effect on performance and emission by integrating the components of trigeneration and storage to the stationary diesel engine. Test results from the experiments also showed that the useful output and total thermal efficiency in case of trigeneration and cogeneration are much higher than single generation. Reduction in smoke and CO_2 emissions were observed with thermal storage integrated micro trigeneration system as compared to single generation. All other major emissions (HC, CO, NOx) increased slightly but were well within permissible range for all the modes. No adverse impacts on any parameter were found while operating in various modes (single generation, single generation with thermal energy storage, cogeneration, cogeneration with thermal energy storage and trigeneration with thermal energy storage).

The experimental results obtained from the present research show that development of a micro size thermal storage integrated trigeneration system is feasible and effective to utilize the resources more efficiently.

TABLE OF CONTENTS

LIST OF FIGURES

LIST OF TABLES

NOMENCLATURE

BSFC	Break specific fuel consumption (kg/kWh)
BTE	Break thermal efficiency (%)
BTu	British thermal units
CHP	Combined heating and power
CCHP	Combined cooling, heating and power
CI	Compression ignition
CO	Carbon monoxide
COP	Coefficient of performance
DG	Diesel generator
DPHE	Double pipe heat exchanger
FOM	Figure of merit
HC	Hydrocarbons
HTF	Heat transfer fluid
HTO	Heat transfer oil
IC	Internal combustion
ICE	Internal combustion engine
LCV	Lower calorific value of fuel (kJ/kg)
LHS	Latent heat storage
LHTES	Latent heat thermal energy storage
mb/d	Million barrels per day
MCHP	Micro combined heating and power
MCCHP	Micro combined cooling, heating and power
NDIR	Non dispersive infrared detector
NO_x	Oxides of nitrogen
PCM	Phase change material
PEMFC	Proton exchange membrane fuel cell
PM	Particulate matter
ppm	Parts per million
SFC	Specific fuel consumption
SHS	Sensible heat storage
SI	Spark ignition
SOFC	Solid oxide fuel cell
Tcf	Trillion cubic feet

TES	Thermal energy storage
TESS	Thermal energy storage system
VA	Vapour absorption

SYMBOLS

C_{pes}	Specific heat of solid phase (kJ/ kg-K)
C_{pex}	Specific heat of exhaust gases (kJ/ kg-K)
$C_{p\ liq\ pcm}$	Specific heat of phase changing material in liquid state (kJ/ kg-K)
C_{ppcm}	Specific heat of phase changing material (kJ/ kg-K)
C_{pw}	Specific heat of water (kJ/ kg-K)
m_w	Mass of water (kg)
Q	Amount of energy stored (kJ)
Q_{dphe}	Thermal energy recovered by DPHE (kW)
Q_{TES}	Thermal energy stored in TES (kW)
Q_{VA}	Thermal energy recovered in VA system (kW)
$T_{f\ liq\ PCM}$	Final temperature of PCM in liquid phase (^{0}C)
T_{wi}	Inlet temperature of water (^{0}C)
T_{wo}	Outlet temperature of water (^{0}C)
$T_{eng\ ex\ gas}$	Engine exhaust gas temperature (^{0}C)
$T_{\ ambient}$	Ambient temperature (^{0}C)
$T_{f\ PCM}$	Final temperature of PCM (^{0}C)
$T_{i\ PCM}$	Initial temperature of PCM (^{0}C)
$T_{\ melt}$	Melting point temperature of PCM (^{0}C)
$T_{i\ liq\ \ PCM}$	Initial temperature of PCM in liquid phase (^{0}C)
T_{wvao}	Final temperature of water in VA system (^{0}C)
T_{wvai}	Inlet temperature of water in VA system (^{0}C)

CHAPTER 1
INTRODUCTION

1.1 Energy demand and crisis

Energy plays an important role in development of any modern society or country. The demand of energy is growing day by day. World consumption of marketed energy is expected to increase from 549 quadrillion British thermal units (Btu) in 2012 to 815 quadrillion Btu in 2040 [1]. Most of the world's energy growth will occur in non-OECD (Organization for Economic Cooperation and Development) nations. Non-OECD energy consumption is expected to increase by 71 % from 2012 to 2040. Table 1.1 shows world's energy consumption by country grouping. Non-OECD Asia, including China and India account for more than half of world's total increase in expected energy consumption over the period of 2012 to 2040 [1].

Table 1.1 World energy consumption by country / region (in quadrillion Btu) [1]

Year → **Region ↓**		**2012**	**2020**	**2025**	**2030**	**2035**	**2040**
OECD	America	118	126	128	131	134	138
	Europe	81	85	87	90	93	96
	Asia	39	43	45	46	47	48
NON OECD	Europe	51	52	55	56	58	58
	Asia	175	223	246	270	295	322
	Middle East	32	41	45	51	57	62
	Africa	22	26	30	34	38	44
	America	31	33	37	40	43	47
Total		**549**	**629**	**673**	**718**	**765**	**815**

Projected increased world consumption of marketed energy from all fuel sources through 2040 is shown in Fig. 1.1.

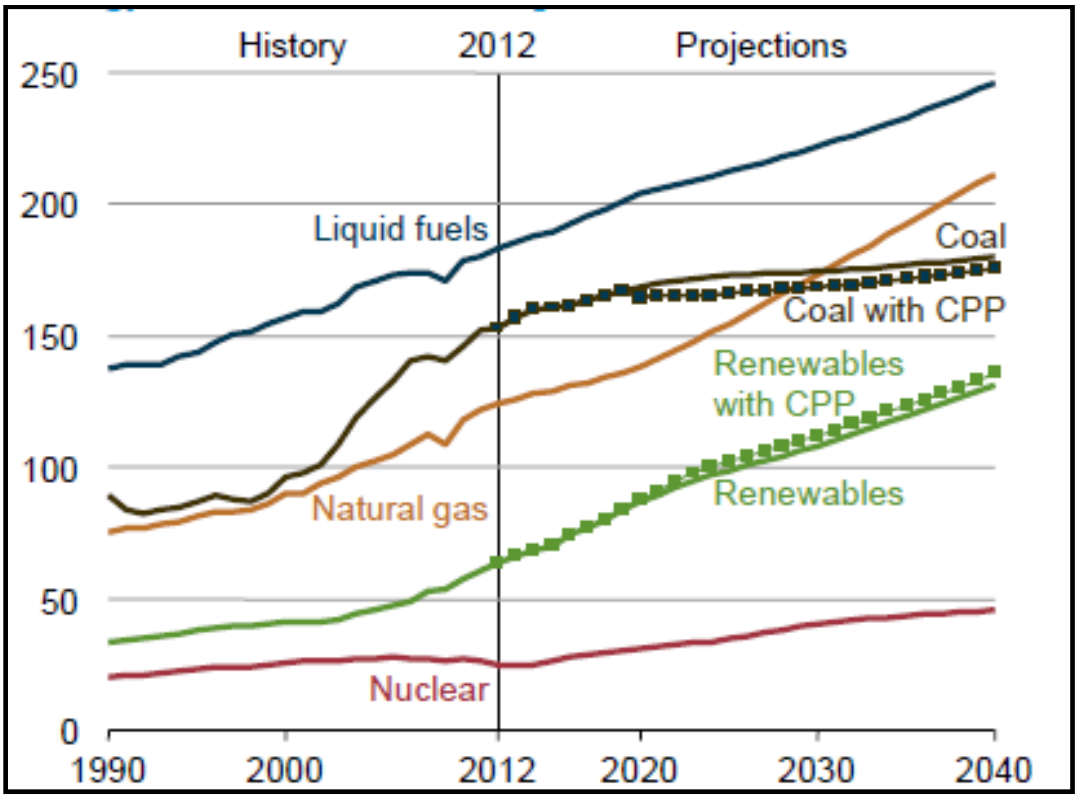

Fig. 1.1 World energy consumption by energy source (in quadrillion Btu) [1]

Fig. 1.1 shows that liquid fuels (mostly petroleum based) will remain the largest source of world energy consumption for many decades to come. Worldwide consumption of petroleum and other liquid fuels is expected to increase from 90 million barrels per day (mb/d) in 2012 to 121 mb/d in 2040. Coal will remain to be the second-largest energy source worldwide behind petroleum and other liquids until 2030. From 2030 to 2040, coal will perhaps be the third-largest energy source, behind both liquid fuels and natural gas. World coal consumption is expected to increase from 2012 to 2040 at an average rate of 0.6 % per year, from 153 quadrillion Btu in 2012 to 180 quadrillion Btu in 2040. Worldwide natural gas consumption is projected to increase from 120 trillion cubic feet (Tcf) in 2012 to 203 Tcf in 2040 i.e. 2.47 % increase per year (taken on straight line) from 2012 to 2040, which is almost 4 times the percentage increase as compared to that of coal.

India is in an early stage of a major transformation, bringing new opportunities to its citizens and moving the country to center stage in many areas of international affairs. India has been responsible for almost 10 % of the total increase in global energy demand since 2000. India's energy demand from 2000 to 2013 has almost been doubled, pushing the country's share in global energy demand up to 5.7 % in 2013

from 4.4 % at the beginning of this century. Almost three-quarters of Indian energy demand are met by fossil fuels. Table 1.2 represents primary energy demand by fuel in India.

Table 1.2 Primary energy demand by fuel in India (in Mtoe) [2]

Year → Fuel ↓	**2000**	**2013**	**2020**	**2030**	**2040**
Oil	112	176	229	329	458
Natural Gas	23	45	58	103	149
Coal	146	341	476	690	934
Nuclear	4	9	17	43	70
Renewable	156	204	237	275	297
Total	**441**	**775**	**1018**	**1440**	**1908**

Coal retains the central position in the mix and in 2013 it accounts for 44 % of the primary energy demand in India. Share of coal is expected to increase to 49 % by 2040. Demand for oil in India is expected to increase from 6.0 mb/d in 2013 to 9.8 mb/d in 2040. Natural gas plays a relatively minor role in the Indian energy mix.

Transport sector is the major consumer of petroleum. In India, the current demand in transport sector is 75 MToE (i.e. 14 % of total energy consumed in India) and it is expected to reach 240 MToE by 2040. Passenger cars' population is expected to rise from 28 million in 2013 to 280 million by 2040 and an additional 30 million more trucks will be on road by 2040 as compared to 2013. 2/3 wheeler population is expected to double by 2040 [2-3]. Fig. 1.2 shows the expected increase in vehicle

population in India and it looks clear that IC engines (gasoline and diesel) will be the main technology in the foreseeable future [4].

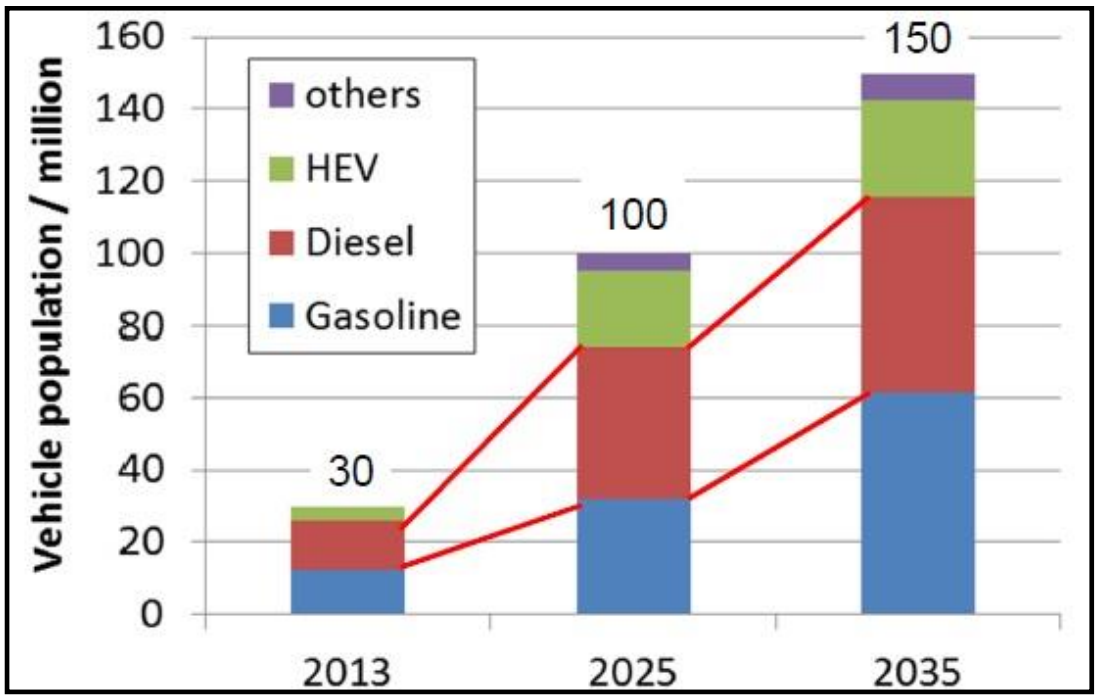

Fig. 1.2 Expected increase of vehicle population in India between 2013 and 2035 [4]

Despite environmental and health concerns, diesel fuelled engine remains a common means of supplying power to heavy-duty vehicles, buses, construction vehicles (CV) and stationary engines because they are quite reliable, extremely durable, having higher fuel efficiency, easy to repair, relatively inexpensive to operate, high-torque (at low speeds) engines. In context of greenhouse gas emissions, due to a diesel engine's inherent fuel economy, diesel engines can compete with other advanced technologies, like hybrid electric vehicles, relative to conventional spark-ignition engines. Diesel-powered vehicles have demonstrated a 30-40% fuel economy advantage over their gasoline counterparts. This translates to about a 20% reduction in CO_2 emissions [5]. Because of the better fuel economy and lower carbon dioxide emissions, diesel engines are popular and significant power train for several applications and shall continue to be in popular use for decades to come. Fig. 1.3 shows the consumption pattern of various petroleum products in India for 2014-15, with diesel having 42% share (more than double of motor spirit, i.e. petrol/gasoline and LPG), and it is quite evident from it that despite all the negatives of diesel, it might take at least couple of decades to find a suitable replacement for diesel as source of energy.

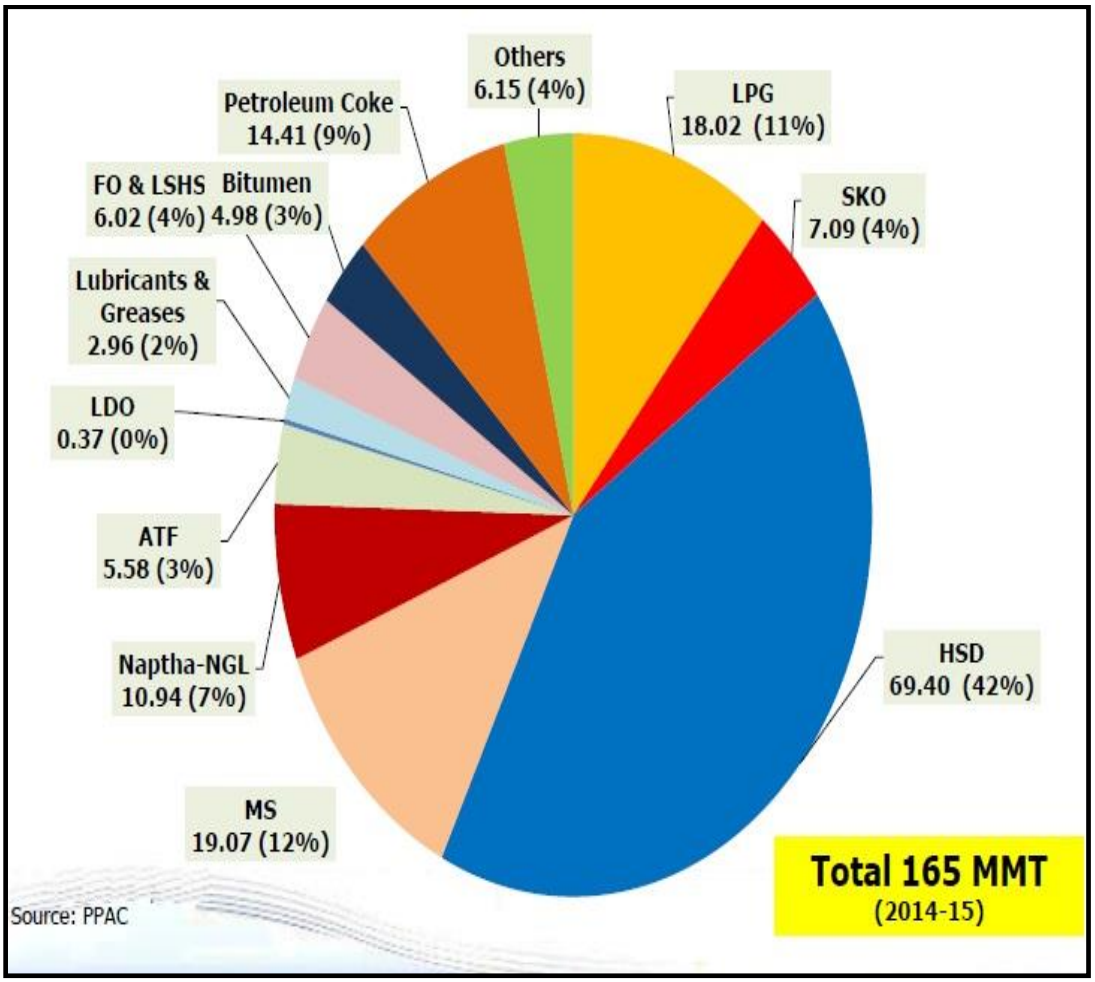

Fig. 1.3 India's consumption pattern of petroleum products in 2014-15 [6].

Fossil fuel reserves are limited and cannot be recycled. Over-exploitation of fossil resources has led to increase in hazardous pollutants also. The uncertainties related to fossil fuels have adversely impacted the developing countries like India, which depend heavily on import of fossil fuels. However, energy supplied from fossil fuels has already been recognized as unsustainable since the energy crisis since 1970s [7-8]. Based on the current conventional prime energy consumption rate, British Petroleum has predicted that major fossil sources, i.e. crude oil, natural gas and coal, are getting depleted quite fast and would be exhausted very soon [7].

Hence, for sustainability of energy there is a great need to identify new sources of energy, and at the same time invention of new and improved methods or technologies to increase energy efficiency in order to reduce the dependency on primary energy sources.

Since a lot of work has already been done in the direction of alternative fuels (alternative source of energy) like hydrogen, bio-diesel, and other additives like

alcohols, the current work focused mainly on improvement in energy efficiency of the existing systems by way of minimizing energy loss. In context of minimizing the energy loss, waste heat recovery as well as thermal energy storage (TES) has attracted a great interest of researchers. Hence, the prime focus of this research was on recovery of waste heat from IC engine exhaust and storage of waste heat using thermal energy storage system (TESS).

1.2 Waste heat recovery

Waste heat may be defined as heat that is rejected from a process at a temperature well above the ambient temperature. When this rejected heat is utilized in any process like heating, cooling, etc. then this heat is known as recovered heat. The system which is used to recover waste heat is known as 'waste heat recovery system'. Waste heat is simply the heat dissipated to the environment [9].

It is an established fact that in an internal combustion engine, near about 30% of heat is carried out by the exhaust flue gases to the environment. In general the temperature of exhaust of a gasoline engines is about 700 °C and temperature of exhaust gas of diesel engine is around 600 °C [10]. A considerable amount of primary fuel can be saved if; some of the waste heat could be recovered then.

There are various techniques available which utilize waste heat from internal combustion engines, thermoelectric generator, simple Rankine cycle, organic Rankine cycle [11-15], six stroke engine [13] and others technologies like combined heating and power systems (CHP or cogeneration), combined cooling, heating and power systems (CCHP or trigeneration), etc. Among several options available for waste heat recovery, to increase overall energy efficiency and to reduce overall emissions, micro-cogeneration and micro-trigeneration are fast growing and emerging techniques in domestic and small-scale applications [16-17]. Description of cogeneration and trigeneration systems for utilization of engine waste heat are given below.

1.2.1 Cogeneration system

Cogeneration is a way of thermodynamically efficient utilization of fuel. Cogeneration is defined as simultaneous production of power and heat [16, 18-20]. Cogeneration is also known as combine heating and power (CHP) system. These systems utilize the

heat contained in the exhaust gases (getting wasted to environment) of power generation systems and thus increase thermal efficiency of the fuel consumed [21]. The energy conversion efficiency in cogeneration system increases to over 80 % as compared to an average of 30–35 % for fuel fired single generation systems [19]. In cogeneration systems, most of the power and heating demands are met simultaneously by a prime mover along with a heat recovery system. Comparison between single generation and cogeneration systems is shown in Fig. 1.4.

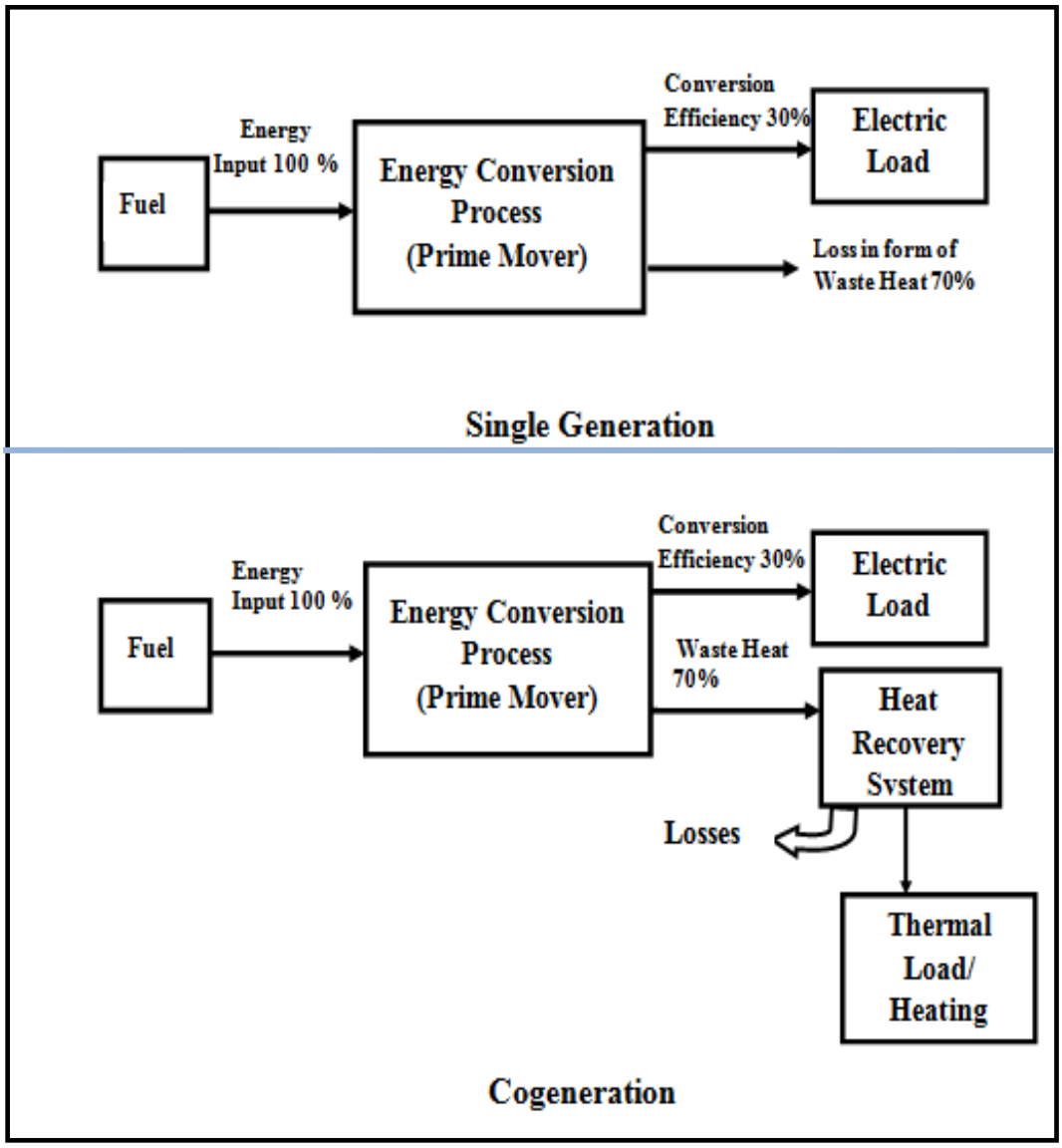

Fig. 1.4 Comparison between single generation and cogeneration system

Small cogeneration systems for domestic and light applications in which electrical power is less than 15 kW are usually called micro-combined heat and power (MCHP) system [7,22,23-24]. The Europe Union has defined a micro cogeneration system with a power output lower than 50 kW [25], considering the real domestic electricity

consumption is usually lower than 15 kW [26-28], the range of micro-cogeneration can be narrowed down to under 20 kW electricity output [29-32].

1.2.2 Trigeneration system

In trigeneration system power, heating and cooling demands are met simultaneously by a prime mover, heat recovery system and thermally activated technology to provide cooling. Trigeneration is also known as combined cooling, heating and power (CCHP) system [16, 33-34]. In simple words, if some thermally activated cooling technology is added to a CHP system to provide cooling effect, the system is called a tri-generation system as shown in Fig. 1.5.

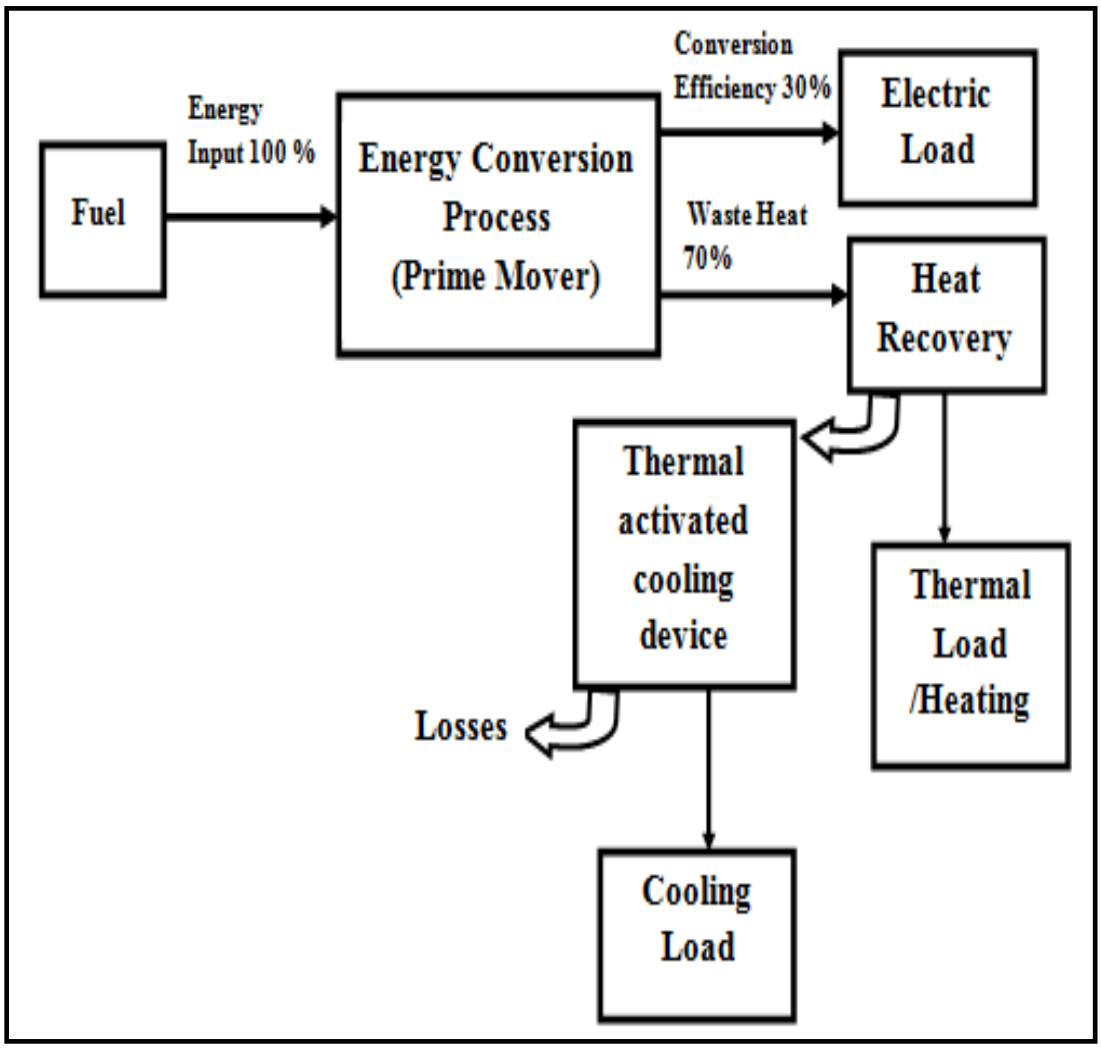

Fig. 1.5 Extension from cogeneration to trigeneration system

Small scale trigeneration power plants, typically, below 15 kW, are called micro-trigeneration plants [7, 22].

The intermittent and time-mismatched demand and availability of waste heat is the major technical constraint that prevents successful implementation of waste heat recovery [35-36].

1.3 Thermal energy storage

Thermal energy storage (TES) technology plays an important role to overcome the problem, of intermittent and time-mismatched demand and availability of waste heat, by way of rationale use of energy as it allows excess thermal energy to be stored for later use [37]. TES can be categorized into sensible, latent and chemical or bond.

1.3.1 Sensible heat storage (SHS)

Sensible heat storage can be defined as heating a liquid or a solid, without changing its phase and thus, storing the excess heat available as sensible heat [38-41]. The amount of energy stored (Q) in SHS depends on the temperature change of the material and can be expressed as:

$$Q = m\, c_p\ \ (T_2 - T_1) \tag{1.1}$$

Where m is the mass of solid or liquid, C_p is its specific heat at constant pressure. T_1 and T_2 are the lower and upper temperatures of the storage medium respectively.

A variety of substances have been used in such type of systems. These include liquids e.g. water, heat transfer oils and certain inorganic molten salts, and solids e.g. pebbles, rocks, refractory, etc. In the case of solids, the material is always in porous form and heat is stored or extracted by the flow of gas or liquid through the pores or voids. The choice of storage medium used depends on the temperature of the application, i.e. water is used for temperatures below 100 °C whereas, refractory bricks and rocks are used for temperatures around 1000 °C [40].

1.3.2 Latent heat storage (LHS)

The heat transfer which occurs when a substance changes its form from one phase to another phase is called the latent heat. When this latent heat is stored in a material (solid and liquid) for a long time it is called latent heat storage. The amount of energy stored (Q) in LHS depends upon the mass (m) and latent heat of fusion / vaporization (l) of the material.

$$Q = ml \tag{1.2}$$

Sometimes it is difficult to operate the system isothermally at the phase change temperature; and the system operates over a range of temperatures T1 to T2 that includes the melting point. Hence, in such a case, the sensible heat contributions also have to be considered and the amount of energy stored in such a heat storage system is given by the sum of the two heat gains (latent heat + sensible heat) as:

$$Q = m\left[\left\{\int_{T1}^{T*} c_{pes}dT\right\} + l + \left\{\int_{T*}^{T2} c_{pel}dT\right\}\right] \quad (1.3)$$

Where, C_{pes} and C_{pel} are the specific heats of the solid and liquid phases and T^* is the melting point [26, 27].

1.3.3 Bond heat Storage

Energy can be stored in a system composed of one or more chemical compounds that absorb or release energy through bond reactions. There are many forms in which heat energy can be stored during bond reactions. An endothermic reversible reaction involves bond storage, which can be reversed when heat release is required. The chemical produced can be stored cold (without losses) and can be transported easily. For storage of thermal energy in bond energy, reversible chemical reactions are preferred [40-41].

The basic principle is: AB + heat ⇔ A + B; using heat a compound AB is broken into components A and B which both can be stored separately; when heat is required bringing A and B together AB is formed and heat is released (exothermic reaction). The heat storage capacity of such a system is the heat of reaction or free energy of the reaction [38-40].

Hence, in light of the above methods, to conserve energy in internal combustion engines, this research work focused on analysis of thermal storage integrated tri-generation system for utilization of engine waste heat for heating and cooling purposes.

1.4 Scope and outline of thesis

The thesis is arranged in six chapters. First chapter is related to the introduction and background of the present research work. The second chapter is about the review of

the current literature in the field of cogeneration/trigeneration technologies, thermal energy storage and combination of cogeneration/trigeneration with thermal energy storage. This chapter also includes research gaps, objectives of current research and research methodology. Third chapter is about the design and development of experimental setup. It includes selection/design and fabrication of various heat exchangers, modified refrigeration unit, measuring instruments and all other components used in development of the entire thermal storage integrated micro-trigeneration system. This chapter also includes detailed experimental plan. Fourth chapter documents the experimental results and discussion. Fifth chapter describes a model to predict the performance of thermal storage integrated micro trigeneration system. The sixth i.e., the last chapter reports the conclusions drawn from the study and future scope of work. In the end, appendices, references, list of publications and profile of the author are presented.

CHAPTER 2
LITERATURE REVIEW

Cogeneration and trigeneration systems are proven technologies for efficient utilization of waste heat. The intermittent and time-mismatched demand and availability of waste heat is the major technical constraint that prevents successful implementation of waste heat recovery [35-36]. A lot of work has already been done in the field of cogeneration / trigeneration and thermal energy storage system. In this chapter findings of previous studies carried out by various researchers in the field of cogeneration/trigeneration technologies and thermal energy storage are presented.

2.1 Theoretical concepts, methods and available technologies in cogeneration/ trigeneration

In cogeneration system, most of the power and heating demand are met simultaneously by a prime mover along with a heat recovery unit. If a thermally activated component for cooling or refrigeration is incorporated in cogeneration system then it will become trigeneration systems or it may be treated as an extended form of cogeneration. Five basic elements are involved in a typical CCHP system. Elements are prime mover (electric power generator), heat recovery system, thermal driven cooling system, management and control system [27, 34]. Detail descriptions of basic elements are as follows

2.1.1 Prime Mover

Prime movers are the keystones of trigeneration/ cogeneration system and play the most crucial role in electricity or mechanical power generation/energy conversion. Since prime movers are crucial therefore, selection of prime movers is of major concerns. The desired qualities of good prime movers are low noise and vibrations, low maintenance, small size and low weight, reliable and simple operation, easy installation and low capital cost [27-28, 43-44]. Various options for prime movers are internal combustion engines, external combustion engines (Stirling engines), Rankine cycle engine and micro gas turbines, and fuel cells [27-28, 43-47].

2.1.1.1 Internal Combustion Engine

Currently two types of internal combustion engines (ICE) are widely used in various applications. One is compression ignition (CI) and other is spark ignition (SI) engine. CI engines are running on diesel as well as other petroleum products (heavy fuel oil or

biodiesel, vegetable oils, etc.) and SI engines are running on natural gas, petrol, etc. Both these engine types (and SI) are suited to co-generation (CHP) and tri-generation (CCHP) systems, since the electrical output of a typical engine generating set is around 30 % of the fuel input, the rest being lost as waste heat, around 50 % of which is recoverable [44]. With lowest capital cost and rang of size reciprocating engines are a proven technology for all CHP / CCHP modes. In addition to the start up capability and good operational reliability, high efficiency at part load operation gives the users a flexible power source, allowing for a range of different energy applications especially as emergency or standby power supply [19, 21, 27, 43, 48]. However, intensive noise and vibration caused by the rotary and reciprocating parts of the ICE will cause an unpleasant experience to users. This results in a higher wear and tear and also indicates a relatively short maintenance interval [7, 22, 44]. Another drawback of the ICE is that it has the highest engine exhaust emission of all the prime movers; in particular the NO_X emission is much higher compared to other prime movers [7]. Despite the limitations of IC engines as described earlier, they have a lot of advantages as well for using them as prime movers for trigeneration systems. Presently, the IC engines are the most widely used prime movers for trigeneration applications [44].

2.1.1.2 Stirling Engine

The Stirling engine is an ECE which operates by cycling hydrogen or helium gas (working gas) between the hot and cold portions. In the hot portion, heat is given to the gas in heater with an external combustion means and it results in swell in the expansion chamber. Further, the working gas is passed to the cold portion, where compression of gas took place in a compression chamber and for next circulation it is cooled down in a chamber [51-54].

Compared to the ICE, the Stirling engine operates with less noise and emission, especially NO_X emission. Further, Stirling engine can be operated using biomass, waste heat and solar energy. The maintenance cost of the Stirling engine is lower than that of the ICE. The major disadvantages of Stirling engines are higher prime cost, higher heat loss and lesser durability of certain parts, and time for warm up. CCHP systems based on Stirling engine have been reported. Stirling engine attained attraction for domestic trigeneration because of its ideal power to heat ratio [51, 55-56].

2.1.1.3 Rankine cycle (RC) engine and micro gas turbines

The definition of scale relating to micro-turbines varies greatly within different literature reviews. Pilavachi [57] categorized micro turbines with a power output less than 150 kW whereas Alanne et al. [58] defined micro turbine with a power output of 25-250 kW. These turbines usually consisted of an air compressor, combustion chamber, gas turbine and a generator. They are characterized by their small size, small number of movable parts and a higher power to weight ratio. In comparison to an ICE, the movable parts present in a micro-turbine are high speed rotary ones; hence it operates smoothly and with high reliability. Further merits of a micro turbine include multi-fuel capabilities and low emissions, mainly due to the low continuous combustion temperature and pressure in the combustion chamber. Nevertheless, extra components such as a rectifier and transformer are needed for a micro turbine to convert the high frequency electricity into commercial power [55, 57, 59]. Despite the high cost and relatively poor part load performance, micro turbines have shown potential to be used in applications.

2.1.1. 4 Fuel cell

Fuel cells are electrochemical energy converters which converts chemical energy in to mechanical energy similar to that of primary batteries [23-24]. Fuel cell operated micro-cogeneration systems are either based on the low temperature proton exchange membrane fuel cell (PEMFC), working at about 80^0C, or are based on the high temperature solid oxide fuel cells (SOFC), working in the temperature limits around 800-1000^0C. Size range for PEMFC is 3-250 kW and for SOFC it is 1-10 MW [23]. Normally hydrogen is used to run the fuel cells, but other options such as natural gas or other fuels by external or internal reforming can also be used [23]. Merits of fuel cells are higher efficiency (up to 60% electric), negligible emissions and absence of noise [23, 30]. The major problem associated with fuel cells is the short lifespan of the membrane and further higher cost of membrane. At this moment, excluding Japan, fuel cell based micro-CHP systems are not available commercially [23].

Major parameters and performance of theses prime movers are shown in Table 2.1:

Table 2.1 Characteristics & performance of prime movers in CCHP system [43, 60-62]

	CI engine	**SI engine**	**Micro-turbines**	**Stirling engines**	**Fuel Cells**
Capacity Range	5 kW-20 MW	3 kW-6 kW	15kW-300 kW	1 kW-1.5 MW	5 kW-2 MW
Fuel used	Gas, propane, distillate oils, biogas	Gas, biogas, liquid fuels, propane	Gas, propane, distilled oils, biogas	Any (Gas, alcohol, butane, biogas)	Hydrogen and fuels containing hydrocarbons
Electrical efficiency (%)	35-45	25-43	15-30	~40	37-60
Power to heat ratio	0.8-2.4	0.5-0.7	1.2-1.7	1.2-1.7	0.8-1.1
Noise	Loud	Loud	Fair	Fair	Quiet
CO_2 emission (kg/MWh)	650	500-620	720	672[a]	430-490
NO_X (kg/MWh)	10	0.2-1.0	0.1	0.23[a]	0.005-0.01
Part load performance	Good	Good	Fair	Good	Good
Life cycle (Year)	20	20	10	10	10-20
Initial cost (dollar/kW)	340-1000	800-1600	900-1500	1300-2000	2500-3500
a- Stirling engine emission characteristics / STM 4-260. Gas-fired distributed energy resource technology.					

2.1.2 Thermally activated refrigeration or cooling technology

If some heat recovery device like heat exchangers, are incorporated in conventional systems (single generation – power only), then system is known as CHP system i.e. major difference between single generation and CHP is that of heat recovery device. Whereas, the important difference between tri-generation (CCHP) systems and conventional systems is that CCHP systems include some cooling components (in addition to heat recovery device) as well. The methods for producing cooling effect utilizing a heat source are called thermally activated cooling technologies. Major refrigeration technologies available are: vapour compression, ejector cycles, absorption and adsorption [49]. Except for vapour compression, all the others can be driven by heat energy.

2.1.2.1 Absorption Refrigeration

Faraday invented absorption refrigeration in 1824. Ammonia vapour was used as a refrigerant and silver chloride as an absorbent for generation of cooling energy. Invention of first ammonia-water absorption chiller took place in 1859, approximately 100 years after the invention of the vapour compression chiller [63].

In simple terms an absorption refrigerator is mainly composed of a generator, condenser, evaporator and absorber. A pair of working fluids is formed by an absorbent and a refrigerant. Currently ammonia-water and LiBr-water has become the most mature working pair. Advantages of vapour absorption system over conventional electric system are: 1) less noise and vibration because of few moving parts; 2) negligible electricity consumption compared to conventional system; 3) waste heat recovery applications; 4) no harmful emissions. They may be actuated by oil, hot water or steam or directly with waste heat. High cost and slow transient response are the major drawbacks [64-66].

The basic cycle of absorption refrigeration is described below and schematic diagram is shown in Fig. 2.1:

a) Heat (QH) is supplied to concentrated solution of refrigerant and absorbent in generator. Due to heat gain high pressure refrigerant start vaporizing and enters into the condenser.

b) After condensation, heat (QI1) is released by the refrigerant before entering to the evaporator;

c) In evaporator low temperature heat QL was absorbed by the refrigerant. By taking heat refrigerant starts evaporating and converted in to low pressure vapours.

d) After the evaporator, refrigerant enters the absorber where it is imbibed by the lean solution coming from the generator and releasing low-grade energy (QI2) to the surroundings. Strong solution is again sent to the generator with the help of pump [7].

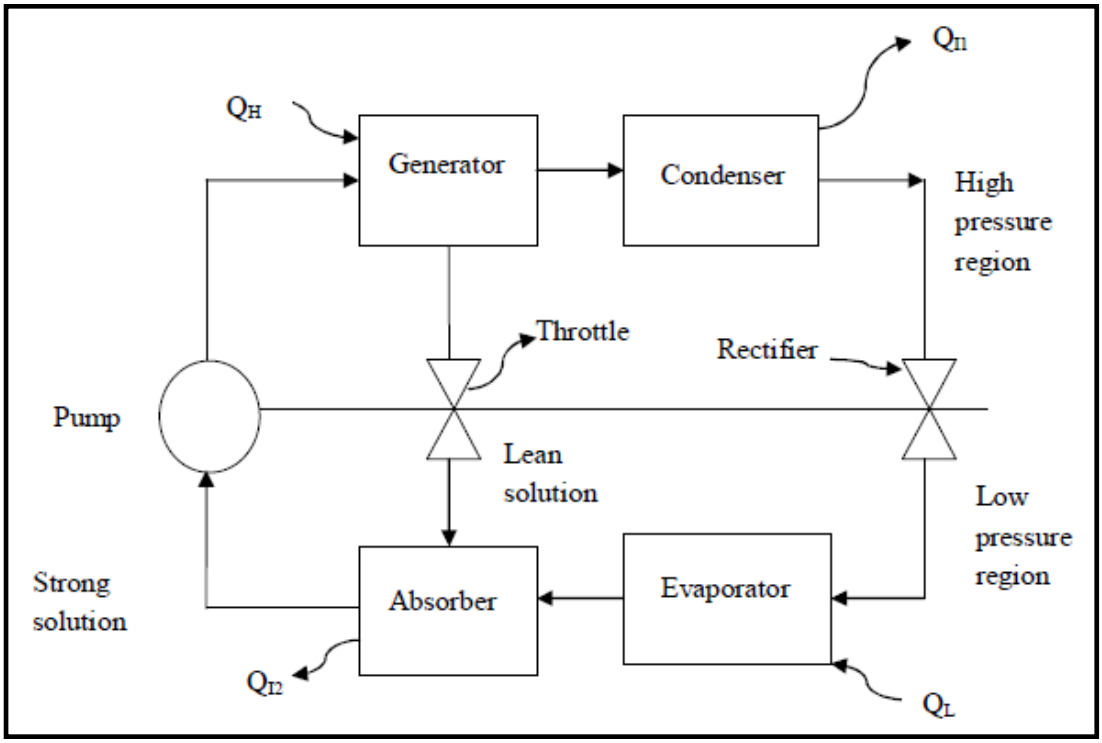

Fig. 2.1 Schematic diagram of absorption refrigeration

In this system compressor, used in vapour compression refrigeration system, was replaced by a generator, absorber, and pump. Waste heat is utilized in generator to heat up the concentrated solution. To remove the water from contained ammonia vapour, a rectifier is necessary required for ammonia-water refrigeration. If this water is not removed from ammonia vapour, will be accumulated in the evaporator, and results in reduced refrigeration efficiency. This rectifier is not necessary in a LiBr-water system, because of the non-volatile property of LiBr. LiBr-water refrigeration cannot be used to meet the freezing demand because of freezing point of the water refrigerant. COP of an absorption refrigeration system is quite low [7].

2.1.2.2 Ejector refrigeration systems:

Ejector or jet pump refrigeration has been used for cooling purposes for many years. This is a thermally driven technology and in a state of development, COP of this system is low as compared to vapour compression systems. Major advantages of this technology is its simplicity, absence of moving part and capability to produce refrigeration using waste heat, solar energy as a source of heat at temperatures above 80° C.

Schematic diagram of ejector refrigeration cycle is shown in Fig. 2.2. Two loops are there in this system, one is power and another one is refrigeration. Low grade energy, Qb, in power loop, is used in generator to vaporize high pressure liquid. Generated high pressure vapours are also known as the primary fluid and flows through the ejector. High pressure vapours are accelerated through the nozzle. In nozzle pressure energy is converted in to kinetic energy, hence, reduction in pressure occurs. This reduction is pressure induces vapour from the evaporator and is known as secondary fluid (point 3). The primary and secondary fluids are mixed in the mixing chamber before moving to the diffuser. In diffuser section, kinetic energy is converted in to pressure energy i.e. recovery of pressure. The heat (Qc) from mixed fluid is rejected to environment in condenser. A portion of fluid leaving the condenser (point 5) is pumped to the boiler for producing power and other portion of fluid is expanded with the help of an expansion device. After expansion it enters in to the evaporator of refrigeration loop (point 6) as a mixture of liquid and vapour. Refrigeration effect (Qe) was produced in evaporator and vapour is then drawn into ejector (point 3). Again the mixed fluid is condensed for repeating refrigeration cycle [67].

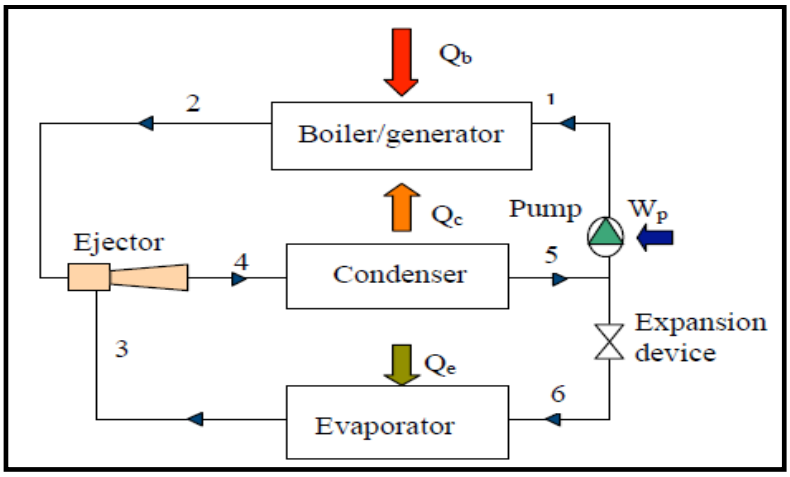

Fig. 2.2 Schematic diagram of ejector refrigeration

2.1.2.3 Adsorption Cooling

Adsorption refrigeration circuit consists of one or more solid adsorbent bed, condenser, expansion valve and evaporator. Solid adsorbent bed adsorbs and desorbs the refrigerant intermittently and provides cooling [64, 68]. Advantages of adsorption technology are: robust technology, few moving parts, low electricity consumption, simple, requires no lubrication, little maintenance, quiet operation, short start-up time, no risk of crystallization, environment friendly, longer chiller life, modularity, readily scalable by additional beds for increased capacity, use of renewable energy resources, can be driven by lower temperature heat source etc. The main limitations are: high vacuum-tight requirement, lower COP, intermittent operation, high cost, less mature technology [66, 68].

2.1.2.4 Desiccant Dehumidifiers

Desiccant dehumidifiers can work alone or in combination with the absorption chillers to meet dehumidification loads. To regenerate the desiccants, low grade heat is required, which can be supplied by the micro CCHP system [64]. Solid or liquid desiccants are capable of absorbing or adsorbing water vapour, working on vapour pressure difference. Materials (desiccant materials) are chlorides of lithium and calcium, zeolite, oxide of aluminum, silica gel, etc. Cooling with solid desiccant is free from chloro-fluoro-carbon (CFC), compact in size and saves energy. Major drawbacks are higher cost and low efficiency [64, 66]. Advantages of desiccant systems are reduced power consumption, reduced grow molds, compact equipment, etc. Limitations include high cost of the desiccant equipment, limited application potential, clogging from foreign particles in the air stream, toxicity, and desiccant degradation if not controlled [66].

2.1.3 Method for heating

Heating requirements like space heating, hot water production, preheating intake air and fuel, dryer, etc. in CHP or CCHP can be fulfilled by utilizing waste heat from engine cooling system or from exhaust gases by using waste heat recovery system. Examples of using waste heat recovery are preheating of primary air for combustion, process or boiler feed water heating, space heating etc. There are various types of heat recovery devices available in the market. The most common heat recovery equipment’s available commercially are recuperators, regenerators, heat wheels, heat

pipes, waste heat boilers, heat pumps, thermo compressors and heat exchanges viz. shell and tube type, double pipe, plate type, run around coil etc. In most micro-trigeneration applications the exhaust gas from a prime mover is passed through a heat exchanger to recover heat or to gain thermal energy from the exhaust.

2.1.4 Existing work in the field of trigeneration/ cogeneration system

Various studies reporting either on the basis of real life installed systems such as hospitals [69], factories [70, 71], supermarkets [72] and hotels [73], or computer operated simulations have already shown the feasibility of tri-generation systems in excess of 50 kW. The new frontier of tri-generation is in the residential and small commercial building sector. Applying tri-generation technology to small residential and small commercial buildings is an attractive option because of the large market potential. This section presents outcome of existing research on real life experimental models and the theoretically modeling techniques for IC engine operated micro trigeneration systems.

Ebrahimi and Keshavarz [74] presented a work to select the best prime mover for a micro CCHP system for a building, in five different climates. For the process of decision –making, four criteria (environmental, technological, economical, and social) and sixteen sub-criteria were used. For making a decision two approaches (algorithms of fuzzy logic and grey incidence approach) were used. Among various options available for prime movers, four main options (conventional separate production, internal combustion engine, micro-gas turbine and Stirling engine) were selected. In pre-design steps other options such as fuel cell and steam turbine were omitted. Using fuzzy logic and the grey incidence approach same results for all the climates were obtained and it was proposed that the worst to best prime movers are micro-gas turbine, conventional separate production, sterling engine and the internal combustion engine.

Basrawia et al. [75] presented the performance of micro gas turbine based CHP and CCHP systems in a buildings located in tropical climate. Performance based on energy, economical and environmental parameters were studied. Cogeneration system consisted of micro gas turbine and an exhaust heat exchanger whereas trigeneration was consisted of micro gas turbine, an exhaust heat exchanger and an absorption heat pump and heat storage. Heat demand was higher during night-time and, hence, heat

storage was essential for storing heat generated during daytime and to be utilized in night. Trigeneration was better compared to that of cogeneration because of more exhaust heat utilization. Energy recovery efficiency in CCHP was of 37% and 80% during day and night time respectively. Further, payback period for the CCHP was also shorter as compared to CHP. Compared to conventional system cogeneration and trigeneration system can also reduce pollutants especially NOx emissions.

Deng et al. [76] using exergy cost method analyzed a micro-trigeneration system. The results reflected that structural theory of thermo-economics is an efficient and systematic tool that provides in depth information related to costs and efficiency of energy conversion processes.

Wu et al. [77] experimentally investigated the micro-CCHP system which mainly consisted of an IC engine with a rated electrical output of 16 kW, an adsorption chiller, and a thermal management controller. Results show that this system can produce 17.7 kW of heating, 6.5 kW of cooling and 16 kW of electrical output. The primary energy ratio reached 0.765 in CHP mode and 0.56 in CCHP mode.

Huangfu et al. [78] discussed the economic & exergy analysis of micro CCHP system using a small IC engine with rated electrical power of 12 kW and an adsorption chiller with refrigeration capacity of 9 kW. Economic evaluation showed that the payback period for this micro-CCHP system was only 2.97 years with a very small initial cost. From exergetic view, the electrical efficiency of gas engine should be enhanced for an improved micro-CCHP system.

Godefroy et al. [49] described the design, testing and mathematical modeling of a small trigeneration system based on a gas engine with 5.5 kW electricity output and an ejector cooling system. Analysis showed that an overall efficiency of around 50% could be achieved.

Kong et al. [79] described an experimental investigation of performance of a micro CCHP system. In this study, LPG and natural fired gas engine was used as a small generator set driven by a small adsorption chiller, which has a rated electric power of 12 kW, a rated cooling capacity of 9 kW and a rated heating capacity of 28 kW. The result showed that in comparison to large trigeneration system, the small trigeneration test facility provided better test rig platform for cooling load, heating load and power

generation and micro trigeneration system can save more primary energy as compared to conventional system.

Angrisani et al. [80] studied a simplified 3-E (Energy, Economic and Environmental) approach to study the performance of a complex small trigeneration energy conversion system. The results showed that in comparison with conventional system, trigeneration system can save primary energy up to 28% and reduce CO_2 emissions up to 36 %.

Wang et al. [81] examined the diesel engine generator based household size trigeneration system. Diesel engine was fuelled with hydrogen. Performance and emission characteristics of a trigeneration system were investigated and compared with single generation and cogeneration systems using ECLIPSE simulation software. The study showed that diesel engine gen set based domestic micro trigeneration system, fuelled with hydrogen was feasible. Results also indicated that trigeneration system produces zero emissions when fuelled with hydrogen.

Wang et al. [82] studied diesel engine generator fuelled with raw jatropha based trigeneration system. The performance and emission characteristics of trigeneration system were compared single generation and cogeneration systems using ECLIPSE simulation software. The results from the study showed that the overall efficiency of trigeneration system was higher and CO_2 emissions of trigeneration system were lower than that of single and cogeneration system.

Badami et al. [83] dealt with an innovative natural gas based CCHP system with electrical, heating, and cooling capacity of 126, 220, 210 kW respectively. The tri-generation plant was composed of a co-generator which used an automotive derived gas fired internal combustion engine coupled to LiCl-water desiccant cooling system to recover heat from the flue gas and from the engine cooling water.

Manzela et al. [50] experimentally studied internal combustion engine exhaust operated vapour absorption refrigeration (ammonia-water). Experiments were carried out for 25%, 50%, 75% and peak load of engine. The impact on engine performance, exhaust emissions, and power economy were evaluated. Steady state of the refrigerator was obtained about 3 hours after the start up of system and steady state temperature was in between 4 ^{o}C and 13 ^{o}C. It was observed, when refrigeration system was installed in the engine exhaust, hydrocarbon emissions were higher and

carbon monoxide emissions were reduced and concentrations of CO_2 remains unaltered.

Lin et al. [17] had designed and realized in laboratory, small diesel engine based household size trigeneration system. Experiments were done to investigate the performance of CCHP and single generation system and engine exhaust emissions. The test results showed that the total thermal efficiency of trigeneration system at the peak engine load reaches up to 67.3%, compared to that of the single generation system. Total thermal efficiency of trigeneration system varied from 205 % to 438 % which was significantly high compared to that of single generation. The CO_2 emission per unit of useful energy output (kWh) from trigeneration was 0.401 kg CO_2/kW h at the engine full load, compared to that of 1.22 kg CO_2/kW h from single generation. Reduction in CO_2 emission per unit of trigeneration output (kWh) was in the range of 67.2 % to 81.4 % compared single generation. It was concluded from the experimental results that the innovative small trigeneration is feasible to generate electricity, produce heating effect and cooling effect simultaneously from a single fuel input.

Cacua et al. [84] presented an experimental study on CCHP system based on a dual fuel engine (diesel-biogas). In this CCHP system, engine exhaust (waste heat) was used for air heating, using a heat pipe exchanger, and for actuating an absorption unit freezer. The heated air was used to dry peppermint using convective trays dryer. At full engine load, the energy efficiency of in diesel and dual mode was 40% and 31%, respectively, and was comparatively higher than that of single generation (23% in diesel and 18% in dual fuel mode). On the other hand, a maximum substitution level of diesel in dual fuel mode was achieved and was 50%.

Ciampi et al. [85] experimentally studied a micro-trigeneration system. Performance of CCHP system as evaluated during three typical days of summer operation and compared with those of a conventional system based on economic, separate energy production and environmental point of views. It was concluded that there is a great ability in micro-trigeneration system to save primary energy, reduce operating cost and decrease CO_2 emissions. Energy saved reduction in operating cost and reduction in CO_2 emission was 20 %, around 39 % and 23 % respectively.

Fong and Lee [86] investigated energy and environmental merits of internal-combustion-engine primed trigeneration (ICEPT). Three types of systems were studied and compared with a conventional chilled water system which was powered

by electricity. The total year-round electricity demand using ICEPT was reduced by 10.4 %, when engine was fueled with natural gas. However, total primary energy saved only in the range from 1.7% to 6.8% with the diesel fueled system. More than 70 % of input energy had been utilized in diesel fueled system and found the best among three types of ICEPT systems. Significant difference was there in COP of absorption chiller and the vapour-compression chiller. The variation in carbon dioxide emission with three types of adopted fuel was significant. Maximum percentage of carbon dioxide was 26.7% for the natural-gas-fueled system.

The major technical constraint that prevents successful implementation of micro-trigeneration or co-generation is intermittent and time mismatched demand and availability of waste heat.

2.2 Studies related to thermal energy storage

Thermal energy storage in a trigeneration system has many functions: reducing mismatch between heat demand and heat supply; storing the heat received from unsteady heat sources; storing excess heat when not required; overcoming the startup phase; avoiding frequent starts/stops. TES transfers heat to storage media during the charging period, and releases it at a later stage during the discharging step [87].

Stritih [88] experimentally studied the characteristics of heat-transfer for finned surface latent-heat storage unit. Solidification and melting processes was studied and characteristics were compared with plain surface heat-storage unit. For the investigation Paraffin (melting point of 30 ^{0}C) was used as an energy storage media. It was selected because it is quite feasible for storage of energy for building applications. The effectiveness was calculated from the quotient of the heat flux with and without fins.

Nallusamya et al. [89] experimentally studied the thermal behavior of a packed bed TES unit used for sensible and latent heat storage. TES unit (Insulated cylindrical tank which was packed with Paraffin filled spherical capsules) was designed, developed and integrated with constant temperature bath/solar collector for performance of the storage unit. To transfer heat from bath/ solar collector, water was used as heat transfer fluid and also as sensible heat storage medium. The significance of time wise variation of HTF and PCM temperatures during charging and discharging processes, performance parameters such as instantaneous and cumulative heat stored were

studied. Based on discharging it was concluded that for intermittent requirement applications, batch wise discharging of hot water from TES was best suited.

Regin et al. [90] presented a review on heat transfer characteristics of TES system using capsules of PCM. It was proposed that to achieve the objective of high storage density with higher efficiency, one of the important methods is use of PCM capsules assembled as a packed bed. Study also includes advancements of available latent heat TES technologies, various aspects of storage such as heat transfer, storage material, encapsulation and new PCM.

Butala and Stritih [91] presented an experimental study on buildings cooling using night time cold accumulation in a phase change material. PCMs suitable for summer cooling were also listed. Experiments were conducted using paraffin with a melting point of 22 ^{0}C as the PCM to store cold during the night time and to cool hot air during the daytime in summer.

Agyenim et al. [92] presented a review on the development, heat transfer enhancement techniques of latent heat TES systems. Various phase change materials (PCMs) investigated over the last three decades were also presented. The review also included the geometry and configurations of PCM containers and a series of numerical and experimental tests undertaken to assess the effects of parameters such as the inlet temperature and the mass flow rate of the heat transfer fluid (HTF). It was concluded that most of the research on phase change problems has been carried out within the temperature range of 0 ^{0}C to 60 ^{0}C suitable for domestic heating/cooling.

Iten and Liu [93] presented a review on procedure to design an effective short term TES using phase change materials.

Pandiyarajan et al. [35] integrated IC engine with a shell and finned tube heat exchanger. The purpose of this integration was to extract heat from the engine exhaust. A thermal energy storage tank was also used to store the excess energy available. Thermal energy storage unit for combined cumulative heat storage (sensible and latent) using cylindrical phase change material (PCM) capsules was designed. The performance of the engine with and without integration was evaluated. It was found that nearly 10–15 % of fuel power was stored as heat in the combined storage system, which was available at reasonably high temperature for suitable application. Various performance parameters pertaining to the heat exchanger and the storage tank such as

amount of heat recovered, heat lost, charging rate, charging efficiency and percentage energy saved were also evaluated.

Dubovsky et al. [94] analyzed a tubular heat exchanger which utilizes the latent heat of a phase change material with an assumption that sensible heat capacity of the liquid PCM and the tubes' material is considered small in comparison with the latent heat of melting of the PCM. In the heat exchanger, the PCM melts inside tubes while air flows across the tube banks. An analytical solution for the overall heat exchange parameters, like heat transfer rate, stored energy and total melting time were obtained and compared with the results of a numerical solution. In addition, the model predicts the results for separate tubes depending on the tube location in the system.

Tay et al. [95] investigated useful latent energy that can be stored within a tube-in-tank phase change TESS with particular reference to off peak thermal storage applications for cooling buildings. Actual useful energy stored within a phase change material (PCM) storage system was coupled to a low energy night time cooling system using a cooling tower. Storage effectiveness was determined and optimized delivering a storage effectiveness of 68% and 75%. This parameter was directly compared to sensible storage systems and it was concluded that tube-in-tank systems can store more than 18 times more useful energy than sensible storage systems per unit volume.

Tay et al. [96] experimentally studied the effectiveness of a tube-in-tank design filled with PCM (salt hydrate) for cold storage applications. From the experimental measurements, the average heat exchange effectiveness of the storage tank was determined and a characteristic design curve was developed which is a function of the measured average NTU.

Mosaffa et al. [97] carried out numerical investigation for the performance enhancement of a free cooling system using a TES unit employing multiple phase changing materials. The TES unit was composed of a number of rectangular channels for the flowing heat transfer fluid, separated by slabs of PCM. Forced convective heat transfer inside the channels was analyzed by solving the energy equation, which was coupled with the heat conduction equation in the container wall. The effect of design parameters such as PCM slab length, thickness and fluid passage gap on the storage performance was also investigated using an energy based optimization. Results suggested that higher COPs are obtained for shorter and thinner PCM slabs.

Kozak et al. [98] carried out experimental and numerical study on a hybrid heat sink. In this sink heat was absorbed by PCM and dissipated to the environment through fins (Aluminum 6061) exposed to the air. A simplified thermal model, based on a two-dimensional enthalpy formulation for the PCM, was also developed for a conservative estimation of temperature evolution. Study addressed the relative contributions of latent/sensible accumulation and heat transfer to the air. It was found that the share of sensible-heat-based accumulation rate tends to increase when the heat input increases.

Majid et al. [99] presented the study on operation and performance of TESS installed at a cogeneration plant for campus cooling. Operating data from 2006 until 2009 were analyzed to evaluate the operating modes, half-cycle figure of merit (FOM) and thermo cline performance of the TESS.

Li et al. [100] presented a novel energy storage system which stores excessive energy in the form of compressed air and thermal heat. This new system allows trigeneration of electrical, heating and cooling power in energy releasing The cooling power from this system was generated by expansion of compressed air instead of using absorption chiller. A new parameter comprehensive efficiency was proposed to evaluate the performance of trigeneration system. Results showed that comprehensive efficiency of the system was very high (50%) in winter and 30% in summer.

Tao et al. [101] investigated the performance of latent heat storage using high temperature molten salt under variable conditions. Numerical investigation was carried out for effect on heat storage rate, effect of tube geometry on melting time and fraction, inlet temperature, velocity. Within the parameters of study, results shows that inlet temperature of the HTF significantly affect the heat storage rate. 53 % reduction in melting time was observed when inlet temperature of HTF increased from 1070 K to 1110 K. More non uniform melting rate and non-uniform distribution of solid liquid interface was observed with high inlet temperature. The important factor that influences much is the velocity of HTF at inlet. Melting time reduces by 45.4 % when inlet velocity increased from 10 m/s to 20 m/s. increasing velocity also resulted in uniform solid liquid interface distribution. Lowest effect of tube diameter was observed on performance. Increasing outer radius from 2.4 cm to 2.8 cm, the change in melting time was only 16.3%, and resulted in more uniform solid liquid interface. It was concluded generally, when the heat load of the heat source is larger, a larger HTF

mass flow rate is suitable to maintain a moderate HTF temperature. And then for the LHS unit, a larger tube diameter is recommendable.

Nomura et al. [102] describes the performance of a direct-contact heat exchanger. Erythritol was used as a storage medium along with heat-transfer oil (HTO). For heat storage unit, cylindrical shell with an inner diameter of 20 cm and a height of 100 cm was used. A nozzle was placed at the bottom of shell, with nine holes of diameter 3.0 mm facing vertically downward. The effects of flow rate of heat transfer oil and the height of PCM layer in the heat storage was studied based on effectiveness, heat release rate, and volumetric heat transfer coefficient. It was observed, when the height of PCM was constant and heat transfer oil flowing uniformly, effectiveness was high and the heat release rate was proportional to the flow rate of HTO. At a height of 0.2 m of PCM the effectiveness observed was 0.83. Further, with increasing HTO flow rate, increase in the average volumetric heat transfer coefficient was observed. These results revealed that the direct-contact heat exchanger can rapidly, efficiently, and compactly release the latent heat of PCM provided that HTO uniformly flows.

2.3 Motivation and research gaps

A remarkable development has taken place in the field of use of trigeneration system and thermal energy storage all over world during the last 2 decades. However, following research gaps were observed from the detailed literature review:

1. Attention has been paid by many researchers in the field of TES. Although the information available in literature about this topic is enormous, there are not many studies on its application with IC engines. The development of TES system is urgently needed for small capacity stationary CI engine considering domestic and small establishments' use.
2. Most of the studies available in the field of energy storage talk about the solar energy storage and storage of heat at lower temperatures. Very few of them are related to IC engine waste heat storage.
3. Various studies available in this field, talk about charging process of TESS, however, very few of them tell about discharging process. Hence, there is a great need to study the discharging process (recovery) of thermal energy storage device.

4. Limited research work has been done in the field of small capacity CI engine operated Micro-Trigeneration. There is need to study Trigeneration/ Cogeneration with small capacity engines.

5. Very few simulation and experimental studies are available in the literature related to integration of thermal storage with cogeneration and trigeneration system. This integration may lead to increase in penetration of Cogeneration and Trigeneration technologies in various applications in developing countries. Hence, feasibility study needs to be done for this type of integration.

6. Very little work has been done on emission resulting from small capacity engine with trigeneration and thermal storage system. No doubt overall energy efficiency would increase (as previous studies suggest) but emissions are also of keen concern in the adoption of these technologies. So there is a need to study the emissions for the above stated condition.

The above research gaps have motivated to carry out research in above field.

2.4 Objectives of current research

After going through the observed research gaps, the following are decided to be the major objectives of the proposed research work:

- To design and develop a thermal energy storage system (TESS) for stationary CI engine exhaust heat and integrate the above TESS with micro-trigeneration/co-generation system for off power and on power operations.

- To evaluate the performance and emissions of TESS integrated micro-Trigeneration system.

- To develop a model to predict the performance of CI engine thermal energy storage (TES) integrated micro-trigeneration.

2.5 Research Methodology

The work was carried out for design and development of thermal storage integrated trigeneration system by recovering waste heat from the engine exhaust. The work was divided into the following episodes:

- Detailed literature survey regarding the CI engines operated micro trigeneration system and TESS.
- Development and installation of load bank, fuel storage and measuring system and air box.
- Test runs of engine with modified system for its durability, accuracy, reliability, and leak-proof requirements. Further improvement/modification, wherever required, in the system developed.
- Evaluation, analysis and comparison of engine exhaust emission (CO_2, smoke NO_x ,CO and HC) at various loads.
- Experimental evaluation with diesel fueled engine for the performance determination and comparison of various parameters such as BTE, BSFC, exhaust gas temperature, etc.
- Design and development of TESS.
- Selection and fabrication of the heat exchanger for heating water by utilizing the waste heat of exhaust gases.
- Development of heat exchanger for generator of VA system and modify VA refrigeration by installing the above heat exchanger.
- Installation of demonstration plant for displaying all components involved in trigeneration system, on real life scale. This included the engine, TESS, heat exchanger for water heating, VA system etc.
- Insulation of TESS, heat exchanger for water heating, VA system to achieve optimal performance.
- Experimental evaluation for feasibility of following three possible combinations for thermal storage micro trigeneration system's performance.

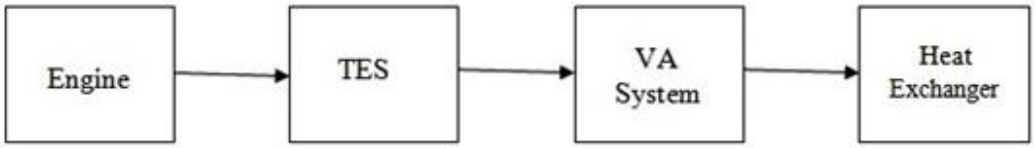

(I)

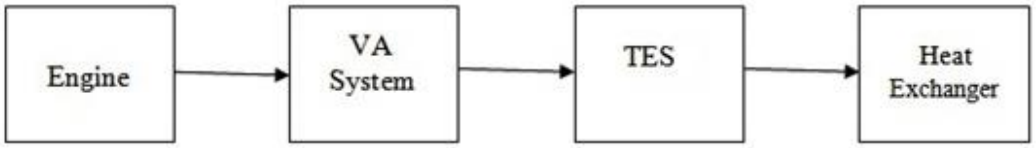

(II)

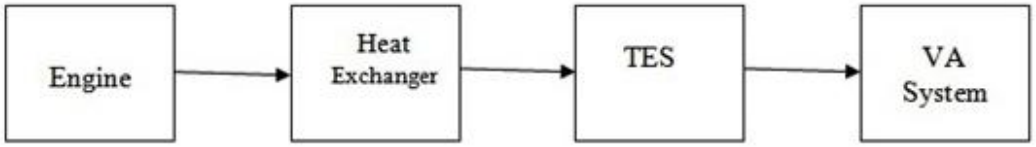

(III)

- Experimental evaluation with feasible combination for thermal storage integrated micro trigeneration system's performance during on power mode/ charging of TESS (when engine was running and exhaust heat was allowed to pass through heat exchanger, TESS and VA system) and off power mode / discharging of TESS (when engine was stopped, air from atmosphere with help of air blower was passed through TESS, where it took heat from TESS and get heated and heated air was supplied to generator of VA system for maintain cooling)
- Emission analysis of thermal storage integrated micro trigeneration system with feasible combination.
- Comparison of performance and emissions of thermal storage integrated micro trigeneration system with the conventional system (single generation).
- Modeling to predict the performance of TES integrated micro-trigeneration system.
- Documentation of the research work.

CHAPTER 3
EXPERIMENTAL SETUP, PLAN AND PROCEDURE

The experimental setup for thermal storage integrated micro trigeneration system consisted of a four stroke, single cylinder, air cooled, stationary diesel engine coupled to dynamometer (an electric dynamometer), integrated with a DPHE for water heating purpose, a TESS and 41 liters vapour absorption refrigeration system for cooling purpose. Positions of these components were changed for various combinations as given in methodology section. Burette meter was used to measure the mass flow rate of fuel, air box was used to measure air flow and K-type (Cr/Al) thermocouples were used to measure temperature at various places. AVL make DITEST (AVL DiGas 4000 light) 5 gas analyzer was used to measure NO_x, CO, HC, CO_2 and O_2 in the exhaust emission from the engine. Smoke (opacity) in exhaust was measured with the help of AVL 437 smoke meter. The detailed description of the instruments used is discussed below.

3.1 Experimental set up

This section deals with development of various components along with working of various measuring equipment.

3.1.1 Engine and dynamometer

Single cylinder, air cooled, stationary diesel engine (TAF1) was chosen as the prime mover of thermal storage integrated micro-trigeneration system. A diesel engine was chosen as a prime mover for this study because it has a lot of advantages over other prime movers. IC engine is inexpensive, reliable and the technology is matured, has low operating cost and high ease of maintenance. Another reason for choosing diesel engine as a prime mover in thermal storage integrated micro-trigeneration system is that it is the most versatile engine widely used in India for agricultural and electricity generation. The complete specification of the engine is shown in Table 3.1.

Table 3.1 Specifications of Kirloskar TAF1 diesel engine

No. of cylinder		1
Bore × Stroke	mm	87.5 × 110
Compression ratio		17.5 : 1
Rated output as per IS: 11170	kW (hp)	4.4 (6)
Rated speed	RPM	1500
Fuel Tank Capacity	Liter	6.5
Rotation while looking at the flywheel		Clockwise
Starting		Hand Start

To determine the brake power electric dynamometer (Power star make) was used. It consisted of an alternator, to apply load electric bulbs were connected. The load was varied by switching on the desired number of electric bulbs. The electrical load bank with control panel is shown in Fig. 3.1 and the specifications of the dynamometer are given in Table 3.2.

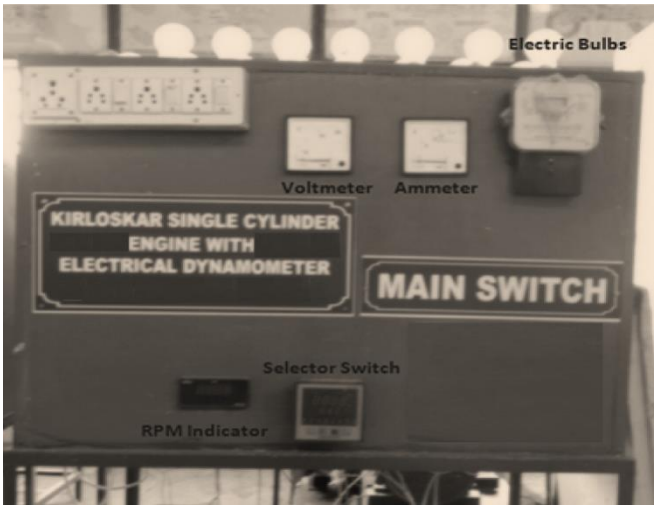

Fig. 3.1 Electric load bank

Table 3.2 Specifications of electric dynamometer

Make	Power star
Model	KBM105
kVA	5
Voltage	230 V
Current	21.7 A
Frequency	50 Hz
Rating	Continuous
Revolutions per minute	1500
PF	1.0

3.1.2 Air flow measurement

To measure the air flow to the engine, an air box (0.60 × 0.60 × 1.20 m^3) was used. At the entrance of one side wall of air box, an orifice (diameter = 25 mm and coefficient of discharge, C_d = 0.6) was fitted. The outlet of the air box was connected to air filter mounted on engine as shown in Fig. 3.2. During operation, pressure inside the box was less than atmospheric pressure outside the box. The pressure inside the air box was measured with the help of U-tube manometer. Air induced per second is given by:

Air induced/second (m^3/s) = $C_d \times A_{orifice} \times \sqrt{\frac{2gh_w\rho_w}{\rho_a}}$

Where, C_d = 0.6

$A_{orifice}$ = 0.000491 m^2

h_w = Manometer difference in m

ρ_w = Density of water (1000 kg/ m^3)

ρ_a = Density of air (1.20 kg/m^3)

Mass flow rate of air can be calculated using the following equation:

Mass flow rate of air = Air induced/second (m^3/s) × Density of air (kg/m^3)

Fig. 3.2 Air box

3.1.3 Fuel flow measurement

Fuel flow measurement is an important step for quantitative determination of brake specific fuel consumption (BSFC). Volumetric fuel flow rate was measured using burette method. A glass burette with calibration marks was connected to the fuel tank and the engine through a tee valve as shown in Fig. 3.3. Initially, fuel line was connected to the engine and burette, so as to fill the burette with the fuel, while the supply of fuel to the engine was not interrupted. In order to measure the fuel consumption the valve was adjusted so that the fuel started flowing from the burette to the engine. The time taken by the engine to consume a fixed volume of fuel was measured with the help of stopwatch. This volume divided by the time gave the volumetric flow rate.

Mass flow rate of fuel = Volume flow rate × Density of fuel

m_f = Volume of fuel consumed / Time taken (in second) * ρ

By putting the value of time taken and density (kg/m^3) in above formula mass flow rate of fuel (kg/s) was calculated.

Fig. 3.3 Fuel measuring system (Burette Method)

3.1.4 Exhaust emission analysis

AVL make DITEST (AVL DiGas 4000 light) 5 gas analyzer, used to analyze the exhaust emission from the engine, is shown in Fig. 3.4. The emissions measured by AVL DiGas 4000 light included NO_x, CO, HC, CO_2 and O_2, out of which, CO, HC and CO_2 were measured by NDIR Technique and NO_x and O_2 were measured by electrochemical sensors. It gives HC and NO_x emissions in PPM and that of other gases in percentage. Smoke (opacity) in exhaust was measured with the help of AVL 437 smoke meter which is shown in Fig. 3.5. Detailed specifications of exhaust gas analyzer and smoke meter are shown in Table 3.3 and Table 3.4 respectively.

Fig. 3.4 AVL DiGas 4000 Light 5-Gas Analyzer

Fig. 3.5 AVL 437 Smoke meter

Table 3.3 Specifications of 5-Gas analyzer [103]

Type	AVL DiGas 4000 light
Object of measurement	CO, HC, CO_2, NO_x, O_2
Measurement Principle	CO, HC, CO_2 → Infrared O_2, NO_x → Electrochemical
Range of measurement	CO: 0…….10 % by vol. CO_2: 0…….20 % by vol. O_2: 0……. 22 % by vol. HC: 0…….20000 ppm vol. NO_x: 0…….4000 ppm vol.
Resolution	CO: 0.01 % by vol. CO_2: 0.1 % by vol. O_2: 0.1 % by vol. HC: 1 ppm vol. NO_x: 1 ppm vol.
Warm up time	15 min. (self) at 20^0C
Speed of response time	Within 15 s for 90 % response
Weight	14 kg
Dimensions	360 mm × 370 mm × 220 mm
Power draw	150 W
Operating Voltage	195…253 V, 47….63 Hz

Table 3.4 Specifications of smoke meter [104]

Type	AVL 437 smoke meter
Measuring value output	Opacity N [%] or absorption k [m^{-1}]
Measuring range	N = 0 ... 100% or k = 0 ... 99.99 m^{-1}
Resolution of displayed values	0.01 % opacity or 0.0025 m^{-1}
Limit of detection	0.1 % opacity
Zero stability	{0.1 % or 0.0025 m^{-1}}/30 min.(drift with zero gas)
Exhaust gas temperature	0 to 600 °C (800°C with high pressure option)
Exhaust gas pressure	-100 mbar to 400 mbar(including pulsation peaks) 0 mbar to3000 mbar with high pressure option
Calibration	Automatic (Self calibration immediately after switch on or at the press of key)
Dimensions	501 mm × 200 mm × 330 mm (Control Unit) 520 mm × 255 mm × 455 mm (Sensor Unit)
Weight	16 kg (Control Unit) 21 kg (Sensor Unit) 6 kg (Trolley)
Power Consumption	600 W (Overall equipment) 500 W (Measuring Chamber Equipment)
Storage Temperature	-30 ^{0}C to +65 ^{0}C
Power Supply	190 to 240 V AC, 50 to 60 Hz, 2.5 A, 11.5 to 36 V DC

3.1.5 Temperature measurement

K-type thermocouples were installed at required points. K-type thermocouples can measure temperatures in the range of -200 °C to 1260 °C. Standard and special limits of error of K-type thermocouple is ± 2.2 °C or ± 0.75 % and ± 1.1 °C or ± 0.4 % respectively. Sensitivity and power consumption of the thermocouple is about 41 $\mu V/^0C$ and 3 mW respectively.

3.2 Design and development of heat exchanger for thermal energy storage

Thermal energy storage system was used to store thermal energy and this stored thermal energy was utilized in actuating the generator of vapour absorption refrigeration system (during off-power condition) for sufficient time to achieve / maintain cooling. Hence, this was the key consideration for designing / selection of heat exchanger. Following steps were adopted for designing / selecting a heat exchanger:

a. Amount of energy required to run the vapour absorption system during off-power condition was calculated. Accordingly, amount of energy needed to be stored in TESS was estimated.

b. Selection of suitable type of heat exchanger.

c. Selection of suitable phase change material for storage of thermal energy.

d. Calculation / selection of dimensional parameters of heat exchanger.

To estimate the amount of energy required to run the vapour absorption refrigeration system initially, refrigeration effect was calculated and after calculation of refrigeration effect, effectiveness of heat exchanger (at the generator of VA system) was taken into consideration to obtain the amount of energy required to run the VA system. Once amount of energy required to run the VA system was obtained, considering various heat losses from TESS and discharging efficiency, amount of energy needed to be stored in TESS was calculated.

From the literature, it was found that from the numerous available options for heat exchangers, shell and tube type heat exchanger was quite simple and the best for charging of phase change materials [92]. Hence, it was decided to design and construct a shell and tube type heat exchanger.

Several researchers have carried out investigations on a wide range of PCMs, subdividing them into organic, inorganic and eutectic PCMs. Factors that must be considered while selecting the phase change material for heat storage purpose are that PCM must possess (a) a melting point in the desired operating temperature range, (b) high latent heat of fusion per unit mass, (c) high specific heat, (d) high thermal conductivity, (e) small volume changes during phase transition, (f) chemical stability, (g) corrosion resistance to container materials, (h) non-toxicity, (i) non-flammability and (j) should be non-explosive. Agyenim et. al. [92] presented a list of PCMs investigated for different applications. Based on the engine exhaust gas temperature (reaching up to 590 ^{0}C at full load), considering temperature drop of exhaust gas before reaching the heat exchanger, the effectiveness of heat exchanger, and exhaust temperature at part load conditions (since the engine will not always run at full load), PCMs with melting point between 100 ^{0}C and 130 ^{0}C were considered . From the available PCMs with melting point in this temperature range the two phase change materials as given in Table 3.5 were short-listed:

Table 3.5 Properties of selected PCMs [92]

S. No.	**Name of PCM**	**Melting Point** (^{o}C)	**Latent Heat** (kJ/kg)	**Specific Heat** (kJ/kg-K)
1	Magnesium chloride hexahydrate ($MgCl_2.6H_2O$)	116.7	168.6	2.61 (Liquid) 2.25 (Solid)
2	Erythritol ($C_4H_{10}O_4$)	117.7	339.8	2.61 (Liquid) 2.25 (Solid)

Magnesium chloride hexahydrate is a toxic compound and also has a much lower latent heat compared to erythritol, hence, erythritol was selected as PCM for this experimental investigation. Erythritol is a naturally occurring polyol produced by bacteria, yeast and fungi. Erythritol is biological sweetener and is used extensively in the food and pharmaceutical industries [105].

Selection / calculation of dimensional parameters of shell and tube type heat exchanger involved consideration of many interacting design parameters which can be summarized as follows:

1. Fluids assignment to shell side and tube side.
2. Specifications of tube parameters - size, layout, pitch and material.
3. Specifications of shell parameters – size, material, baffle spacing and clearance.

Since erythritol was selected as the phase change material (cold medium), its mass was to be kept constant in the system, hence, it was decided to fill erythritol inside shell and exhaust gases (hot medium with moving mass) were designed to pass through the tubes.

As per the design manual [106] most common outer diameters of tubes are 1.875 cm and 2.54 cm. For greater heat transfer area smallest diameter is preferred and hence, outer diameter (tube) of 1.875 cm was selected.

After finalizing the size of the tube, the size of shell was obtained. The size of the shell was so that the back pressure will remain in allowable limit. The temperature and back pressure relationship is given in Appendix A.1. Simplified Delware method was used to compute shell-side pressure drop. The equation for shell side pressure drop is:

$$\Delta P = 1.6 \times 10^{-20} f G^2 d_s (n_b+1) / d_e s \varphi$$

Where,

f	=	Friction factor (dimensionless)
G	=	Mass flux (kg/s.m^2)
d_s	=	Shell internal diameter (m)
n_b	=	Number of baffles
s	=	Specific gravity of fluid
d_e	=	Equivalent diameter
φ	=	Viscosity correction factor

The value of friction factor, equivalent diameter and viscosity correction factor were taken from the graphs [106].

Based on the above pressure drop and easy availability in market, shell diameter was selected as 34.6 cm. After selecting shell diameter numbers of tubes were calculated. A thumb rule was used to find the number of tubes i.e. for heat exchanger diameter of the shell is taken as 1.5 to 2 times that of the diameter of tube bundle [107]. Following formula was used to find the number of tubes

$$D_b = d_0 \left(\frac{Nt}{k}\right)^{1/n}$$

Where,

D_b = Bundle diameter

d_0 = Outer diameter of tube

N_t = Number of tubes

K = Constant and value is taken from reference table i.e. 0.215 [l06]

n = Constant and value is taken from reference table i.e. 2.207 [l06]

Table 3.6 Specifications of shell and tube type heat exchanger

Parameter	**Value**
Hot side fluid	Engine exhaust (Tube)
Cold side medium	Erythritol (Shell Side)
Shell material	Mild steel
Shell height	42.0 cm
Shell diameter	34.6 cm
Tube material	Mild steel
Tube diameter	1.875 cm
No of tubes	45
No of fins	4 on each tube

With above equation 45 numbers of tubes were calculated and square pattern arrangement was selected because it simplifies cleaning and has lower shell side pressure drop. Specifications of developed shell and tube type heat exchanger are given in Table 3.6.

Next step after obtaining the dimensions of shell and tubes was fabrication of heat exchanger. 21 thermocouples were placed at three different horizontal planes at a height of 10 cm, 20 cm and 30 cm respectively from the bottom of TESS. Fig. 3.6 shows the position of thermocouples in the shell. Photographic view related to fabrication of various components of shell and tube type heat exchanger is shown in Fig. 3.7. Insulation was done in 3 layers with the help of glass wool, asbestos rope covered on the top by plaster of Paris.

This heat exchanger had inlet and outlet (for exhaust gas) as diverging and converging sections respectively. Diverging section was used at bottom side of shell to expand the exhaust gas for better heat transfer between exhaust gas and tubes. Converging section was used at top of the shell to allow easy escape of the exhaust gas.

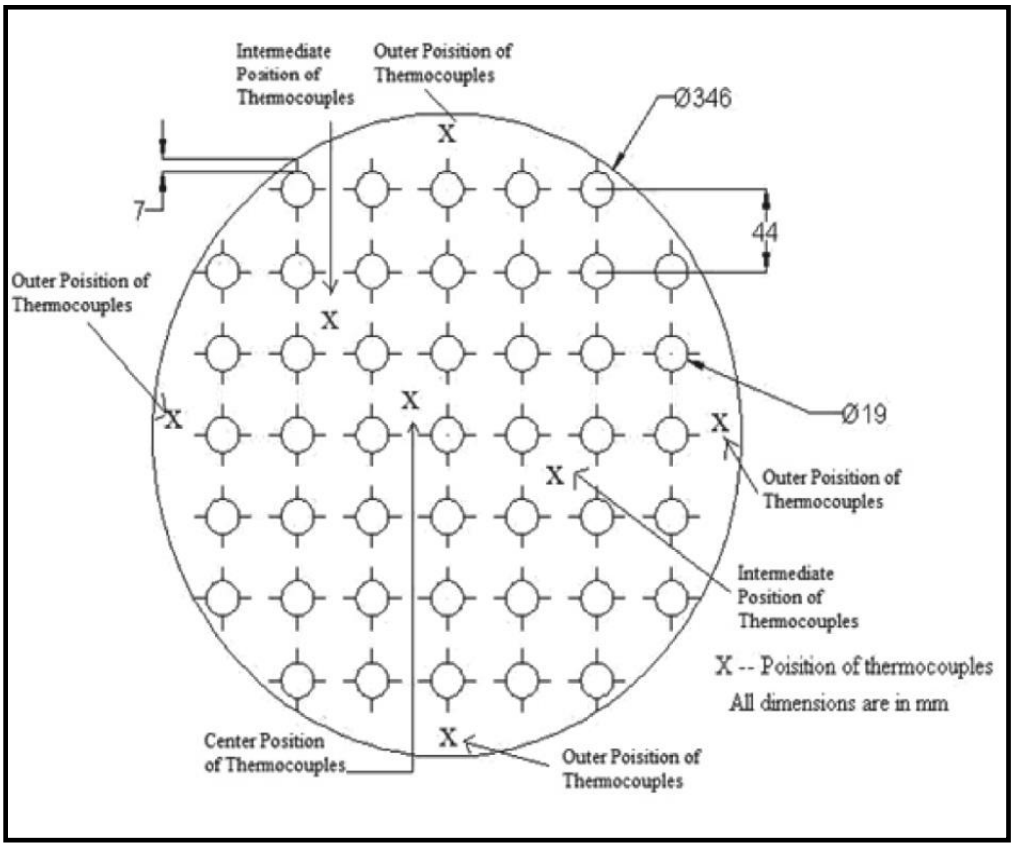

Fig. 3.6 Position of tubes and thermocouples in shell

Fig. 3.7 Photographic view of various components of shell and tube heat exchanger

After development of heat exchanger tests were also conducted with PCM having higher melting point than erythritol. From the list of available PCM, Sodium Nitrate

($NaNO_3$) with melting point 310 ^{0}C was selected for test. The temperature and energy from the engine exhaust gas was not sufficient to completely melt $NaNO_3$. Therefore the idea of using $NaNO_3$ as a storage medium for TESS was dropped.

3.3 Design and development of double pipe heat exchanger

A double pipe heat exchanger of mild steel was designed and fabricated for providing hot water. The heat exchanger was designed to recover maximum amount of heat available in the engine exhaust i.e. at full load condition of the engine.

Using the formulae given in handbook [108] for double pipe heat exchanger, heat exchanger was designed. Since the heat exchanger was used to heat water using exhaust gas of engine, hence, diameter of inner tube was restricted to diameter of exhaust line of engine and hot exhaust gases were made to flow through the inner tube. Cold water was passed through outer tube. Key points of design were energy availability in the exhaust of the engine, inlet temperatures (hot fluid inlet temperature and cold fluid inlet temperature), etc. Following equations were used for designing the double pipe heat exchanger:

The flow cross sectional area (A_c) was calculated using the following equation:

$$A_c = A_{\text{outer pipe}} - A_{\text{inner pipe}}$$

The flow wetted perimeter (P) was calculated using the following equation:

$$P = \pi\, d_{\text{outer pipe}} + \pi\, d_{\text{inner pipe}}$$

The hydraulic diameter (D_h) was calculated using the following relation:

$$D_h = 4A_c / P$$

The value of Reynolds number (R_e) was determined by the following expression:

$$R_e = \rho V D_h / \mu$$

The calculation of the friction factor (f) was done using the following expression:

$$f = (0.790 \ln Re_D - 1.64)^{-2}$$

Knowing the Prandtl Number (Pr) for this application to be Pr = 0.7, the Dittus-Boelter equation was used to obtain the value of Nusselt number (N_u) as given below :

$$Nu = 0.023 Re^{\frac{4}{5}} Pr^n$$

Where, n = 0.4 for heating, and

n = 0.3 for cooling of the fluid.

Using convection correlations for non-circular tubes, the convective heat transfer coefficient (h) was calculated using the following expression:

$$Nu = hD_h / k$$

The major heat transfer resistance is due to the inner tube. This resistance was calculated by neglecting the thermal resistance (R_t) inside the inner tube using the following equation:

$$R_t = 1 / \pi d_{inner\ pipe}\, lh$$

From the value of R_t as mentioned above, the value of UA was calculated by the following equation:

$$UA = 1 / R_t$$

Number of transfer units (NTU) was calculated by knowing the value of UA and minimum capacity rate (C_{min}) by the following expression:

$$NTU = UA / C_{min}$$

Here, the value of C_{min} ($C = m \times c$) was obtained for the hot fluid and value of maximum capacity rate (C_{max}) was obtained for cold fluid. Then the value of effectiveness (ϵ) was calculated by knowing the value of capacity ratio ($C = C_{min} / C_{max}$) using the following equation:

$$\varepsilon = \frac{1\text{-}\exp\{\text{-}NTU(1\text{-}C)\}}{1\text{-}C\exp\{\text{-}NTU(1\text{-}C)\}}$$

Specification and pictorial view of double pipe heat exchanger is given in Table 3.7 and Fig. 3.8 respectively.

Fig. 3.8 Pictorial view of double pipe heat exchanger

Table 3.7 Specification of double pipe heat exchanger

Parameter	Value
Fluid	Engine exhaust (Inner tube) Water (Outer tube)
Diameter of outside tube	5.08 cm
Diameter of inside tube	3.81 cm
Length of outside tube	67.70 cm
No. of passes per shell	Single
Contact area of water (outer tube) with hot fluid (inner tube)	810 cm^2

3.4 Modification in vapour absorption refrigeration system

Electrolux vapour absorption system, with a capacity of 41 liters and heat input of 95 Watts, was used for cooling purpose. This type of cooling system is also called three fluids absorption system. The three fluids used in the system were ammonia, hydrogen and water. Ammonia was used as refrigerant because it possesses most of the desirable properties for refrigerant. Hydrogen being the lightest gas was used to increase the rate of evaporation of liquid ammonia passing through the evaporator. Water was used as a solvent because it has the ability to absorb ammonia readily. Fig. 3.9 shows the working of electrolux type vapour absorption refrigerator.

The vapour absorption system cycle is as follows. The ammonia liquid leaving the condenser flows downward under gravity to the evaporator where it meets hydrogen gas. The hydrogen gas which is being fed to the evaporator permits the liquid ammonia to evaporate at a low pressure and temperature according to Dalton's principle. The mixture of ammonia and hydrogen passes to the absorber. In absorber, weak ammonia solution in water is also added coming downward from water separator with gravity flow. Water absorbs ammonia in absorber and hydrogen returns

upwards from absorber to evaporator. Hence, strong solution of ammonia in water passes from absorber to the generator where it is heated and ammonia vapour with traces of water vapour rises off to the water separator. Water is separated out from ammonia in water separator and a weak solution of ammonia is returned downward to the absorber with gravity flow. The ammonia vapour rises from the separator to the condenser where it is condensed to ammonia liquid, hence, completing the cycle.

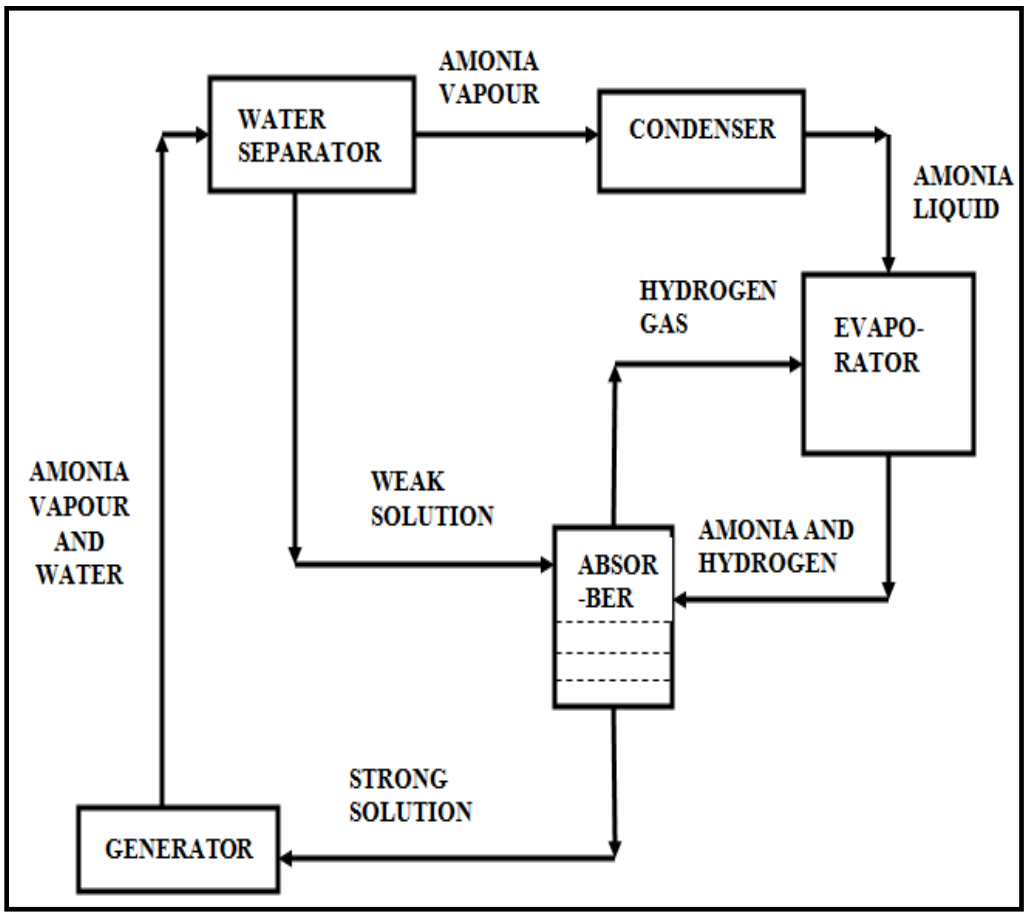

Fig. 3.9 Electrolux type vapour absorption refrigeration system

The generator of the VA refrigerator used in this study was modified to utilize the waste heat of engine exhaust gases. For the above purpose, a counter flow, double pipe heat exchanger was designed, fabricated and installed. In this double pipe heat exchanger, the generator tube was used as the inner tube and a mild steel pipe was taken as outer pipe. The length of the outer pipe of heat exchanger was fixed according to the maximum vertical length available at the generator but the diameter of the outer pipe was varied within the restricted space available between the generator tube and evaporator chamber in order to adjust the effectiveness of the heat

exchanger which could provide the required heat transfer rate at the generator. The same design procedure as given in design of double pipe heat exchanger section was adopted to select the outer diameter of pipe.

The length of the outer pipe was taken as 0.216 m as per the maximum space available at the generator side. Considering the limited space availability and requirement of an insulation layer surrounding the outer pipe, the diameter of the outer pipe was selected as 1.5” i.e. 38 mm. Photographic view of the heat exchanger fitted in VA system is shown in Fig. 3.10.

The heat exchanger for generator thus developed was well insulated outside by three alternative layers of glass wool, asbestos rope and plaster of Paris of 3 mm thickness each. This insulation was basically provided to prevent the flow of heat from the generator to the evaporator.

Fig. 3.10 Photographic view of heat exchanger fitted in VA system

3.5 Integration of various components

For the trigeneration with thermal energy storage, various components (double pipe heat exchanger, shell and tube type TESS and modified VA refrigeration system) were integrated to the engine with the help of piping and valves. For various combinations as given in methodology section, position of components was changed accordingly. To achieve single generation with thermal energy storage, TESS was integrated directly to the engine. Components with the help of various valves and piping were arranged in such a manner that rest of the modes (CHP, CHP with TES and CCHP with TES), could be achieved by controlling the valves only without disturbing the positions of various components. The physical set-up and valve positions are explained in the next section – 'Experimental plan and procedure' with the help of Table 3.8.

3.6 Experimental plan and procedure

Experimental test plan and performance parameters are discussed in this section. The experimental investigation of the performance of thermal storage integrated micro-trigeneration system was divided in various steps. In the very first step all the components (engine, double pipe heat exchanger, thermal energy storage system and vapour absorption refrigeration system) were arranged in three different combinations as explained earlier in methodology section to find the most feasible solution. Photographic views of all the three combinations i.e. (i) Engine + TESS + VA system + Heat exchanger; (ii) Engine + VA system + TESS + Heat exchanger and (iii) Engine + Heat exchanger + TESS + VA system are shown in Fig. 3.11, 3.12 and 3.13 respectively.

After finding the feasible combination i.e. the combination III (Engine + Heat exchanger + TESS + VA system), experimental investigation of the performance of the thermal energy storage integrated micro-trigeneration system was carried out to suit the conditions of single generation, cogeneration (CHP), cogeneration with TES and trigeneration (CCHP) with TES modes. For single generation with TES mode TESS was integrated directly to the engine. The schematic diagram of experimental setup with feasible combination is shown in Fig. 3.14.

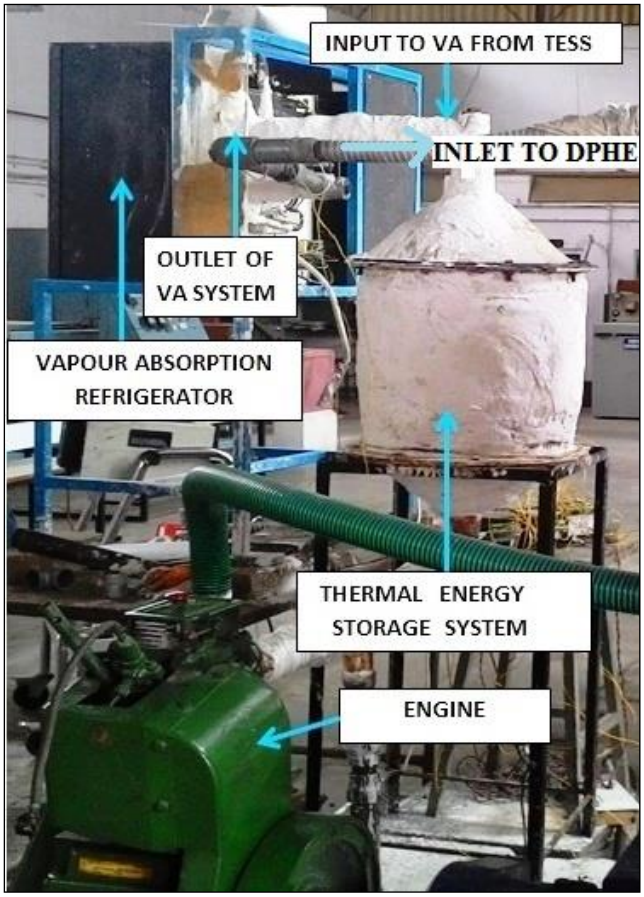

Fig. 3.11 Photographic view of experimental setup with combination I

(Engine + TESS + VA system + Heat exchanger)

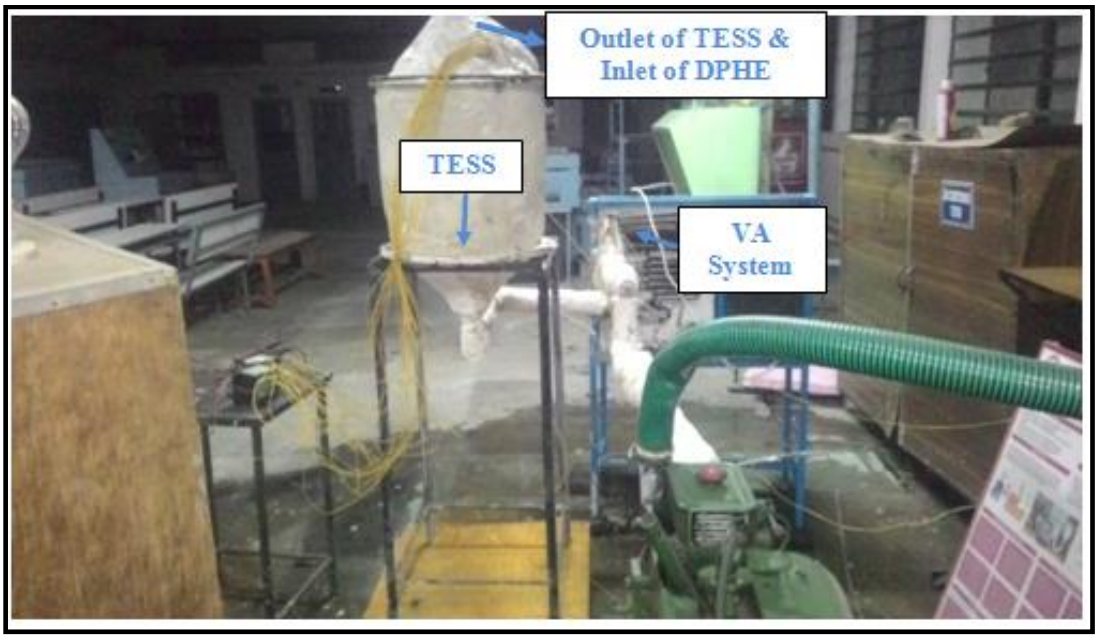

Fig. 3.12 Photographic view of experimental setup with combination II

(Engine + VA system + TESS + Heat exchanger)

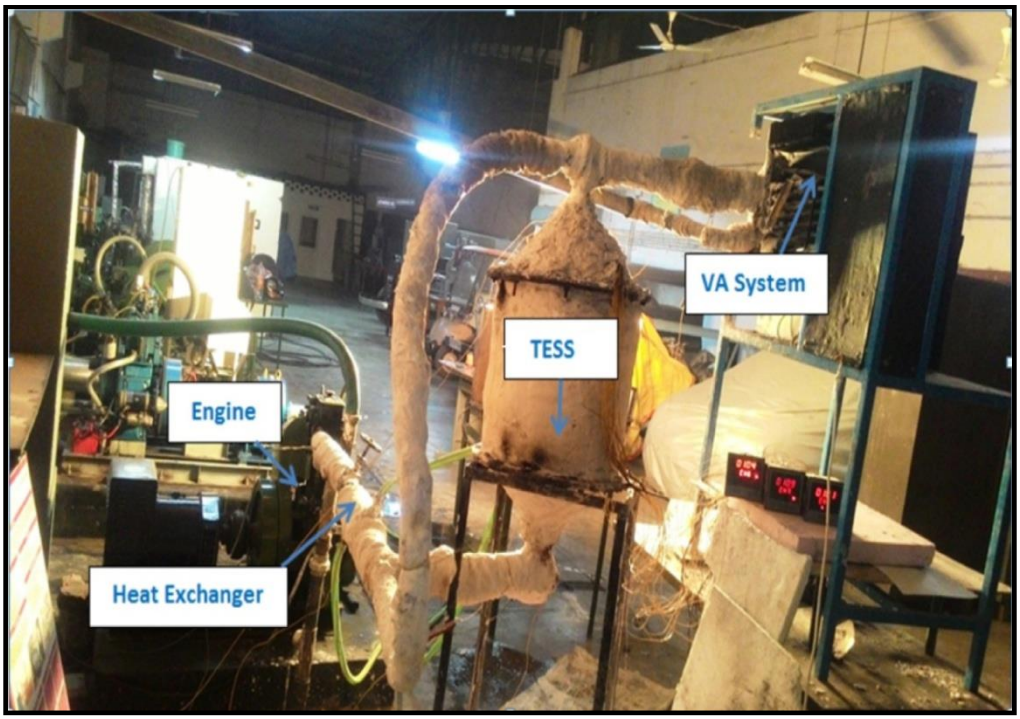

Fig. 3.13 Photographic view of experimental setup with combination III (Engine + Heat exchanger + TESS + VA system)

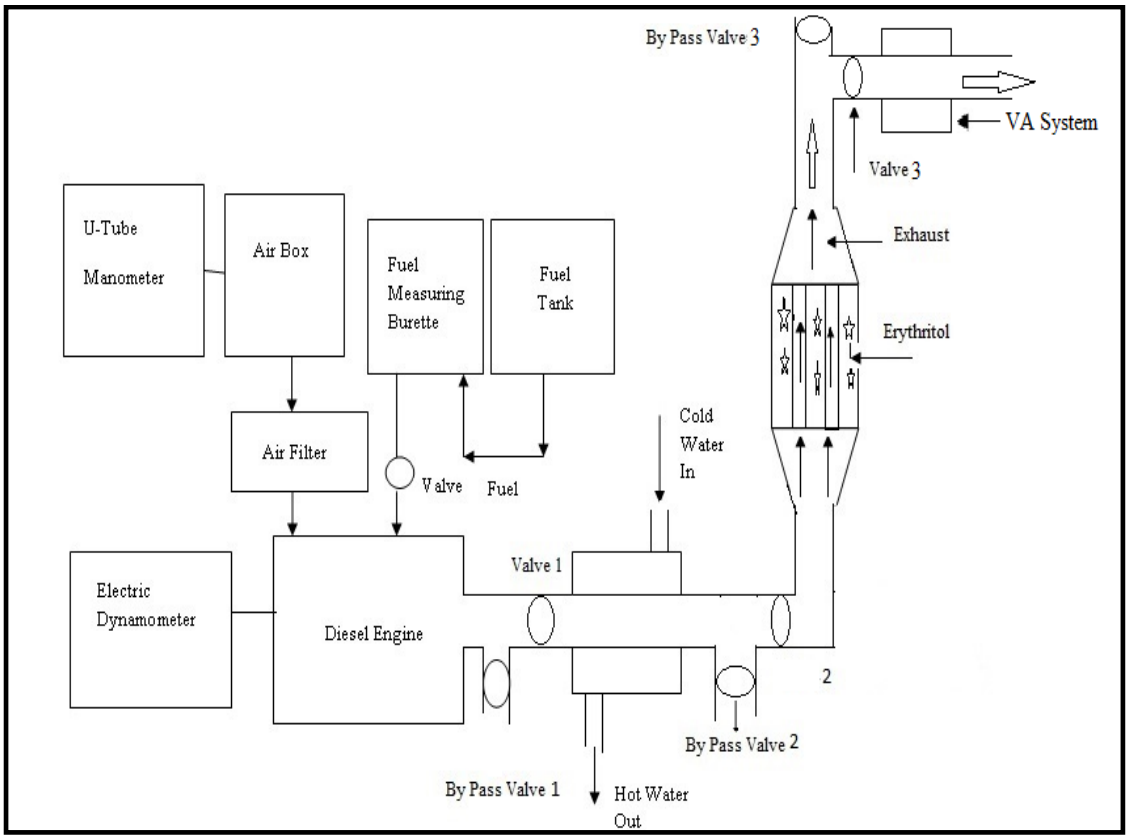

Fig. 3.14 Schematic diagram of experimental setup for feasible combination

Table 3.8 Position of valves for various steps

Test Mode	Bypass Valve 1	Bypass Valve 2	Bypass Valve 3	Valve 1	Valve 2	Valve 3
Single Generation (2nd step)	Open	Closed	Closed	Closed	Closed	Closed
Cogeneration (CHP) (4th step)	Closed	Open	Closed	Open	Closed	Closed
Cogeneration with thermal energy storage (CHP with TES) (5th step)	Closed	Closed	Open	Open	Open	Closed
Trigeneration with thermal energy storage CCHP with TES (6th step)	Closed	Closed	Closed	Open	Open	Open

In the second step, a series of tests were carried out to evaluate the engine generator performance when it was to be run on a single generation system (base case). In the third step, a series of tests were conducted to evaluate the performance of single generation with TES mode. In the fourth step, a series of tests were conducted to evaluate the performance of cogeneration (CHP) mode. In the fifth step, a series of tests were conducted to evaluate the performance of cogeneration (CHP) with TES mode. In sixth and the last step, a series of tests were conducted to evaluate the performance of trigeneration (CCHP) with TES mode. Valve positions for various steps are shown in Table 3.8 and valve locations are shown in Fig. 3.14.

3.6.1 Performance of engine generator working on single generation system

A number of tests were performed on single generation system to determine the engine generator performance and emissions. While varying the engine load between idle to full load, various parameters were recorded e.g. power output, fuel consumption, exhaust temperature and emissions (CO, CO_2, NO_x, HC and smoke). As per the schematic diagram of the whole set up as shown in Fig. 3.14, only bypass valve 1 was opened and rest of the valves were kept closed for single generation

system. Exhaust gases coming from engine were passed to atmosphere through bypass valve 1.

3.6.2 Performance of single generation with thermal energy storage

A number of tests were performed to determine the performance and emissions for single generation with TES. Experimental setup for the same is shown in Fig. 3.15. Experiment was carried out in two stages. First stage was charging of TESS and the second stage was discharging of TESS. In the first part of first stage, the inlet valve to the TESS was closed and bypass valve was opened i.e. TESS was not integrated with the engine. At this stage, various parameters of the engine viz., brake thermal efficiency (BTE) and brake specific fuel consumption (BSFC) and emissions (CO, CO_2, NOx, HC and smoke) were recorded and evaluated.

In the second part of first stage, initially the inlet valve to the TESS was closed to obtain the steady state, and on the accomplishment of the same, inlet valve to the TESS was opened and the bypass valve was closed. Hence, the exhaust was passed through the TESS and various parameters (BTE, BSFC and temperatures at various places in TESS) and emissions (CO, CO_2, NOx, HC and smoke) were observed / calculated.

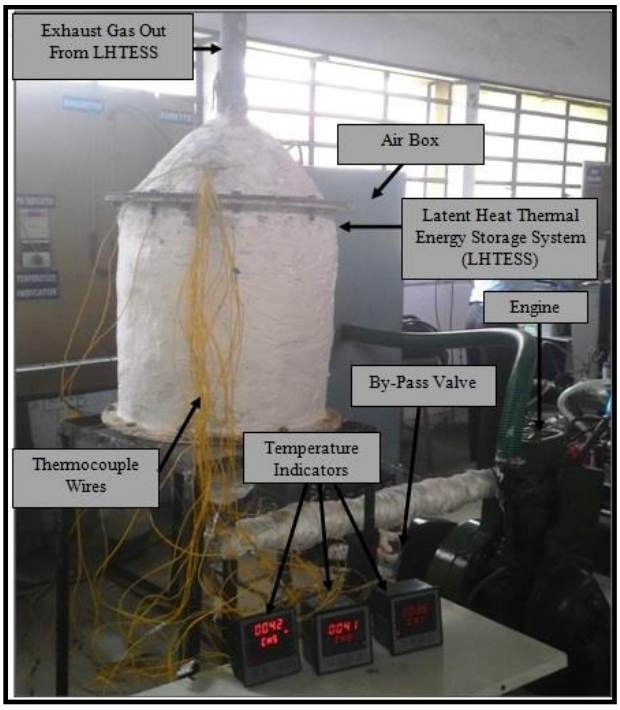

Fig. 3.15 Experimental setup for single generation with TES

In the second stage (discharging), the engine was kept off and an air blower was used to blow air from the bottom of the TESS and hot air was obtained at the top of latent heat thermal energy storage system (LHTESS or TESS). This discharging process is shown in Fig. 3.16.

Fig. 3.16 Discharging of TESS

3.6.3 Performance of cogeneration (CHP) system

In the cogeneration (CHP) mode, exhaust gases from engine were passed through valve 1 to a double pipe heat exchanger and bypass valve 2 was open as shown in schematic diagram of the whole setup in Fig. 3.14. Rests of the valves (bypass valve 1, 3 and valve 2, 3) were kept closed. While varying the engine load between idle to full load, various parameters were recorded e.g. power output, fuel consumption, temperatures of cooling water at entry and exit points of both, engine and heat exchanger, water flow rate and emissions (CO, CO_2, NO_x, HC and smoke).

3.6.4 Performance of cogeneration (CHP) with thermal energy storage system

In the cogeneration (CHP) with TES mode, exhaust gases from engine were passed through valve 1 and valve 2 to a double pipe heat exchanger, TESS and to atmosphere through bypass valve 3 as shown in schematic diagram of the whole setup in Fig. 3.14.

Rests of the valves (bypass valve 1, 2 and valve 3) were kept closed. While varying the engine load between idle to full load, various parameters were recorded e.g. power output, fuel consumption, temperatures of cooling water at entry and exit points of both, engine and heat exchanger, water flow rate, temperatures at inlet and outlet of TESS, and emissions (CO, CO_2, NO_x, HC and smoke).

3.6.5 Performance of trigeneration (CCHP) with thermal energy storage system

Experiments for performance of CCHP with TES were carried out in two stages. First stage belonged to charging of TESS and second stage belonged to discharging of TESS. In the first part of first stage, the inlet valves to the double pipe heat exchanger, TESS, VA system (valves 1, 2 and 3 and bypass valves 2 and 3 as shown in schematic diagram of the whole setup in Fig. 3.14) were kept closed and bypass valve 1 was opened (stage similar to that explained in section 3.6.1).

In the second part of first stage, initially the inlet valves to the double pipe heat exchanger, TESS, VA system (i.e. valves 1, 2 and 3 and bypass valves 2 and 3 as shown in schematic diagram of the whole setup in Fig. 3.14) were kept closed and bypass valve 1 was kept open until steady state was obtained, and on the accomplishment of the steady state, bypass valves 1, 2 and 3 were kept closed and inlet valves (valves 1, 2 and 3) to the heat exchanger, TESS and VA system were opened. At this condition, the exhaust was allowed to pass through the heat exchanger, TESS and VA system. Various parameters were recorded e.g. power output, fuel consumption, temperatures of cooling water at entry and exit points of both, engine and heat exchanger, water flow rate, temperatures at inlet and outlet of TESS and VA system and emissions (CO, CO_2, NO_x, HC and smoke).

In second stage, the engine was off. An air blower blew the air from the bottom of the TESS (through bypass valve 2) and hot air was used (through valve 3) to actuate the VA system. In this recovery process, only bypass valve 2 and valve 2 and 3 were kept open and rest of the valves were kept closed. The recovery was done until the temperature of VA refrigerator cabin became constant while supplying hot air with the blower. Flow chart of various stages is shown in Fig. 3.17, 3.18 and 3.19.

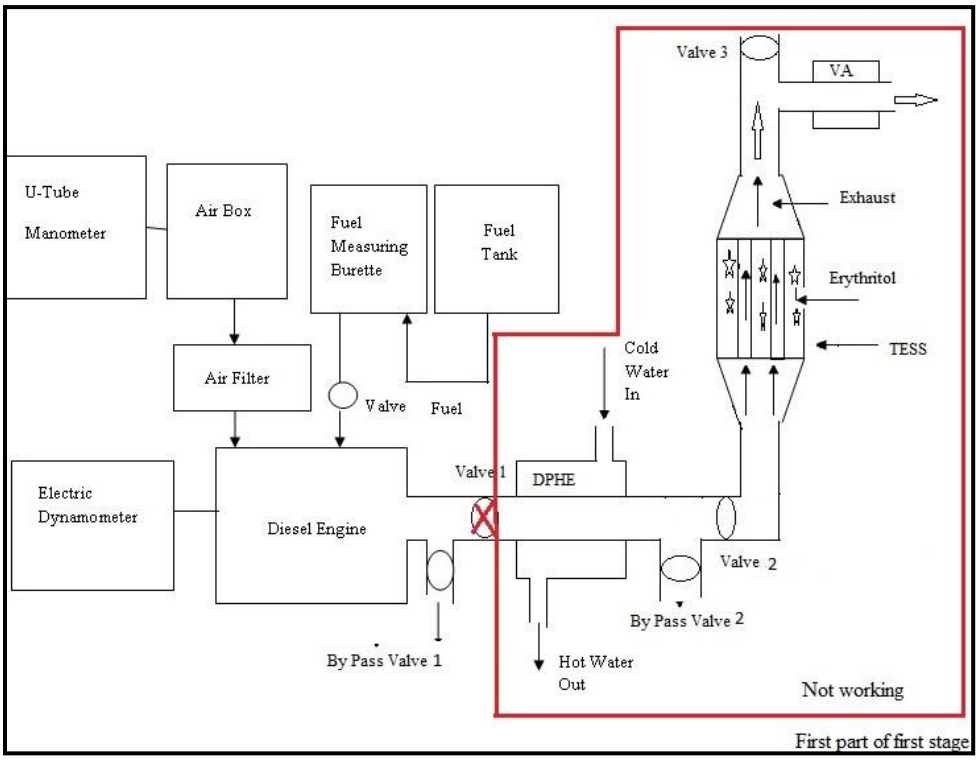

Fig. 3.17 Flow chart for 1st part of 1st stage

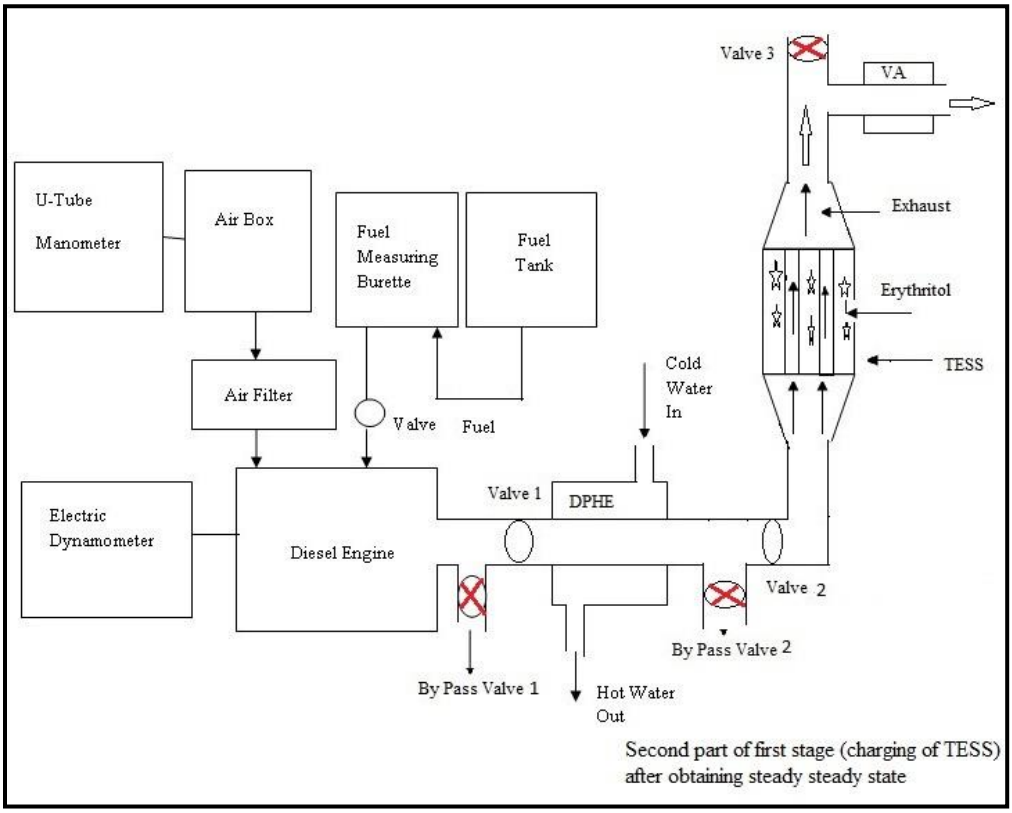

Fig. 3.18 Flow chart for 2nd part of 1st stage

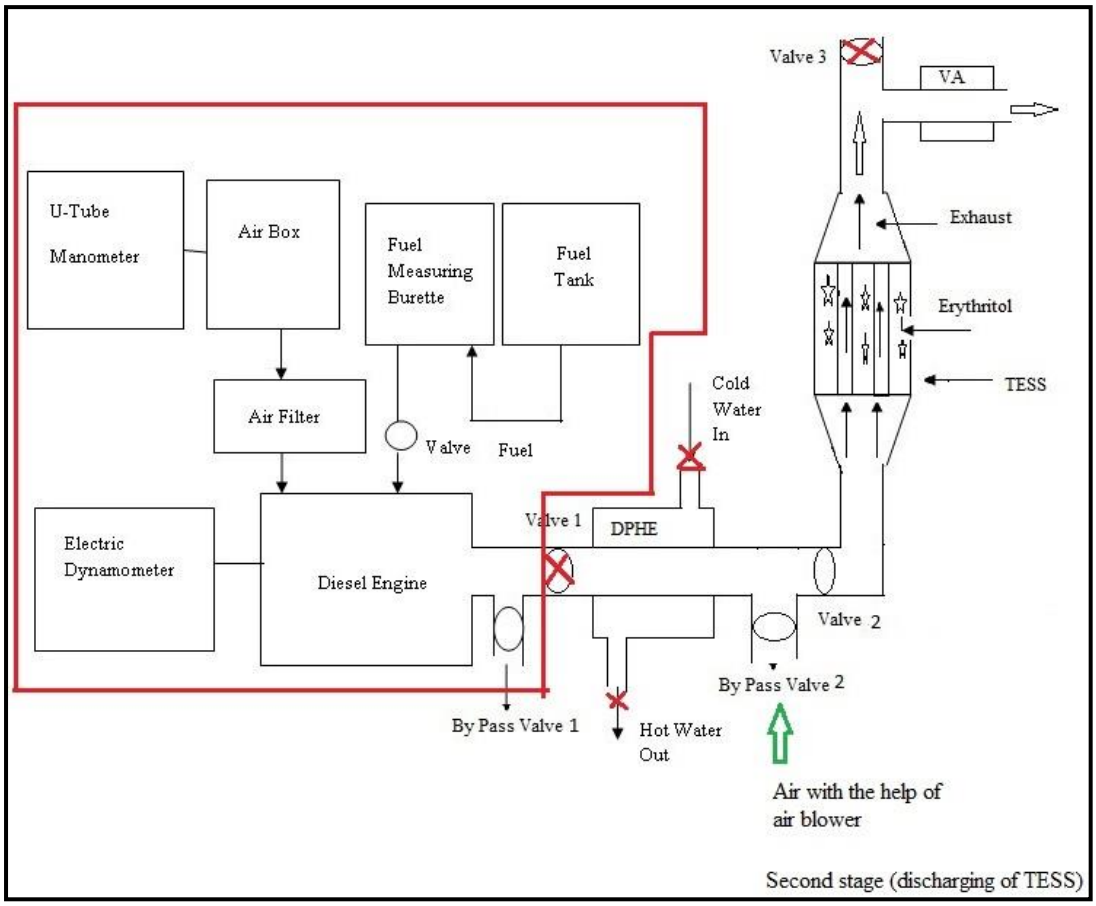

Fig. 3.19 Flow chart for 2nd stage

To estimate the performance of thermal energy storage integrated micro-trigeneration system, the engine was operated at different loads. At the steady state stage, a record of different data was generated by taking the readings of engine generator power output, fuel consumption and different temperatures. Temperatures at inlet and outlet of TESS, heat exchanger, VA system generator, engine exhaust, and temperature of erythritol powder at different places were taken at every 10 minutes' interval, until the steady state in temperature of refrigerant at inlet to evaporator of VA system was achieved and maintained for half an hour. For the performance evaluation of VA, various parameters were recorded and evaluated.

For calculation of heat input to the generator of VA system, exhaust gas temperature at inlet and outlet to the generator of VA system was recorded. The refrigeration effect was calculated by placing a known quantity of water (2 kg) inside the cabin of VA refrigeration system in a vessel and noting down the initial temperature. By continuously supplying the heat to the generator of VA, the temperature of refrigerant at inlet to evaporator of VA system started decreasing and reached a minimum value

of -4.2 ^{0}C. By supplying more heat there was no change in this temperature and hence, it was assumed that steady state in refrigerant temperature was obtained.

At this steady state (with refrigerant temperature of -4.2 ^{0}C) heat was supplied for 30 minutes. Due to this, heat from water was extracted by cold refrigerant and temperature of water decreased. Final temperature of water (in the vessel) after 30 minutes was recorded and used for calculating the refrigeration effect. Time for above change in temperature of water from initial temperature was recorded and refrigeration effect was calculated. The engine was stopped when the steady state in temperature of refrigerant inlet to evaporator of VA system was achieved and maintained for half an hour. After stopping the engine discharging of TESS was done. The process was repeated at different loads.

3.7 Thermodynamic energy analysis

The following performance parameters were calculated for the system based on the energy principle:

Brake specific fuel consumption (BSFC): Brake specific fuel consumption is an important parameter that shows how efficiently an engine is converting fuel into work. BSFC is defined as the ratio of fuel consumed in kg/h to the brake power and the expression of BSFC is given as:

$$\text{BSFC} = \frac{\text{fuel consumed in kg/h}}{Brake\ power\ in\ kW} \quad \text{kg/kWh}$$

Thermal energy content in fuel input is given by:

$$Q_{fi} = \dot{m}_f * LCV \qquad kW \tag{1}$$

Thermal energy carried by the exhaust gases is given by:

$$Q_{exhaust} = \dot{m}_{ex} C_{p_{ex}} \{T_{eng.ex.gas} - T_{ambient}\}\ kW \tag{2}$$

Thermal energy recovered by double pipe heat exchanger (heating) is given by:

$$Q_{DPHE} = \dot{m}_w C_{p_w} \{T_{wo} - T_{wi}\} \qquad kW \tag{3}$$

Thermal energy stored in thermal energy storage system is given by:

$$Q_{TES} = m_{pcm}[C_{p\ pcm}\{T_{f\ pcm} - T_{i\ pcm}\} + Latent\ heat\ of\ PCM + C_{p\ liq\ pcm}\{T_{fliq\ pcm} - T_{i\ liq\ pcm}\}]/time\ \ kW \tag{4}$$

Thermal energy recovered in VA system is given by:

$$Q_{VA} = m_w C_{p_w} \{T_{wvai} - T_{wvao}\}\ /time\ \ kW \tag{5}$$

Total useful energy for combined heating, cooling and power with storage is given by:

$$Q_{thcps} = Electric\ output + Q_{DPHE} + Q_{TES} + Q_{VA} \quad kW \tag{6}$$

Brake thermal efficiency (BTE): Brake thermal efficiency is one of the important parameters of engine performance because it gives a measure of net power developed by the engine, which is available for use at the engine output shaft, with respect to the heat supplied in the form of fuel. Thermal energy efficiency (%) for the diesel engine is given by:

$$\eta_p = \frac{Electricoutput}{Q_{fi}} * 100 \tag{7}$$

Thermal energy efficiency (%) for combined heating, cooling and power with storage is given by:

$$\eta_{\mathrm{Chcps}} = \frac{\mathrm{Q_{thcps}}}{\mathrm{Q_{fi}}} * 100 \tag{8}$$

Percentage energy saved is calculated using:

$$\mathrm{Q_{Saved}} = \frac{\mathrm{Q_{DPHE}} + \mathrm{Q_{TES}} + Q_{VA}}{\mathrm{Q_{fi}}} * 100 \tag{9}$$

3.8 Thermodynamic exergy analysis:

The following equations (eq. 10-21) were used to determine the performance parameters of thermal energy storage integrated cogeneration system based on exergy principle:

The input exergy to the diesel engine is given by:

$$e_f = 1.04 Q_{fi} \quad kW \tag{10}$$

Exergy recovered in double pipe heat exchanger (heating) is calculated using:

$$e_{DPHE} = \dot{m}_w C_{p_{ex}} [\{T_{wo} - T_{wi}\} - \mathrm{T_o} \ln(\frac{T_{wo}}{T_{wi}})] \tag{11}$$

Exergy present in thermal energy storage is given by:

$$e_{TES} = \frac{m_{pcm} C_{p\,pcm}}{time} \left[\{T_{f\,pcm} - T_{i\,pcm}\} - T_o\, ln(\frac{T_{f\,pcm}}{T_{i\,pcm}})\right] + \frac{m_{pcm} * Latent\ he\ PCM}{time} \left[1 - \frac{T_o}{T_{melt}}\right] \quad kW \tag{12}$$

Exergy recovered in VA system is given by:

$$e_{REF} = \frac{m_w}{Time} C_{p_w} [\{T_{wvai} - T_{wvao}\} - \mathrm{T_o} \ln(\frac{T_{wvao}}{T_{wvai}})] \tag{13}$$

Total exergy for combined heating and power is calculated using:

$$e_{thp} = \text{Electric output} + e_{DPHE} \quad (14)$$

Total exergy for combined heating, power with thermal storage is given by:

$$e_{thps} = \text{Electric output} + e_{DPHE} + e_{TES} \quad (15)$$

Total exergy for combined cooling, heating, power with thermal storage is given by:

$$e_{tcchp} = \text{Electric output} + e_{DPHE} + e_{TES} + e_{REF} \quad (16)$$

Exergy efficiency (%) of diesel engine is given by:

$$\eta_{exergy,p} = \frac{\text{Electricoutput}}{e_f} * 100 \quad (17)$$

Exergy efficiency (%) for combined power and heating is calculated using:

$$\eta_{exergy\ Chp} = \frac{e_{thp}}{e_f} * 100 \quad (18)$$

Exergy efficiency (%) for combined power, heating with thermal storage is calculated using:

$$\eta_{exergy\ Chps} = \frac{e_{thps}}{e_f} * 100 \quad (19)$$

Exergy efficiency (%) for combined power, cooling and heating with thermal storage is given by:

$$\eta_{exergy\ Chps} = \frac{e_{tcchp}}{e_f} * 100 \quad (20)$$

Exergy saved is thus calculated as:

$$e_{saved} = \frac{e_{DPHE} + e_{TES} + e_{REF}}{e_f} \quad (21)$$

CHAPTER 4
RESULT AND DISCUSSIONS

In this chapter, various engine performance parameters like BTE and BSFC were evaluated for single generation, single generation with TES, cogeneration (CHP), cogeneration with TES and trigeneration (CCHP) with TES modes at different load conditions i.e. zero load to full load. Performance parameters like effectiveness for heat exchanger; charging efficiency, energy storage and recovery efficiency for TESS; and COP for vapour absorption system were evaluated. Comparative analyses of engine emissions (CO, HC, NOx, CO_2 and smoke) for different modes were done. Three sets of readings were taken for all cases and following sections show the test results of average values of the three tests for each parameter. Error analysis is discussed in Appendix A.2.

4.1 Performance parameters for single generation with thermal energy storage (TES) system

In this section, performance parameters like engine performance, time vs. temperature plot for TESS, charging efficiency, recovery efficiency, and percentage energy saved, etc. are reported and discussed.

4.1.1 Engine performance parameters

Engine performance parameters like brake thermal efficiency (BTE) and brake specific fuel consumption (BSFC) were considered. Brake Thermal Efficiency (BTE) is one of the important parameters of engine performance because it gives a measure of net power developed by the engine, which is available for use at the engine output shaft, with respect to heat supplied in the form of fuel. Specific fuel consumption is also an important parameter that shows how efficiently an engine is converting fuel into work. Variation in BTE and BSFC, plotted against load for conditions when engine was operated only for single generation; and when engine was operated only for single generation integrated with TESS; are shown in Fig. 4.1 and 4.2 respectively.

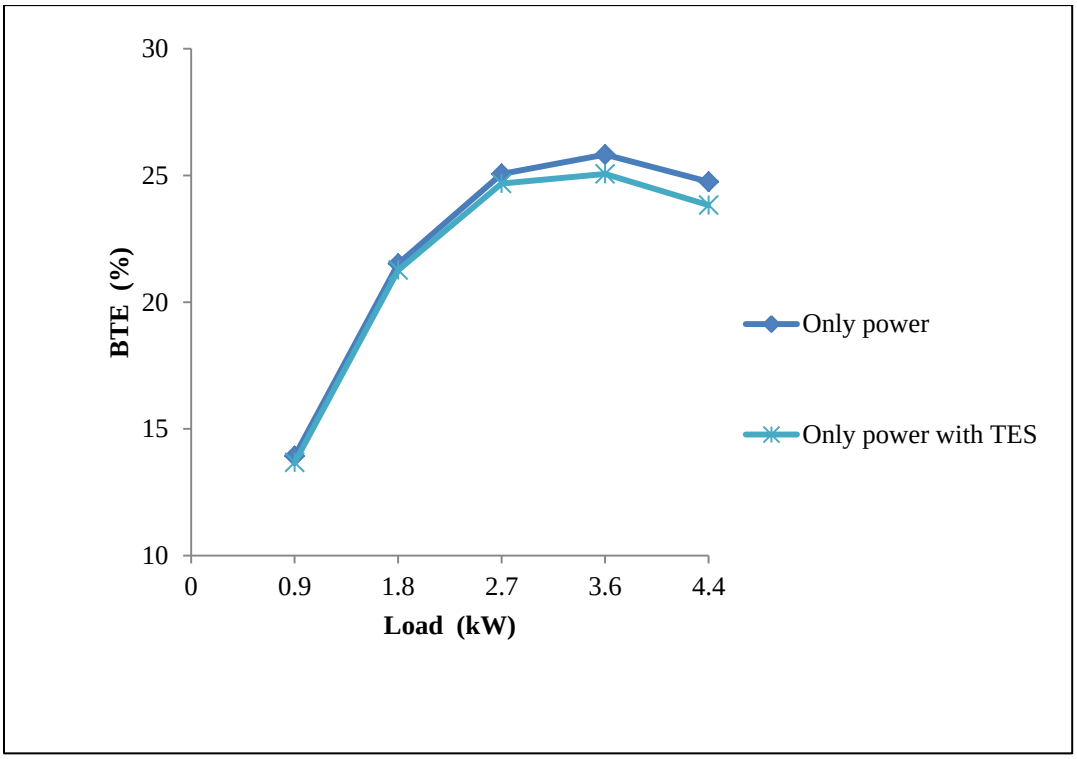

Fig. 4.1 Variation in BTE against loads with and without TESS

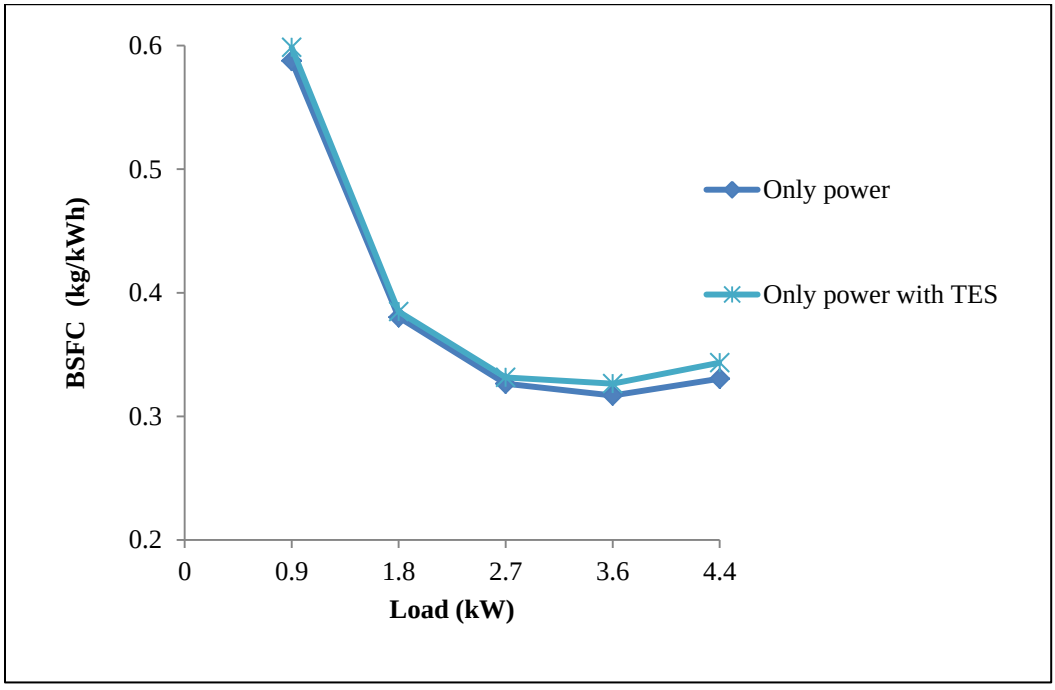

Fig. 4.2 Variation in BSFC against loads with and without TESS

It has been observed from these plots that the BTE was slightly low and BSFC was slightly high when engine was integrated with TESS. Variation in BTE is in the range of 1.2 to 3.8 % and variation in BSFC is in the range of 1.2 to 3.9 %.

4.1.2 Variation in temperature with respect to time at various places in TESS during charging

Performance of TESS was concerned with heat transfer from flowing exhaust gas to energy storage medium (erythritol) and vice versa. Hot exhaust gas flows from bottom to top of the shell and tube type heat exchanger (TESS) and heat transfer takes place from exhaust gas to erythritol during charging process.

Fig. 4.3 and 4.4 show the rise in temperature of erythritol (phase change material, to reach the melting point temperature from atmospheric temperature, approx. 30 ^{0}C) at various places in TESS with respect to time and variation in temperature with time at different positions on a fixed plane at a load of 4.4 kW during charging of TESS respectively.

At 117.7 ^{0}C (Approximately 118 ^{0}C), erythritol started melting and since then, the temperature of erythritol, as obtained from all the 21 thermocouples remained unchanged (at 118 ^{0}C) until the entire amount of erythritol melted. The duration of this temperature stability was different at different loads due to the difference in heat carried by exhaust at different loads. The stability in temperature was due to the latent heat absorption by erythritol during the phase change. As soon as the entire erythritol was melted, there was further increase in temperature again due to specific heat absorption by liquid erythritol. Hence, when the temperature started rising again after stabilizing at melting point (118 ^{0}C) for quite some time, it was understood that entire erythritol was melted and then the engine was stopped. All the thermocouples showed the same temperature (118 ^{0}C) when the entire erythritol was melted.

It has been observed from Fig. 4.3 that there is approximately constant rise in temperature in TESS. At a load of 4.4 kW, temperatures reached above the melting point temperature (after complete melting of erythritol) in 65 minutes. Similar results were obtained at other loads also except for time. At various loads viz., 1.8 kW, 2.7 kW and 3.6 kW, the time to reach above the melting point was 155 minutes, 135 minutes and 100 minutes respectively. Due to higher exhaust gas temperature at higher loads the time taken to reach the melting point was lesser.

From Fig. 4.4 it can be seen that rise in temperature of erythritol at center position was higher as compared to outer (peripheral) position. This was due to the fact that exhaust

was passing through a diverging section and hence, most of the effect of exhaust was at center tubes.

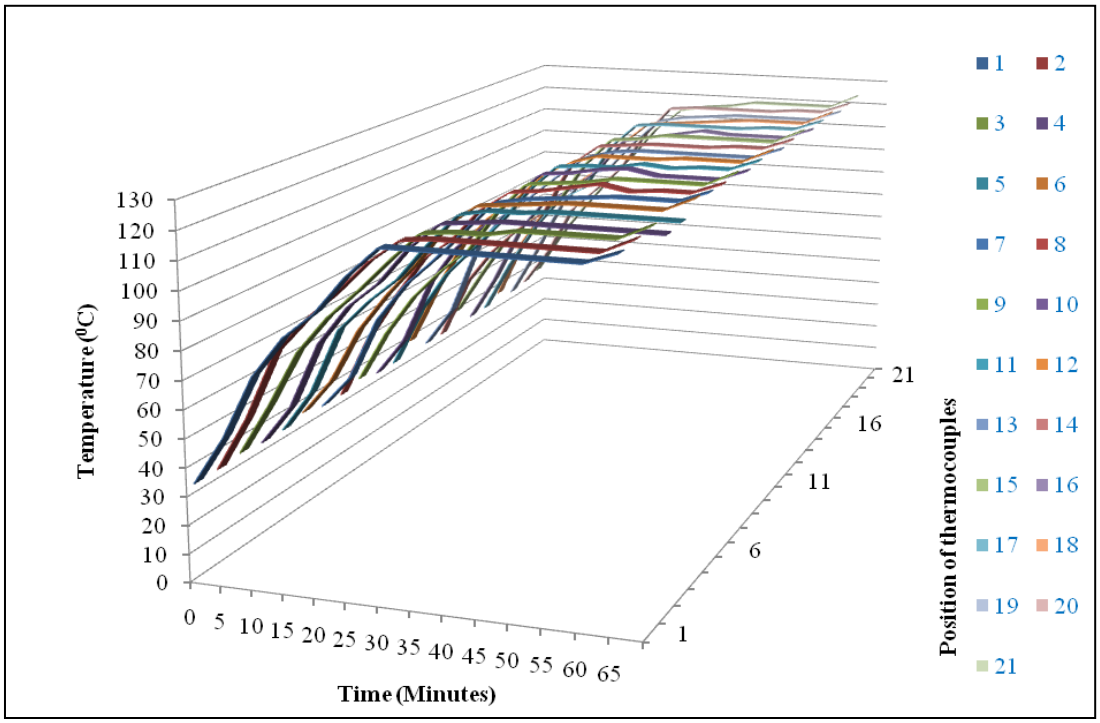

Fig. 4.3 Variation in temperature with time at various places in TESS during charging at a load of 4.4 kW.

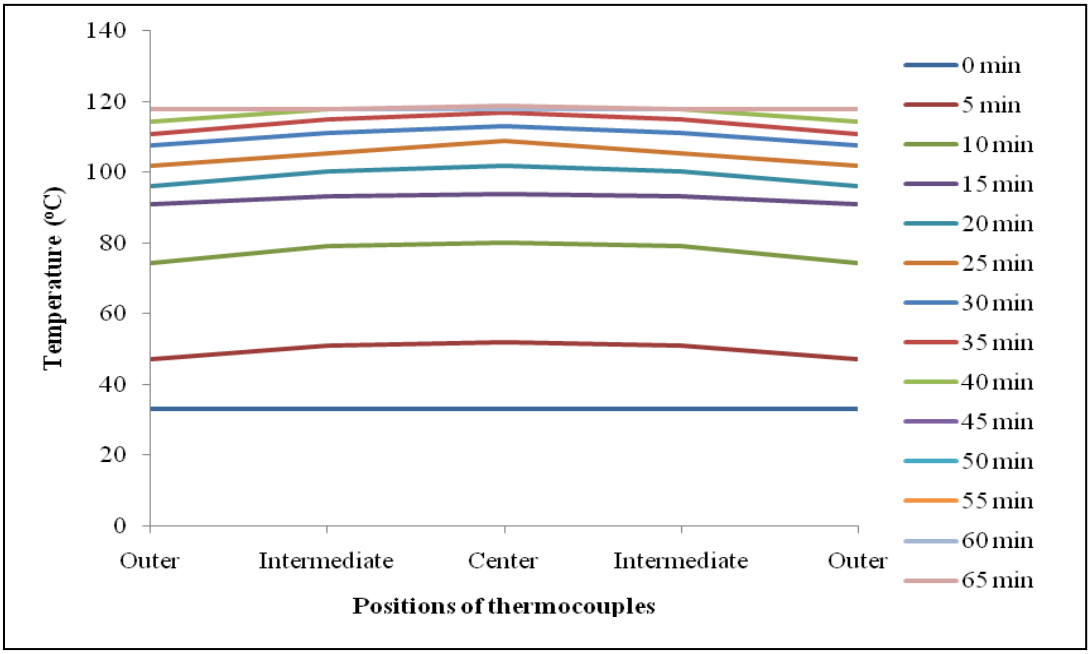

Fig. 4.4 Variation in temperature with time at different positions on a fixed plane at a load of 4.4 kW during charging of TESS

4.1.3 Time - Temperature relationship at various loads during charging of TESS

The rise in temperature of PCM erythritol (to reach above the melting point temperature, from atmospheric temperature) with respect to time at various loads is shown in Fig. 4.5. From these plots it was seen that the slope of rise in temperature was less at lower loads and it increased as the load increased. This means that heat rate (heat given to erythritol per minute) increased as the load was increased. Since the heat rate increased with load, time required for temperature rise of erythritol decreased with increase in load. This was due to the fact that at higher loads the temperature of exhaust gases was quite high and hence, the temperature difference between erythritol and exhaust gas was more due to which, amount of heat transfer increased and time to heat erythritol decreased. Similarly, at lower loads, temperature of exhaust gases was less compared to temperatures at higher load, hence, temperature difference between erythritol and exhaust gases was less, due to which rate of heat transfer decreased and time to heat erythritol increased.

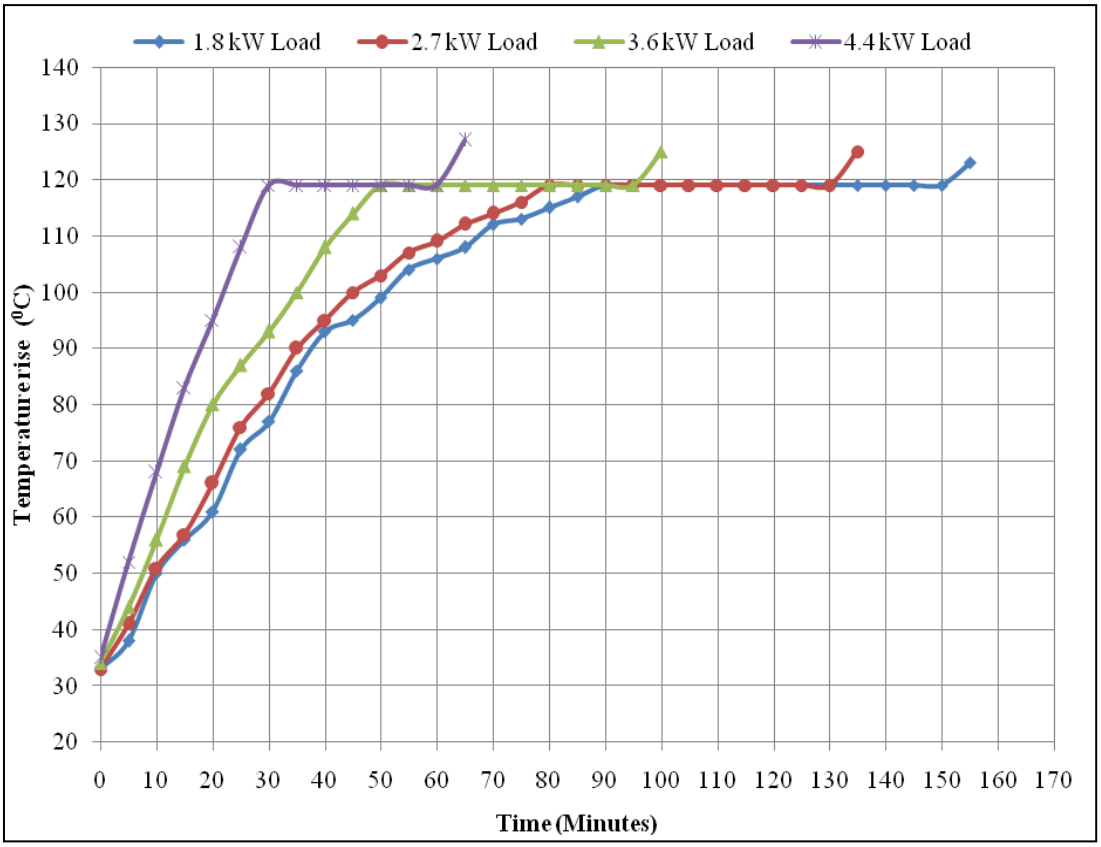

Fig. 4.5 Variation in temperature with respect to time at various loads during charging of TESS

4.1.4 Charging Efficiency

The charging efficiency is defined as the ratio of energy content in the storage tank to the actual energy supplied during the charging process. Fig. 4.6 shows the charging efficiency at different loads.

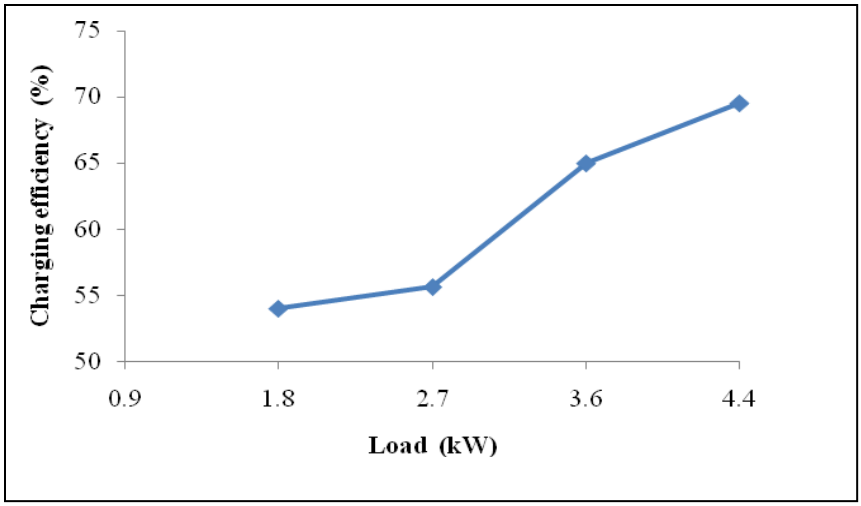

Fig. 4.6 Charging efficiency at different loads

Charging efficiency varied from 53.90 to 69.53 % at different loads. Highest charging efficiency i.e. 69.53% was obtained at peak load of 4.4 kW. This was due to the fact that at higher loads the temperature of exhaust gas was high and hence, engine needed to be run for lesser time for the required heat gain by erythritol. Due to running of engine for lesser time, the heat supplied to the TESS was less and hence, charging efficiency was more at higher loads. The charging efficiency was certainly adversely impacted due to heat losses by convection and radiation despite of all the insulations provided.

4.1.5 Variation in temperature with respect to time at various places in TESS during discharging

During discharging process, air at atmospheric temperature was blown into TESS from bottom with the help of air blower. In this process heat transfer took place from erythritol to air. During this process temperature of air increased and that of erythritol decreased. Fig. 4.7 shows the drop in temperature of erythritol at various places in TESS with respect to time. Fig. 4.8 shows the variation in temperature with time at different positions on a fixed plane during discharging of TESS.

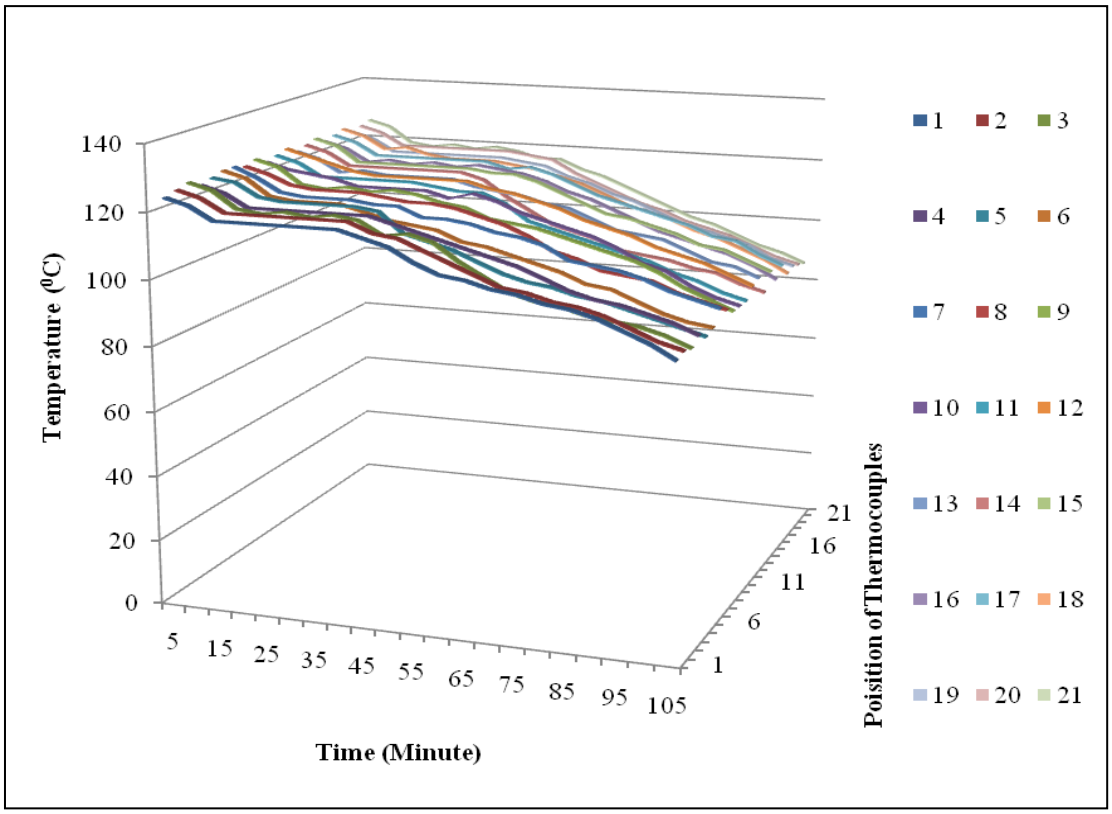

Fig. 4.7 Variation in temperature with respect to time during discharging of TESS

It has been observed from Fig. 4.7 that there was approximately constant decrease in temperature in TESS at various places in TESS.

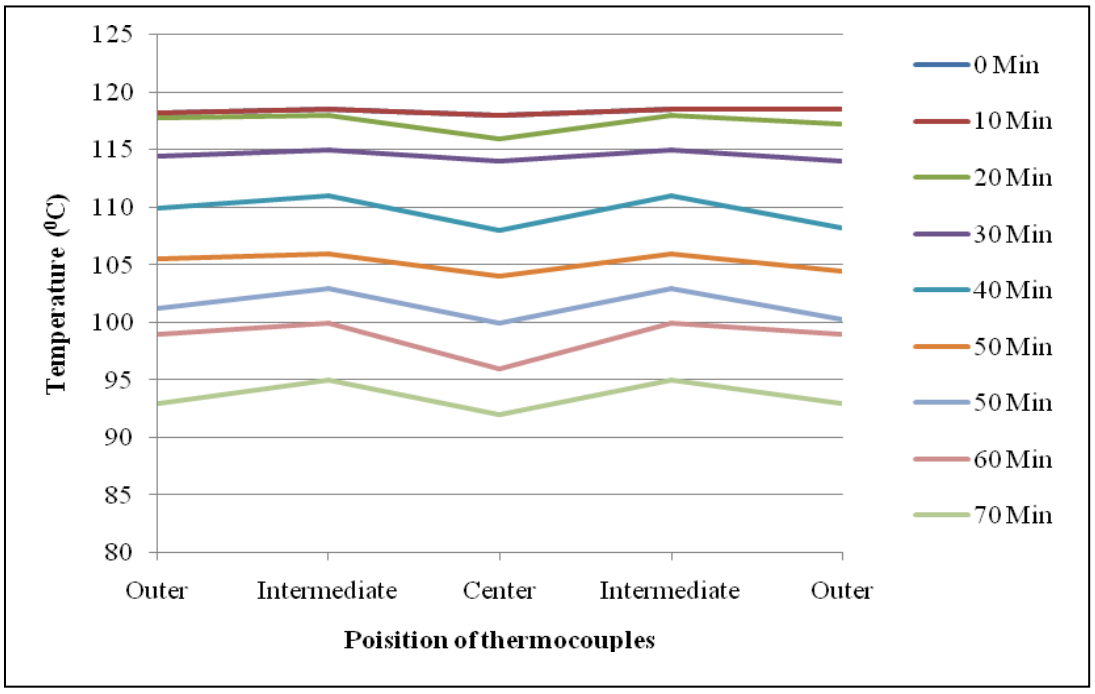

Fig. 4.8 Variation in temperature with time at different positions on a fixed plane during discharging of TESS

From Fig. 4.8 it can be seen that temperature drop during discharging at center position and outer position was more as compare to intermediate position. This might be due to the fact that heat loss to the environment at outer position was more as compared to intermediate position. Again air was passing through the diverging section, hence, most of the effect of air was at center tubes due to which temperature drop at center was more.

4.1.6 Heat recovery efficiency

Heat recovery efficiency is ratio of heat recovered (during discharging) from the TESS to the total heat stored by TESS during charging. Fig. 4.9 shows the amount of heat stored during charging and heat recovered during discharging. It can be seen from the graph that only 38 % of the total heat stored in TESS was recovered during discharging.

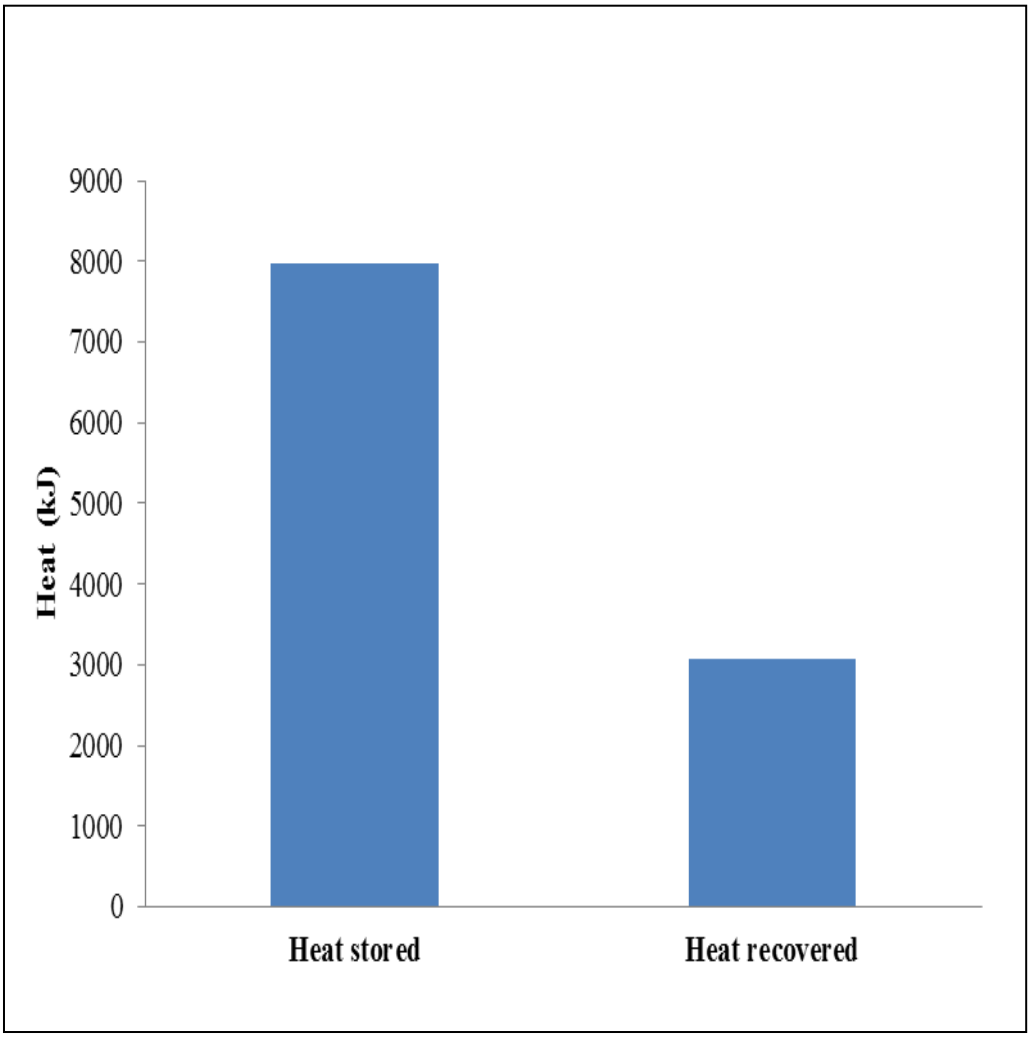

Fig. 4.9 Relation between amount of heat stored and heat recovered

4.1.7 Percentage energy saved

Percentage energy saved is indicative of percentage of fuel needed over and above to produce energy equal to the amount of energy saved by introducing the TESS. The percentage energy saved at different loads is given in Fig. 4.10. It can be noted from the graph that a considerable amount of energy in the fuel can be saved. Maximum energy saved was 11.33 % at the peak load i.e. 4.4 kW.

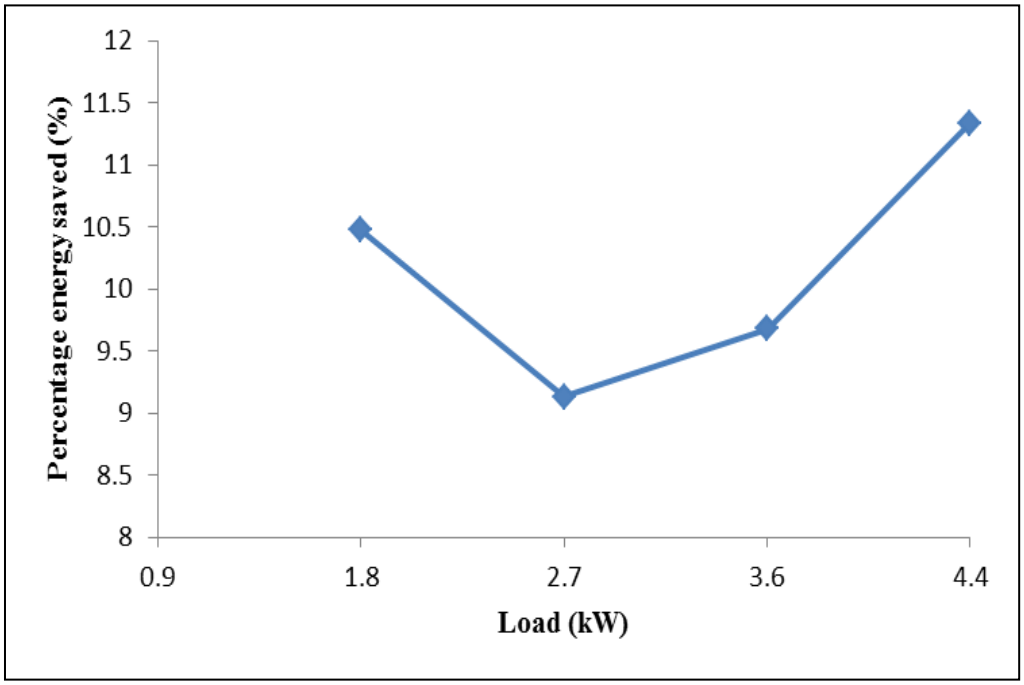

Fig. 4.10 Percentage energy saved at various loads

4.2 Performance parameters for cogeneration (CHP) system

In this section performance parameters related to cogeneration (CHP) system like engine performance parameters, effectiveness of double pipe heat exchanger, useful energy output and percentage energy saved are discussed.

4.2.1 Engine performance parameters

Variations in BTE and BSFC have been plotted against load for single generation (only power) and cogeneration (CHP), and are shown in Fig. 4.11 and 4.12 respectively. In CHP system, engine was integrated with double pipe heat exchanger.

BTE and BSFC for both the cases (for single generation and cogeneration) were found to be nearly the same as shown in Fig. 4.11 and 4.12 respectively which indicates that there was no significant effect of integration of double pipe heat exchanger on the performance of engine.

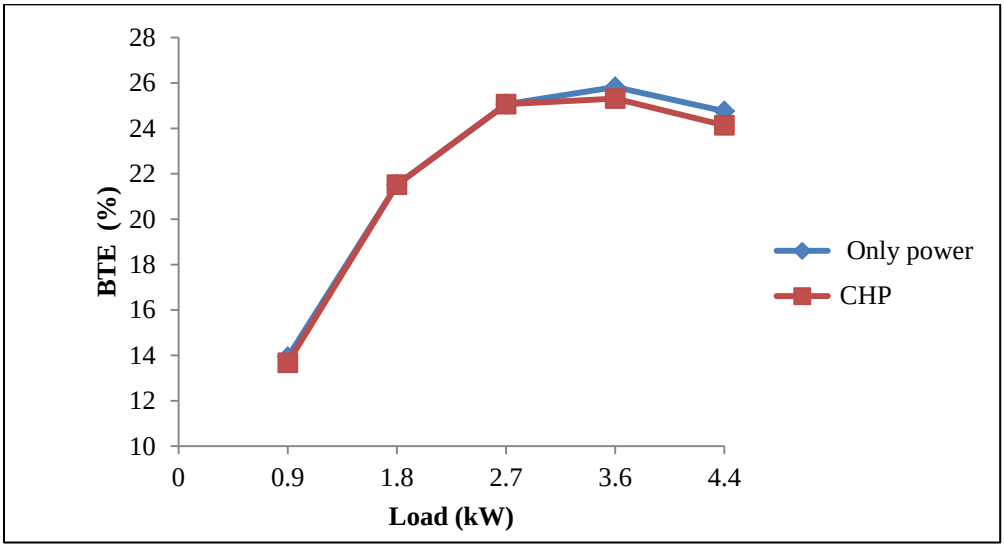

Fig. 4.11 Variation in BTE against load for single generation and cogeneration (CHP)

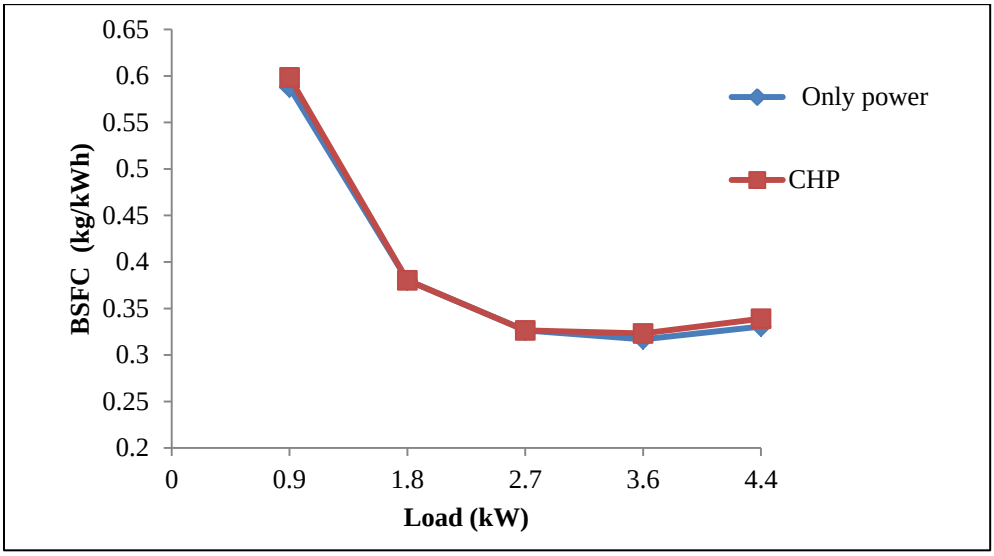

Fig. 4.12 Variation in BSFC against load for single generation and cogeneration

4.2.2 Effectiveness of double pipe heat exchanger

Effectiveness of heat exchanger is defined as the ratio of the actual amount of heat transferred to the maximum possible amount of heat transfer. The effectiveness of double pipe heat exchanger at various loads with different mass flow rates of water is shown in Fig. 4.13.

Effectiveness of heat exchanger at 3.0 liters per minute (LPM) mass flow rate of water was maximum for all load conditions. It can be seen that at a mass flow rate of 1 LPM the effectiveness was minimum and as mass flow rate increased effectiveness

increased. But beyond mass flow rate of 3 LPM the effectiveness of heat exchanger decreased. This might be due to the fact that at higher mass flow rates, the temperature difference between hot fluid inlet to double pipe heat exchanger and hot fluid outlet decreased.

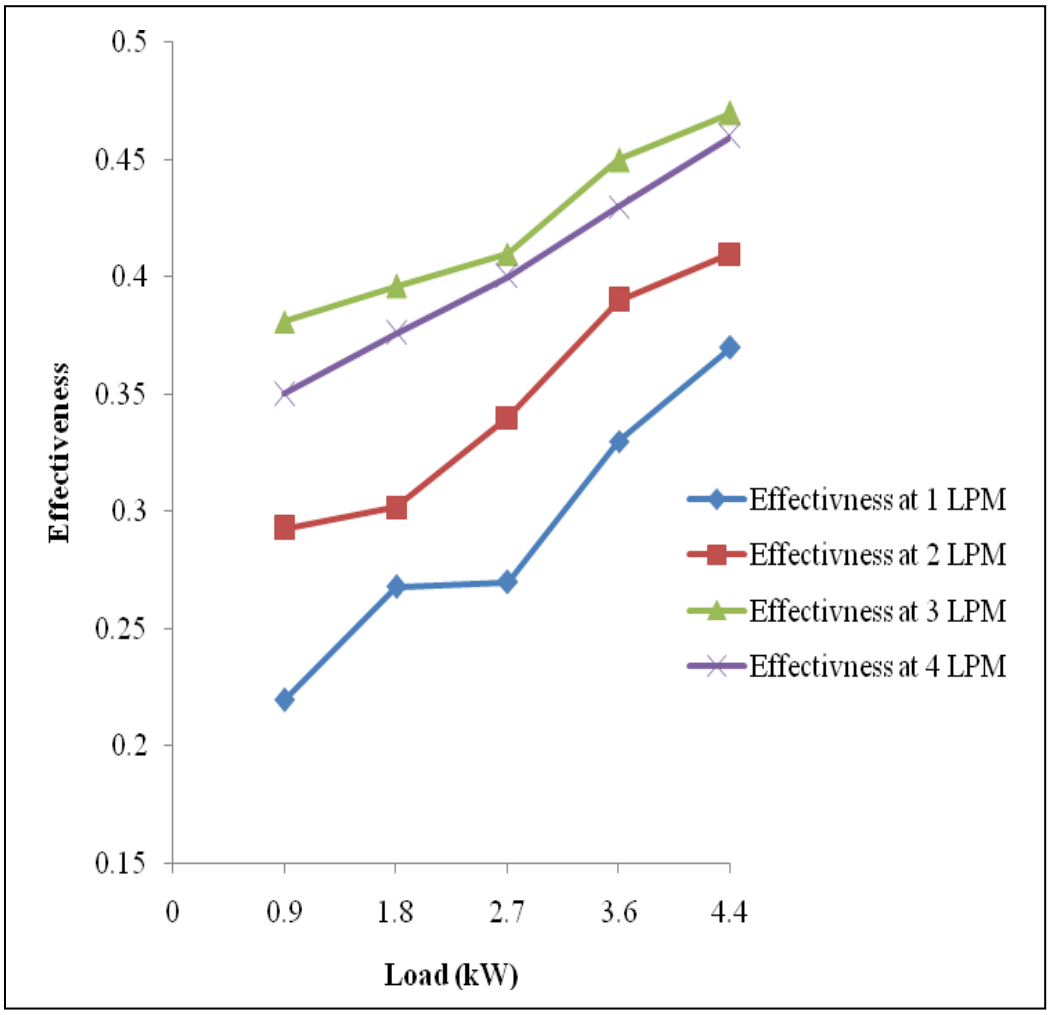

Fig. 4.13 Effectiveness of heat exchanger at various engine loads for various mass flow rates of water

4.2.3 Useful energy output

Total useful energy output of CHP system is calculated as the summation of electrical output and heat recovered by double pipe heat exchanger. Fig. 4.14 shows the useful energy output at various loads for single generation (only power) and cogeneration (CHP) system.

Significant increase in amount of useful energy output was observed when engine was integrated with double pipe heat exchanger. The useful energy output for combined heating and power system varied from 1.36 kW at 0.9 kW engine load to 6.47 kW at 4.4 kW engine load i.e. an increase of approximately 50% compared to that of single generation. This was due to the utilization of engine waste (exhaust) heat for water heating purpose.

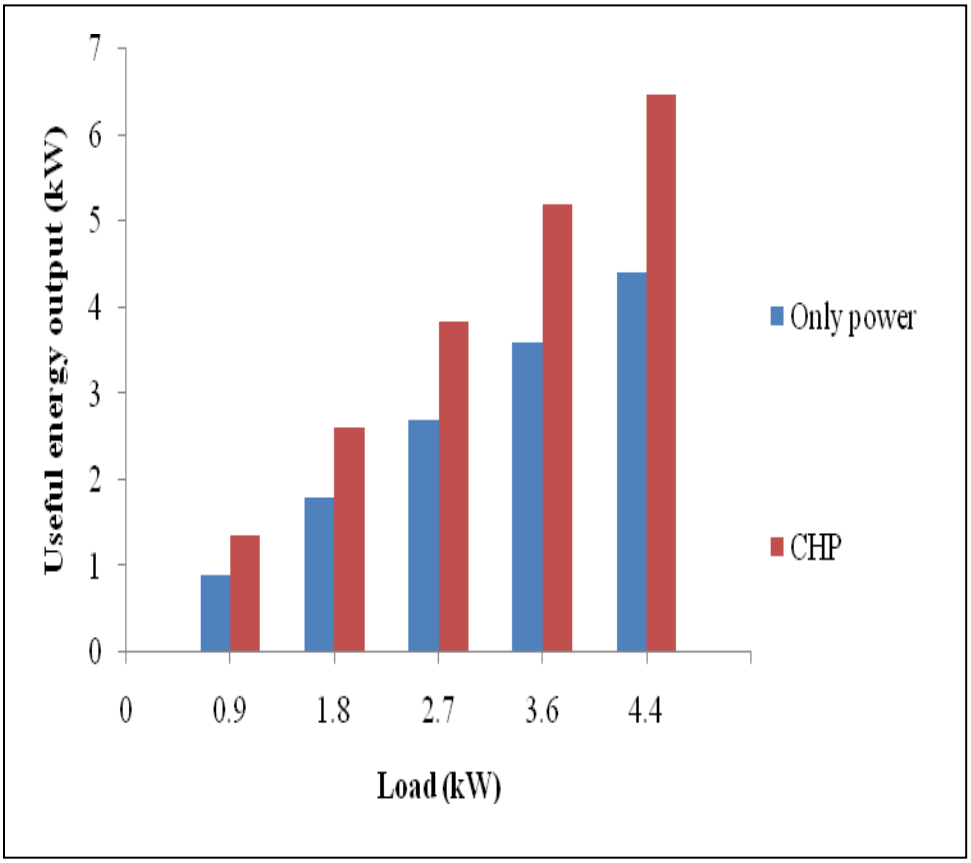

Fig. 4.14 Useful energy output at various engine loads for single generation and CHP modes

4.2.4 Thermal energy efficiency of CHP system

Thermal energy efficiency of CHP system is defined as the ratio of useful energy output in CHP to the thermal energy content in input fuel. Thermal energy efficiency for single generation (only power) and cogeneration at various loads is shown in Fig. 4.15.

With utilization of exhaust heat for heating purpose, thermal efficiency of CHP system increased significantly as compare to single generation system. Maximum

efficiency was obtained at a load of 3.6 kW and value of maximum efficiency in case of CHP was 36.6 %. Increase in the thermal efficiency was in the range of 41 to 48 %.

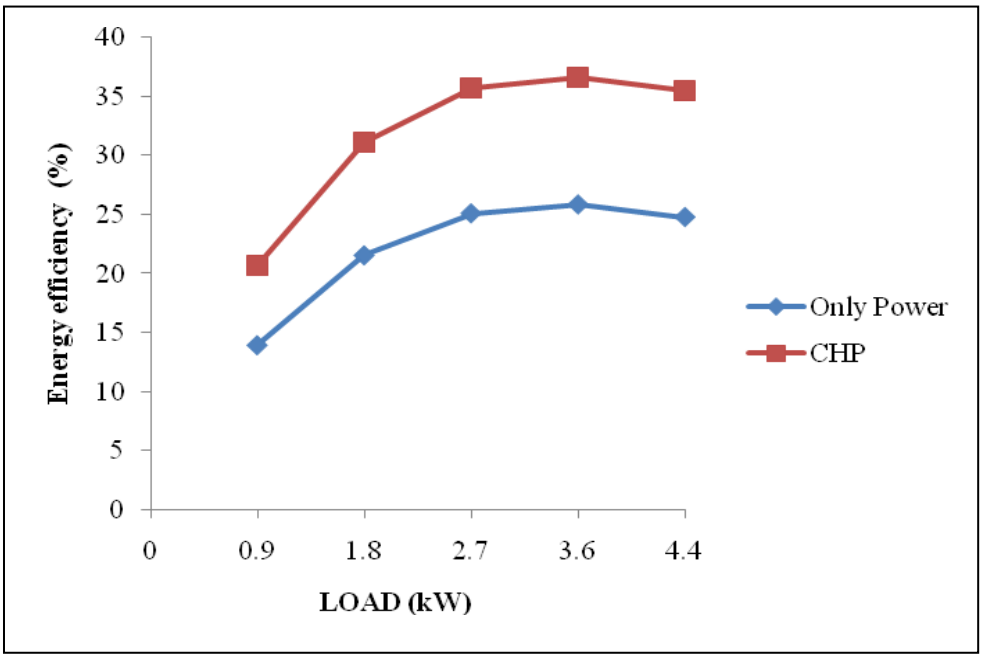

Fig. 4.15 Energy efficiency at various engine loads for single generation and CHP modes

4.2.5 Percentage energy saved in CHP

Percentage energy saved is indicative of percentage of fuel needed over and above to produce energy equal to the amount of energy recovered by introducing the double pipe heat exchanger. The percentage energy saved at different loads in CHP mode is given in Fig. 4.16.

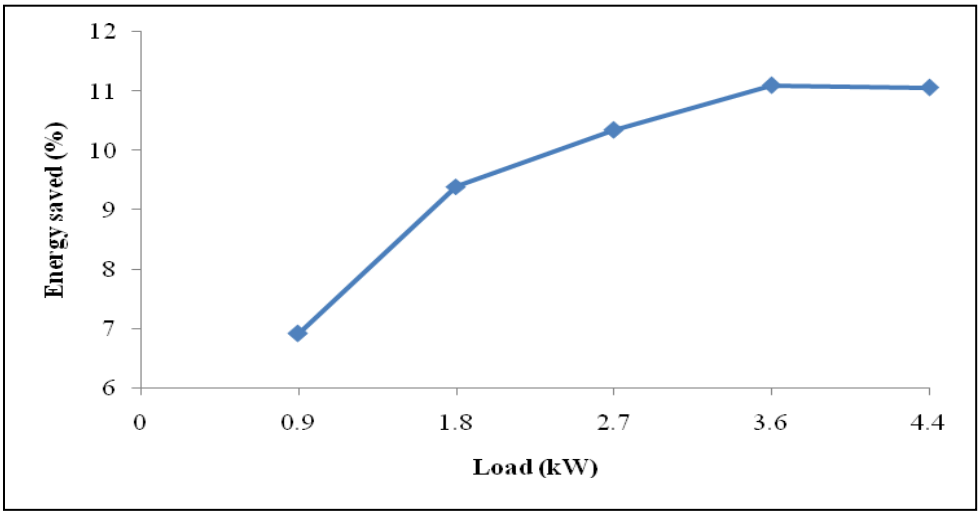

Fig. 4.16 Percentage energy saved at various loads in CHP mode

It can be noted from the graph in Fig. 4.16 that by integrating double pipe heat exchanger or converting single generation into CHP mode considerable amount of energy contained in fuel can be saved. Maximum energy saved was 11.09 % at 80 % of peak load i.e. at 3.6 kW.

4.3 Performance parameters for cogeneration (CHP) with thermal energy storage system

In this section performance parameters related to engine, DPHE and TESS are discussed. Useful energy output based on combined effect of integration of DPHE and TESS to engine is reported in this section.

4.3.1 Engine performance parameters

Variations in BTE and BSFC have been plotted against load for single generation and cogeneration (CHP) with TESS, and are shown in Fig. 4.17 and 4.18 respectively. In CHP with TES, engine was integrated with both double pipe heat exchanger and TESS.

Slight decrease in BTE and slight increase in BSFC was found when engine was integrated with DPHE and TESS as compared to single generation. Variation in BTE was in the range of 2.35 to 5.01 % and variation in BSFC was in the range of 2.4 to 5.2 %.

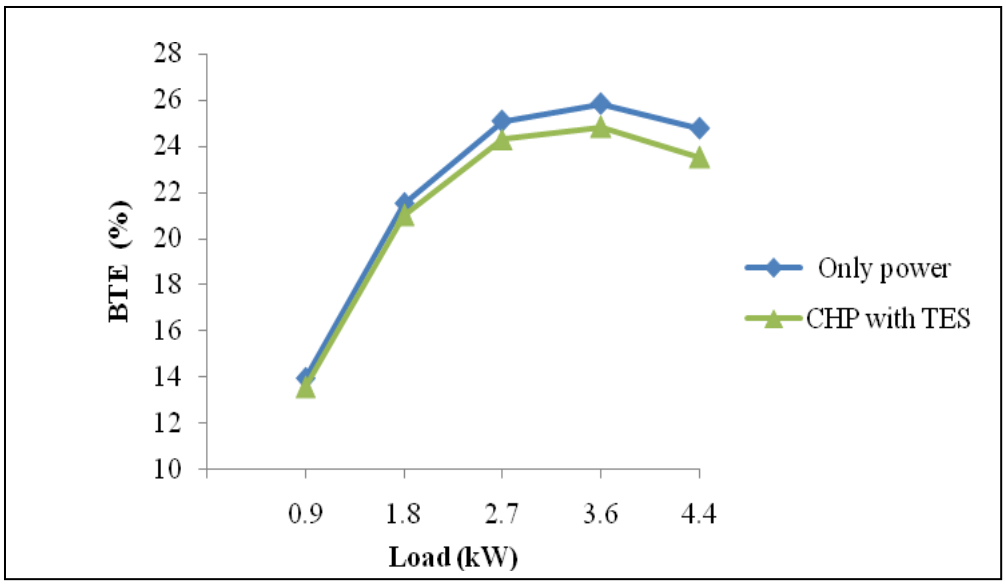

Fig. 4.17 Variation in BTE against load for single generation and cogeneration with TESS

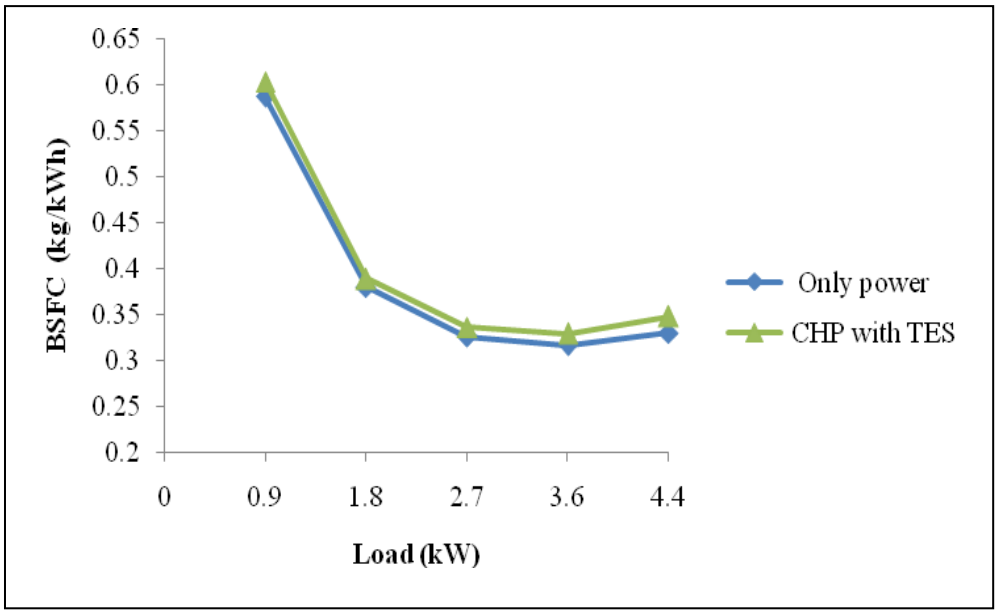

Fig. 4.18 Variation in BSFC against load for single generation and cogeneration with TESS

4.3.2 Useful energy output

Total useful energy output of CHP with TESS is calculated as the sum of electrical output, heat recovered by DPHE and thermal energy stored in TESS. Fig. 4.19 shows the useful energy output at various loads for single generation (only power) and cogeneration (CHP) with TES.

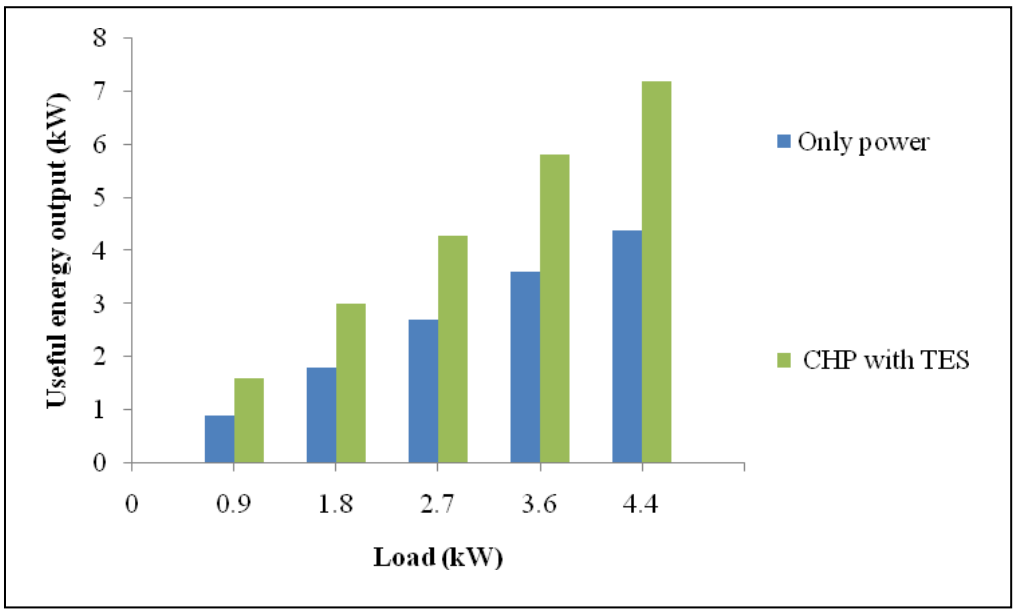

Fig. 4.19 Useful energy output at various engine loads for single generation and CHP with TESS

Significant increase in amount of useful energy output was observed when engine was integrated with double pipe heat exchanger and TESS. The useful energy output for combined heating and power with storage system varied from 1.61 kW at 0.9 kW engine load to 7.20 kW at 4.4 kW engine load i.e. an increase in the range of 63 % to 80 % compared to that of single generation. This increase in useful energy was due to the heat recovered from engine exhaust for water heating purpose in double pipe heat exchanger and storage of thermal energy in TESS.

4.3.3 Thermal energy efficiency of CHP with thermal energy storage system

Thermal energy efficiency of CHP with TES is defined as the ratio of useful energy output in CHP with TES to the thermal energy content in input fuel. Thermal energy efficiency for single generation (only power) and cogeneration with TES at various loads is shown in Fig. 4.20.

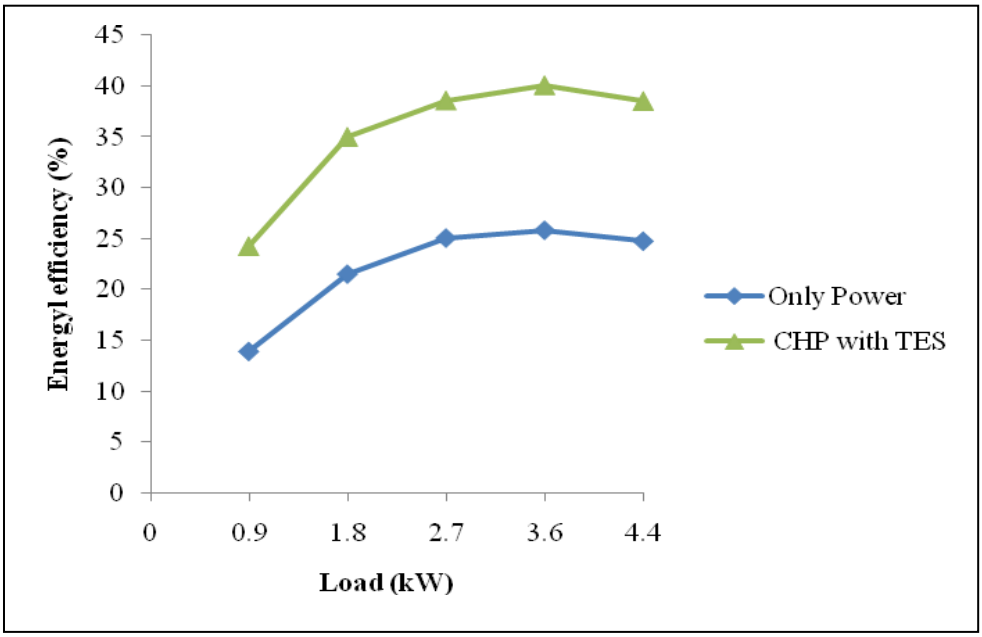

Fig. 4.20 Energy efficiency at various engine loads for single generation and CHP with TESS

With utilization of exhaust heat for water heating purpose and TES, energy efficiency was increased significantly as compare to single generation system. Maximum efficiency was obtained at a load of 3.6 kW and value of maximum efficiency in case of CHP with TES was 40.06 %. Increase in energy efficiency for CHP with TESS was found to be in the range of 53 % to 62 %. The increase in energy efficiency in the case

of CHP with TESS as compared to that in single generation was quite high because exhaust heat was utilized by two systems, viz., double pipe heat exchanger and TESS.

4.3.4 Percentage energy saved in CHP with TESS

Percentage energy saved is indicative of percentage of fuel needed over and above to produce energy equal to the amount of energy saved by introducing the storage system and heat exchanger. The percentage energy saved at different loads in CHP mode with TESS is given in Fig. 4.21.

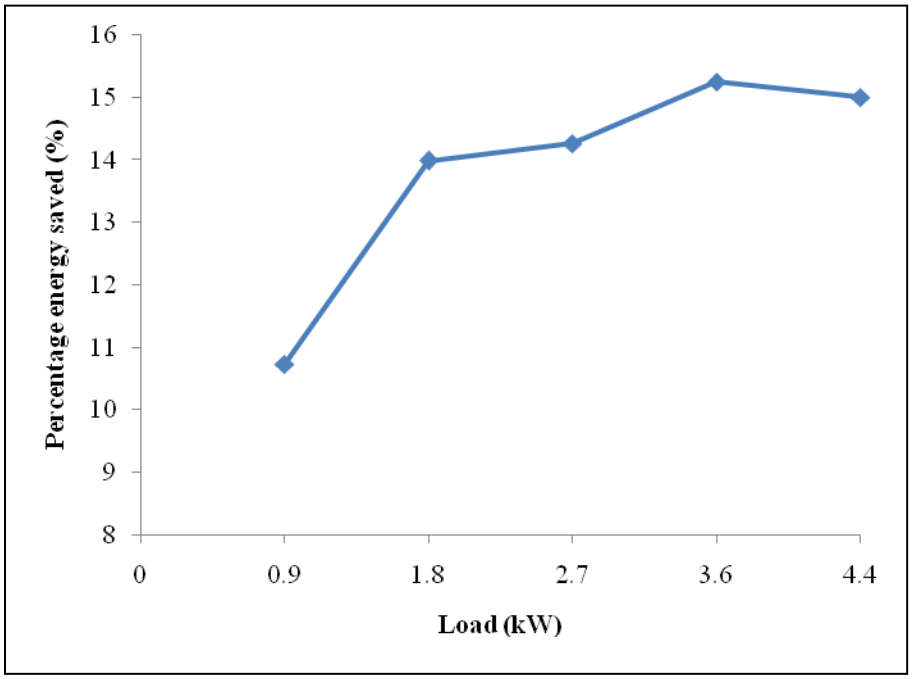

Fig. 4.21 Percentage energy saved at various loads in CHP with TESS

Maximum energy saved in CHP with TESS was obtained at a load of 3.6 kW and the value of percentage energy saved at 3.6 kW was 15.27 %. Since brake thermal efficiency was highest at about 80 % engine load, hence, maximum percentage energy saved was also obtained at this load.

4.4 Performance parameters for trigeneration (CCHP) with TESS

All three combinations given in previous chapter were investigated. Trigeneration with storage could be achieved only at full load condition. Hence all combinations were investigated at full load condition.

In 'I' combination when heat was supplied to VA system via TESS, it was found that temperature of erythritol reached above 190 ^{0}C when the cooling was first achieved. However, at this temperature erythritol started evaporating and started coming out

from TESS with exhaust gas due to which white smoke was obtained at engine exhaust and also value of CO emission in exhaust gas became high. Hence, this combination was found non-feasible.

In 'II' combination when exhaust heat was supplied directly to VA system to achieve cooling, it was found that refrigerator cabin temperature of VA system started rising instead of decreasing. This was because of the fact that the exhaust temperature was quite high when it was supplied to generator of VA system; and due to this heat loss from VA generator; refrigerator cabin temperature was also high. This heat, which was lost by VA generator, was gained by cabin of VA refrigerator. Though there was insulation, but the temperature difference between ambient and exhaust was quite high and space available for insulation was limited due to construction of VA system. Hence, this combination was also found non-feasible.

In 'III' combination when exhaust heat was supplied to TESS via heat exchanger and then to VA system, problems associated with combination I and II were resolved and in this combination, system was working properly. Hence, it was found that 'III' combination was feasible and all other investigations were carried out using III combination.

In this section, engine performance parameters, useful energy output, results related to VA system and performance of TESS during off-power condition related to combination III are presented. In this combination, engine was coupled with double pipe heat exchanger, TESS and VA system. Energy was stored in TESS using erythritol as energy storage medium initially; and after this, thermic fluid was used as TES medium.

4.4.1 Engine performance parameters

Test results of BTE and BSFC for base case (only power) and CCHP with TESS were plotted against load as shown in Fig. 4.22 and 4.23 respectively. It was observed from these plots that the BTE in CCHP with TESS was slightly low as compare to that for base case. Similarly BSFC was slightly high in CCHP with TESS as compare to that for base case. This decrease in BTE and increase in BSFC might be due to the effect of back pressure in exhaust line of engine due to the presence of various additional components in the exhaust path.

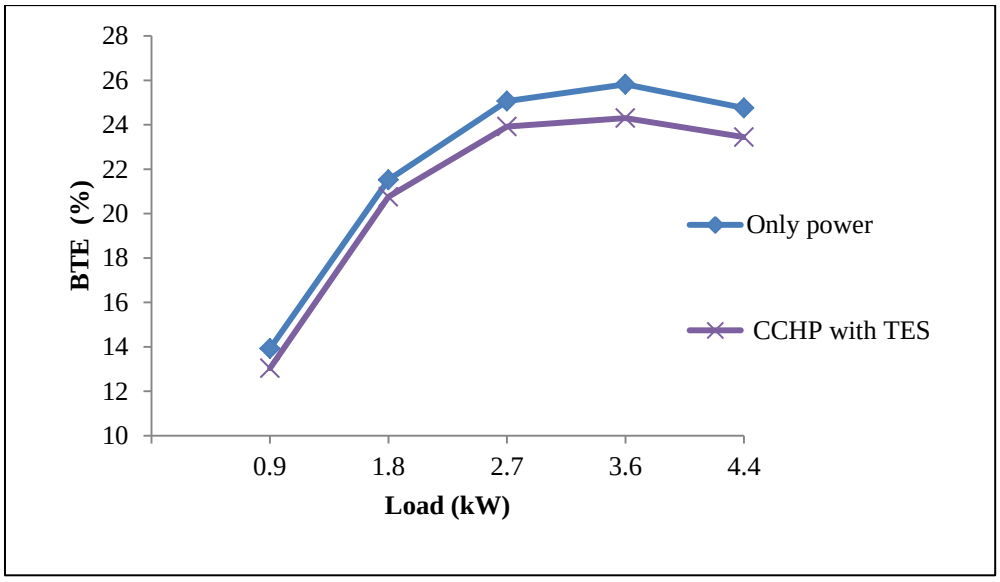

Fig. 4.22 Variation in BTE against load for single generation and CCHP with TESS

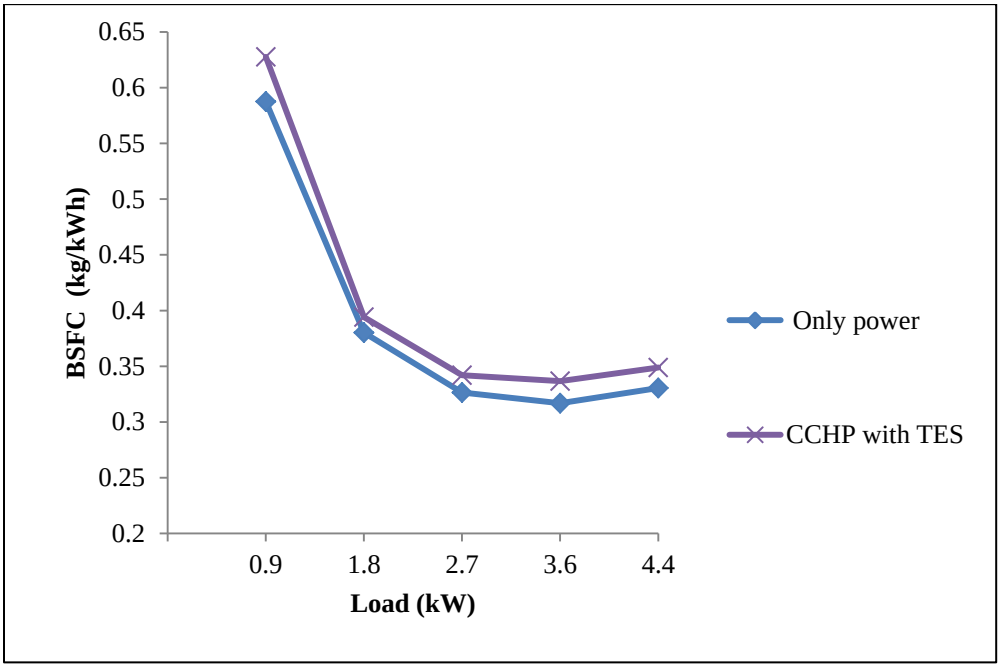

Fig. 4.23 Variation in BSFC against load for single generation and CCHP with TESS

4.4.2 Useful energy output in CCHP with TESS using erythritol as energy storage medium

Total useful energy output of CCHP with TESS was calculated as the sum of electrical output, heat recovered by double pipe heat exchanger, thermal energy stored in TESS and heat removed from water in VA system (refrigeration effect). Fig. 4.24 shows the

useful energy output at various loads for single generation (only power) and trigeneration (CCHP) with TESS.

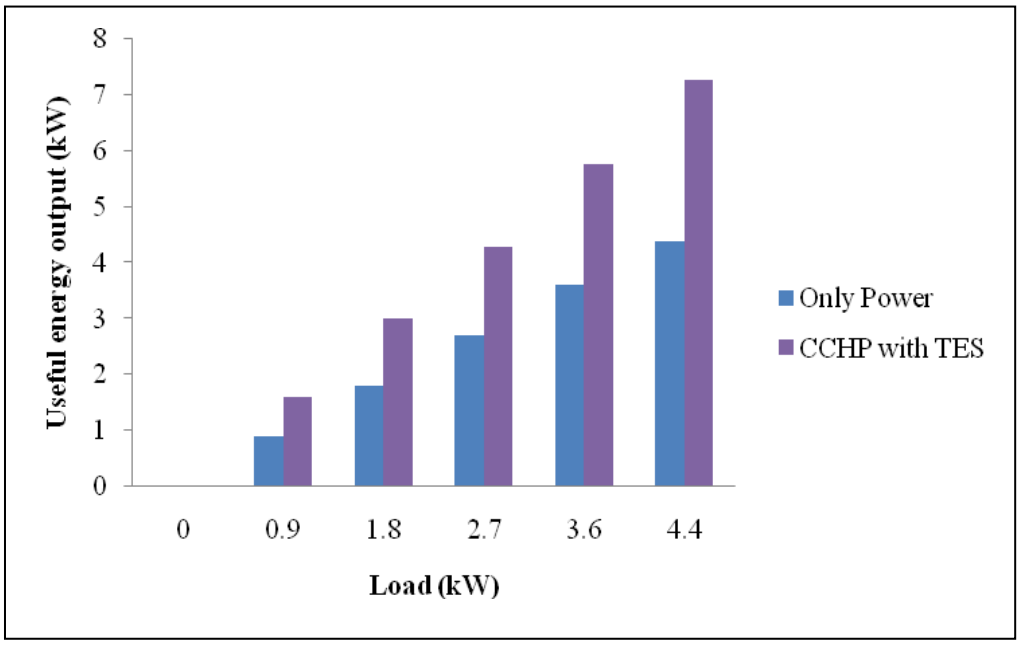

Fig. 4.24 Useful energy output at various engine loads

The useful energy output for CCHP with TESS varied from 1.61 kW at 0.9 kW to 7.27 kW at 4.4 kW load. Significant increase in amount of useful energy output was observed in CCHP with TESS mode. This was due to utilization of engine exhaust heat for heating, cooling and thermal energy storage purposes.

4.4.3 Performance of VA system

During on-power mode hot exhaust gases were allowed to pass through the heat exchanger, and due to this, temperature of refrigerant in the VA generator started increasing. Water was placed in a vessel inside the cabin of VA refrigeration system. As temperature of refrigerant in VA generator increased, temperature of refrigerant inlet to evaporator started increasing, and this resulted in increase in temperature of cabin of VA refrigeration system. When the temperature of refrigerant in generator rose above 95 ^{0}C there was a sudden drop in refrigerant inlet temperature to evaporator. At this point, cooling effect started with a continuous drop in the temperature of refrigerant at inlet of the evaporator. The minimum refrigerant temperature obtained at the inlet to the evaporator was -4.2 ^{0}C. This minimum temperature was maintained constant by supplying heat continuously to the VA

generator. Within 30 minutes, 9 ^{0}C drop in refrigeration cabin temperature was observed and drop in water temperature (kept in the vessel) was 3 ^{0}C.

Coefficient of performance (COP) is normally used to evaluate the performance of VA systems. COP is defined as the ratio of refrigeration effect to the heat supplied to generator of VA system. Using various observations as given in methodology section for refrigeration effect and heat input to generator, refrigeration effect and heat input was calculated. Since cooling in VA was obtained at full load condition only, COP of VA was calculated at full load condition only which was found to be 0.11.

4.4.4 Performance of TESS during off-power mode using erythritol as energy storage medium

During off-power mode amount of energy stored in TESS was used to actuate the generator of VA system using air blower as given in methodology section during discharging of TESS. The heated air was supplied to the generator of VA system. It was observed that up to 20 minutes there was no change in the refrigerator cabin temperature of VA system when hot air from TESS was supplied to the generator of VA system. It was also observed that the refrigerator cabin temperature started increasing after 6 minutes of stopping the supply of engine exhaust to the generator of VA system (in on-power mode); in contrast to 20 minutes when hot air was supplied from TESS to the generator of VA system (in off-power mode). This indicates that stored energy in TESS had sufficient heat to maintain the temperature of refrigerator cabin for 20 minutes.

4.4.5 Performance of TESS during off-power mode using thermic fluid as storage medium

To increase the duration of cabin cooling stability, it was observed that either storage medium must be heated at higher temperature or the storage medium should be replaced. It is already seen in the feasibility of I combination that storage temperature of erythritol is limited due to vaporization of erythritol. The erythritol gained the temperature near 140 ^{0}C when engine was stopped in combination III. At this temperature recovery was done and due to recovery at this lower temperature the amount of heat required in generator of VA system was obtained for a smaller duration. Hence, constant temperature in VA cabin was obtained for smaller duration during off-power mode.

Due to temperature limitation of erythritol, heating to higher temperature could not be achieved with erythritol and hence, a thermic fluid named 'Thermia' was used as storage medium (replacing erythritol). Thermia was heated up to 190 ^{0}C during charging as against 140 ^{0}C in case of erythritol. By changing the storage medium, there was no effect on the performance of engine, double pipe heat exchanger and VA system.

During off-power mode amount of energy stored in TESS was used to actuate the generator of VA system using air blower as given in methodology section during discharging of TESS. The heated air was supplied to the generator of VA system. It was observed that up to 50 minutes there was no change in the cabin temperature of VA system when hot air from TESS was supplied to the generator of VA system. It was also observed that the cabin temperature started increasing after 6 minutes of stopping the supply of engine exhaust to the generator of VA system (in on-power mode); in contrast to 50 minutes when hot air was supplied from TESS (with Thermia as medium) to the generator of VA system (in off-power mode). This indicates that stored energy in TESS (with Thermia as medium) had sufficient heat to maintain the temperature of cabin for 50 minutes.

4.5 Comparative analysis of single generation, CHP, CHP with TESS and CCHP with TESS

4.5.1 Engine Performance Parameters

Test results for BTE and BSFC for base case (only power), CHP, CHP with TESS and CCHP with TESS were plotted against load as shown in Fig. 4.25 and 4.26 respectively.

It was observed from these plots that the BTE in CHP mode was slightly low as compared to the base case and slightly high compared to CHP with TESS as also CCHP with TESS. Similarly BSFC was slightly high as compare to base case, slightly low compare to CHP with TESS as also CCHP with TESS. This decrease in BTE and increase in BSFC might be due to the effect of back pressure in exhaust line of the engine. As number of component in exhaust line increased, back pressure also increased and hence, performance of engine decreased.

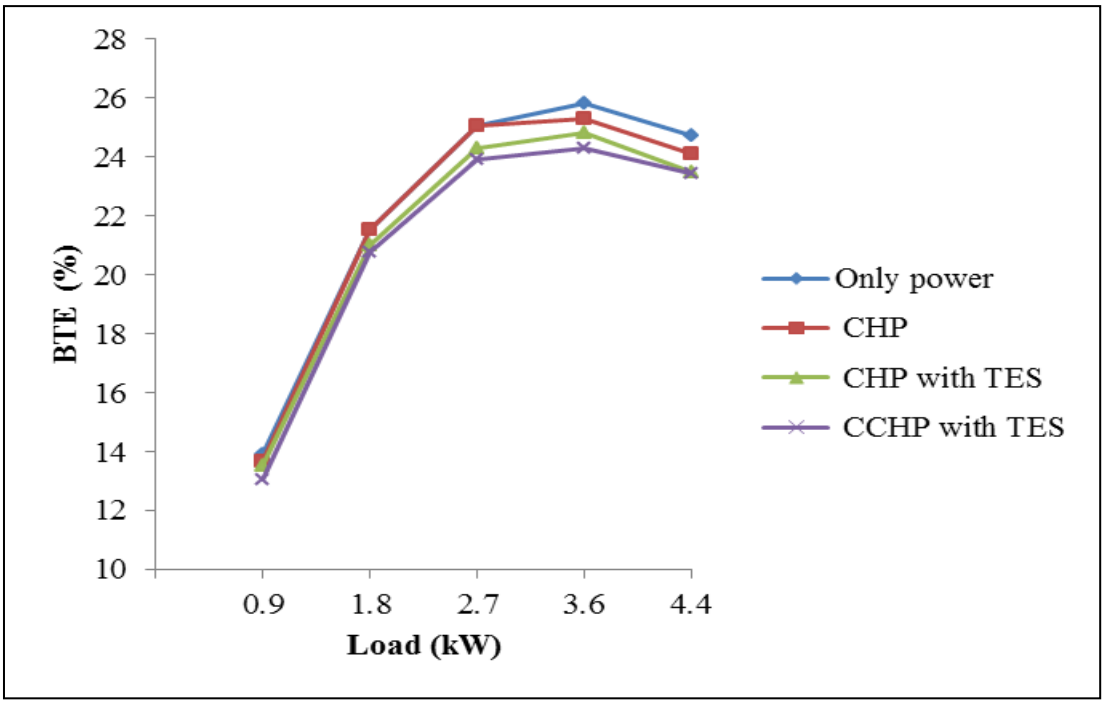

Fig. 4.25 Variation in BTE against load for various modes

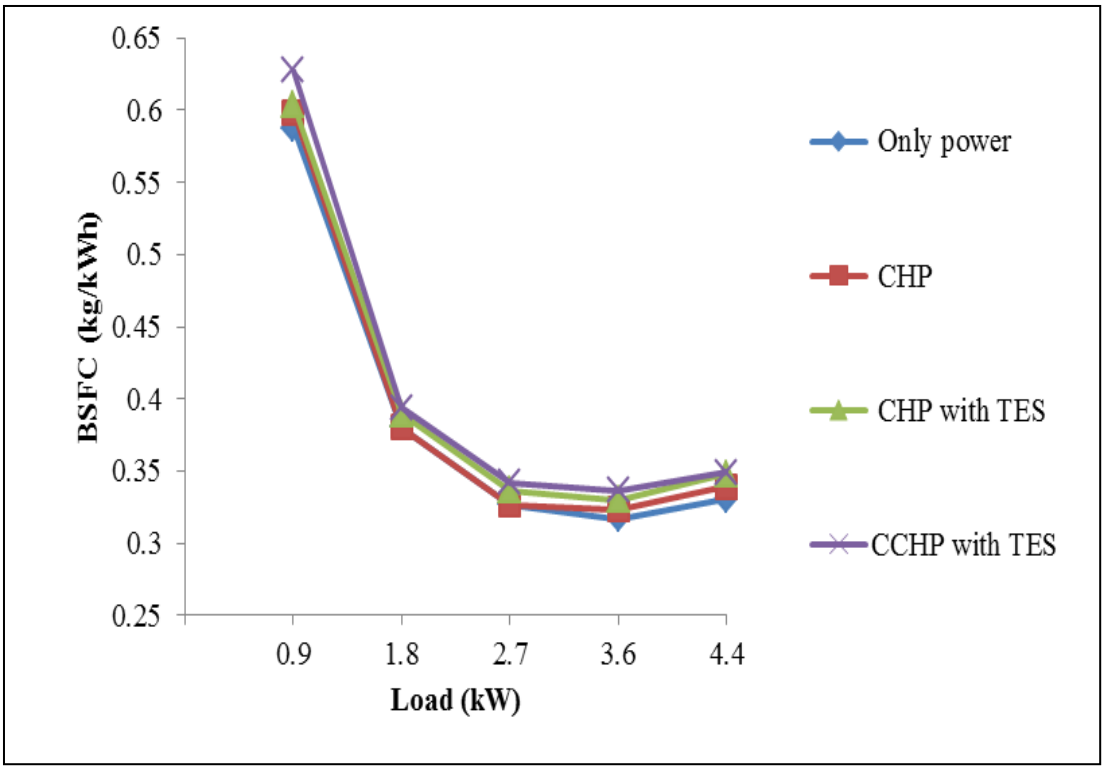

Fig. 4.26 Variation in BSFC against load for various modes

4.5.2 Useful energy output

Fig. 4.27 shows the useful energy output for various modes at different engine loads. The useful energy output for CCHP with TESS varied from 1.61 kW at 0.9 kW to

7.27 kW at 4.4 kW load compared to 1.61 kW, 1.36 kW and 0.9 kW at 0.9 kW load and 7.21 kW, 6.47 kW and 4.4 kW at 4.4 kW for CHP with TESS, CHP and only power respectively.

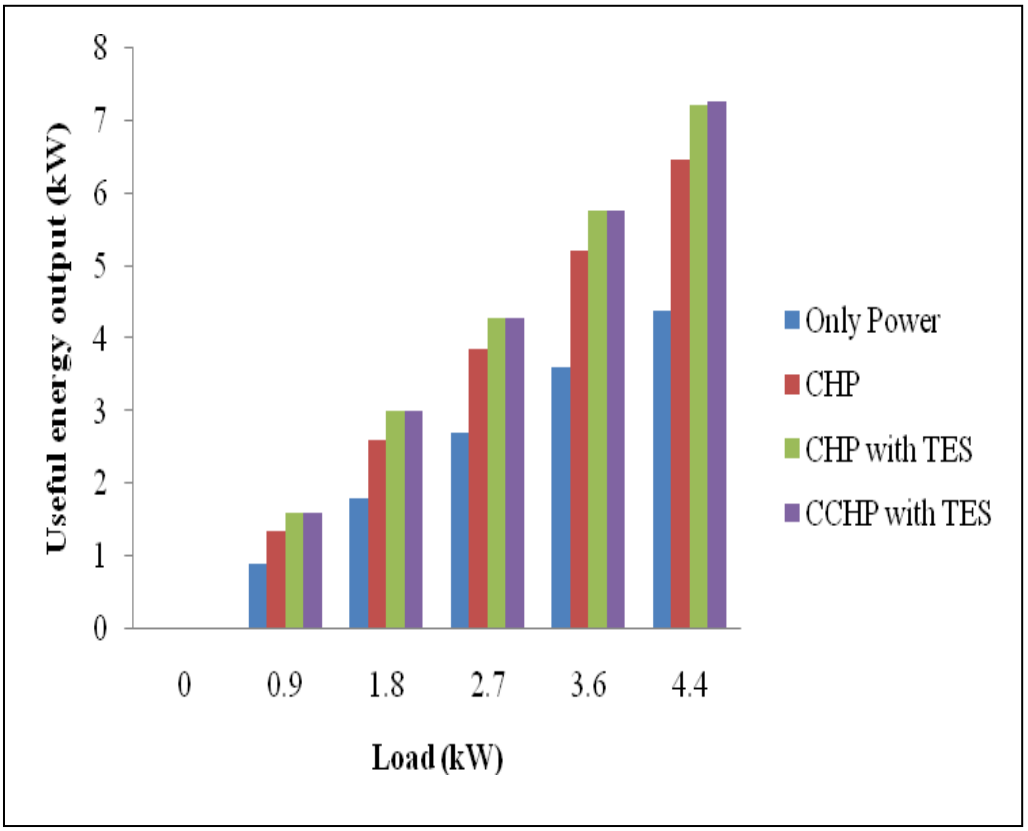

Fig. 4.27 Useful energy output at various engine loads for various systems

Significant increase in amount of useful energy output was observed on utilization of waste heat for the purpose of heating water / cooling / TES individually or in different combinations. At a load of 0.9, 1.8, 2.7 and 3.6 kW useful outputs are same for CHP with TESS and CCHP with TESS because at these loads cooling was not achieved.

4.5.3 Percentage energy saved

The percentage energy saved at various loads for CHP, CHP with TESS and CCHP with TESS are given in Fig. 4.28. At a load of 0.9, 1.8, 2.7 and 3.6 kW, percentage energy saved was same for CHP with TESS and CCHP with TESS because at these loads cooling was not achieved. The value of percentage energy saved at full load for CHP, CHP with TESS and CCHP with TESS was 11.03 %, 15.016 % and 15.303 % respectively. This indicated that there was a significant saving of energy in CCHP with TESS mode as compared to CHP and CHP with TESS modes.

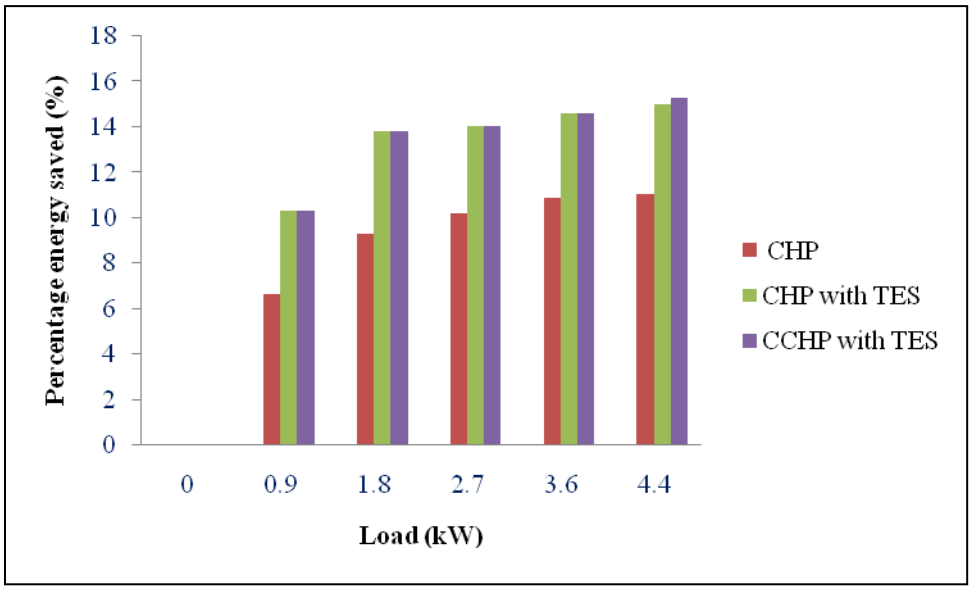

Fig. 4.28 Percentages energy saved at different loads for various systems

4.5.4 Exergy efficiency for various operating modes

Various exergy parameters as defined in Chapter 3 were evaluated at various engine loads and values were tabulated as shown in Table 4.1. Exergy efficiency for various operating modes at different engine loads is shown in Fig. 4.29. It was noted from the graph that a considerable amount of exergy in the fuel could be saved by utilization of waste heat in various modes. Maximum exergy saved was 5.23 % and occurred at the peak load of 4.4 kW in CCHP with TESS mode. Exergy saved increased as the load increased. This was due to the fact that at higher load, the temperature of exhaust was quite high.

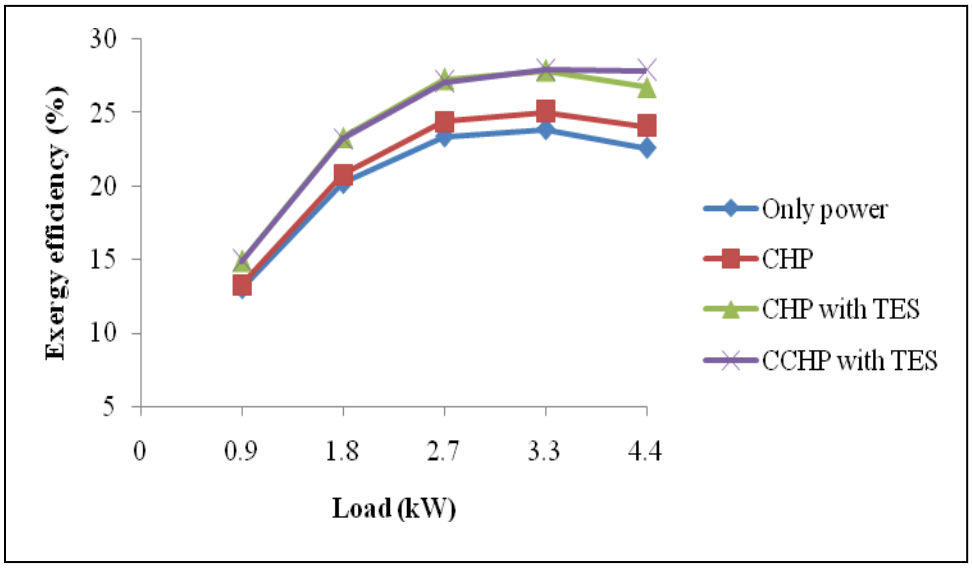

Fig. 4.29 Exergy efficiency for various operating modes at different engine loads

Table 4.1 Parameters for exergy analysis

S. No.	**Parameter**	**Load 0.9 kW**	**Load 1.8 kW**	**Load 2.7 kW**	**Load 3.6 kW**	**Load 4.4 kW**
1.	The input exergy to the diesel engine	6.911	8.909	11.554	15.091	19.460
2.	Exergy recovered in double pipe heat exchanger	0.0175	0.051	0.118	0.179	0.284
3.	Exergy present in thermal energy storage	0.113	0.226	0.317	0.440	0.538
4.	Exergy recovered in VA system	0.0	0.0	0.0	0.0	0.195
5.	Total exergy for combined heating and power	0.917	1.185	2.818	3.779	4.684
6.	Total exergy for combined heating, power with thermal energy storage	1.030	2.078	3.136	4.219	5.222
7.	Total exergy for combined cooling, heating, power with thermal energy storage	1.030	2.078	3.136	4.219	5.420
6.	Exergy efficiency (%) of diesel engine	13.022	20.203	23.367	23.854	22.610

S. No.	Parameter	Load 0.9 kW	Load 1.8 kW	Load 2.7 kW	Load 3.6 kW	Load 4.4 kW
7.	Exergy efficiency (%) for combined power and heating	13.276	20.784	24.397	25.042	24.073
8.	Exergy efficiency (%) for combined power, heating with thermal storage	14.911	23.331	27.145	27.959	26.838
9.	Exergy efficiency (%) for combined power, cooling, heating with storage	14.911	23.331	27.145	27.959	27.850
10.	Exergy saved	1.889	3.128	3.777	4.104	5.23

4.6 Emission analysis for single generation, CHP, CHP with TESS and CCHP with TESS

In this section emissions of CO, HC, NO_x, CO_2 and smoke from single generation, CHP, CHP with TESS and CCHP with TESS at various loads are discussed. The aim of these tests was to carry out comparative analysis of engine exhaust emissions of single generation, CHP, CHP with TESS and CCHP with TESS.

Among the gaseous pollutants emitted by diesel engines, NOx is the most significant. NOx is formed due to high in-cylinder temperature and excess oxygen availability during combustion. As the load increases, in-cylinder temperature increases, producing more NOx. Fig. 4.30 shows the variation of NOx with engine load for comparison between various modes of operation.

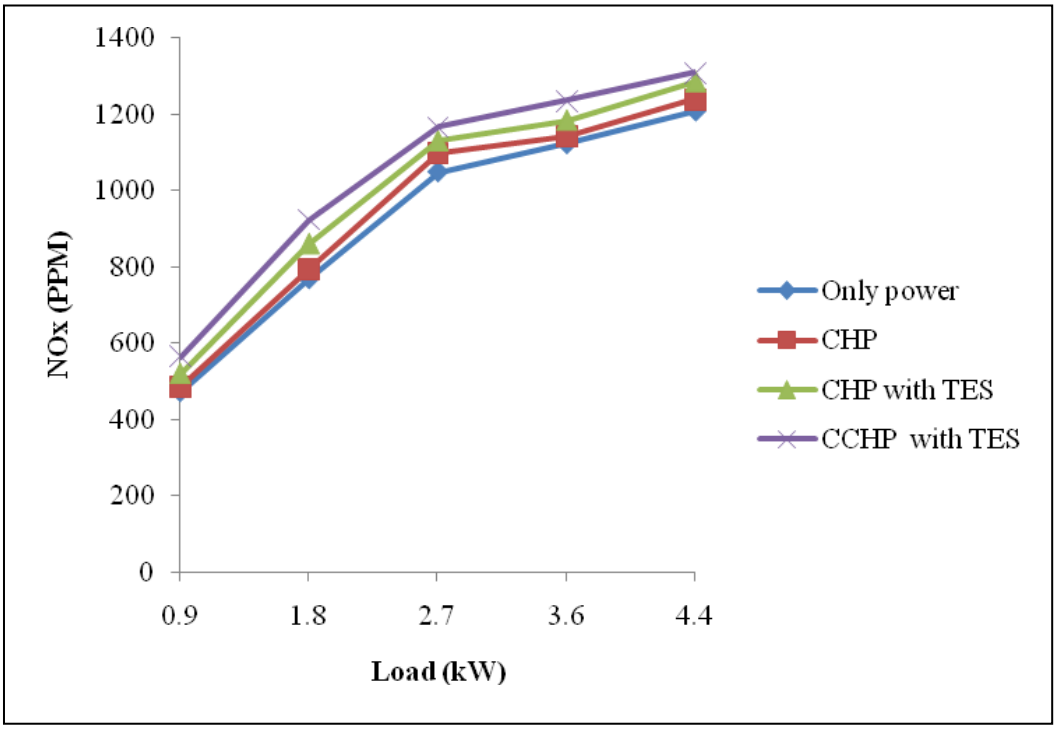

Fig. 4.30 Variation of NOx emission with engine load for different operation modes

Smoke in engine exhaust is the result of incomplete combustion or thermal cracking (pyrolysis) of fuel. Smoke from exhaust is a visible indicator of improper combustion in the engine. As the load increases, larger fuel injection combined with lack of oxygen in the cylinder contributes to a very quick rise in smoke emission [30]. Fig. 4.31 shows the variation of smoke with engine load for comparison between various operating modes.

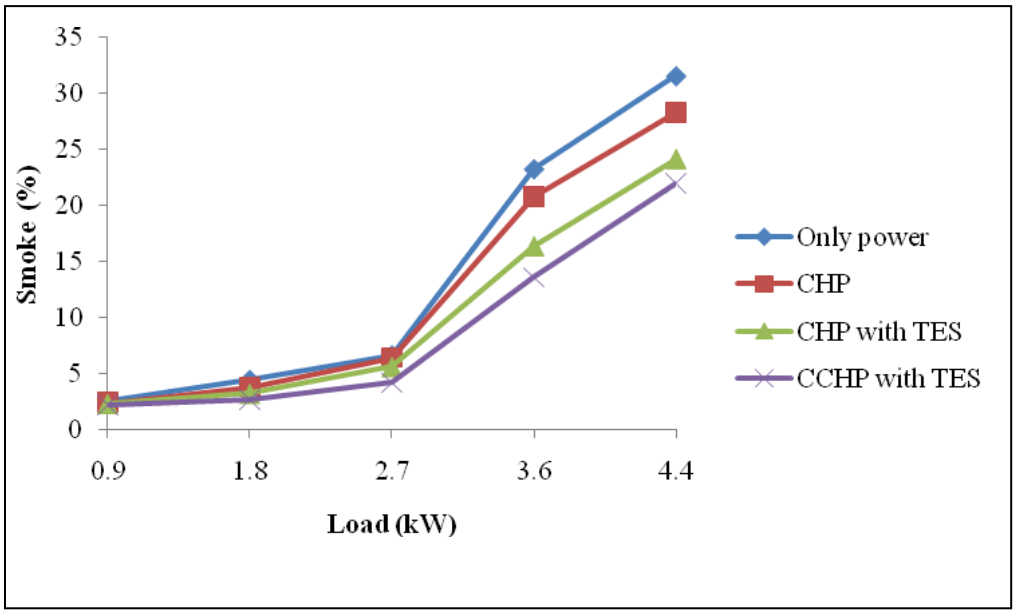

Fig. 4.31 Variation of smoke emissions with engine loads for different operation modes

CO is formed due to incomplete combustion of fuel. From Fig.4.32 it is clear that at idle or low load conditions CO emission was high due to low operating temperatures and incomplete combustion of fuel. With the increase in load, both, the operating temperature and mixing of fuel increases, resulting in reduction of CO emission. But at high loads, the available oxygen for combustion becomes lesser (lean air-fuel ratio), resulting in increased CO emission.

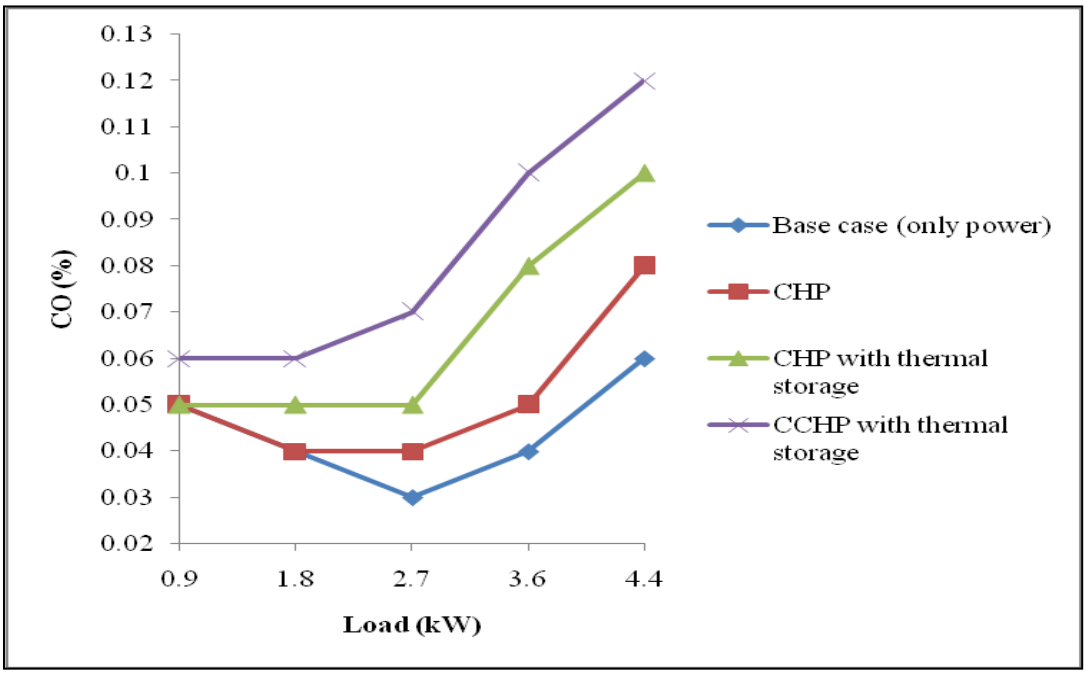

Fig. 4.32 Variation of CO emission with engine loads for different operation modes

Fig. 4.33 shows the variation of unburned hydrocarbon with engine load for comparison between various operating modes.

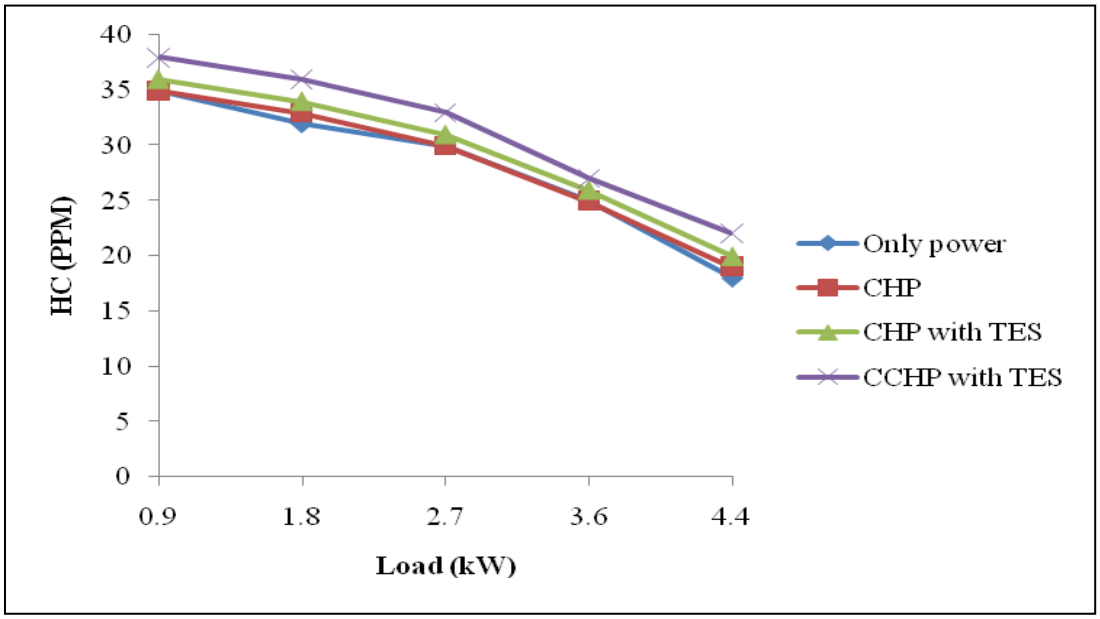

Fig. 4.33 Variation of HC emission with engine loads for different operation modes

CO_2 emission increased with the increase of engine load in all modes. Fig. 4.34 shows the variation of CO_2 with engine load for comparison between various operating modes.

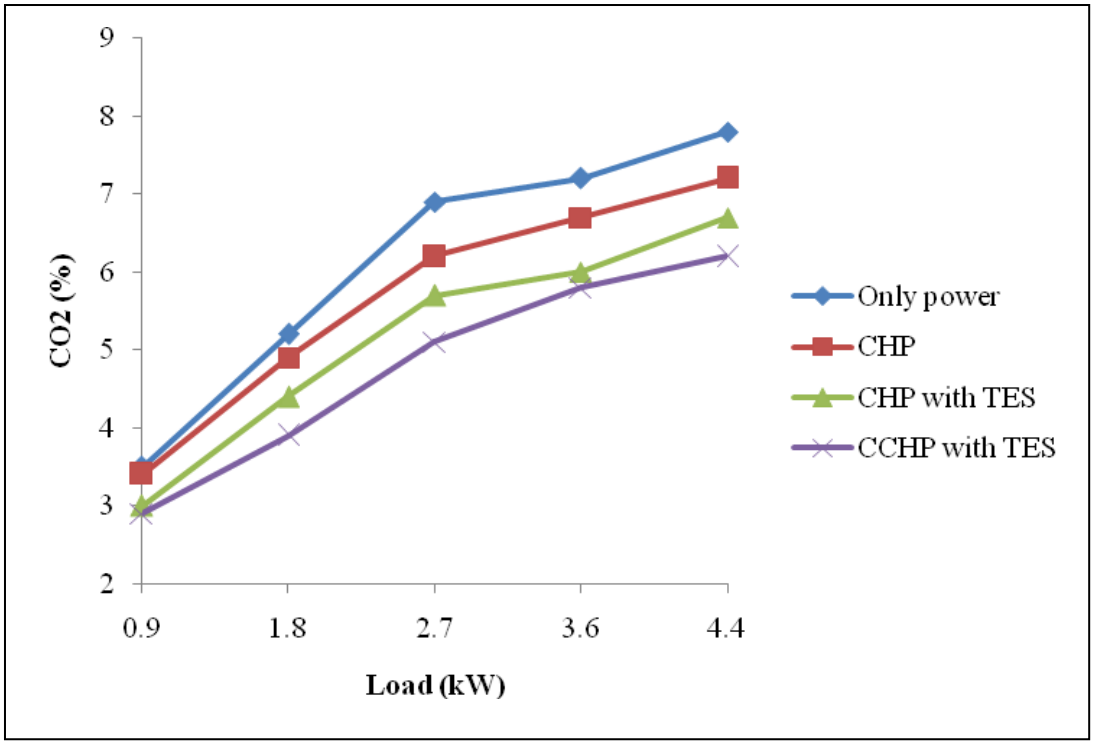

Fig. 4.34 Variation of CO_2 emissions with engine loads for different operation modes

Fig. 4.30 to 4.34 show the variation of NO_x, smoke, CO, HC and CO_2 respectively with engine load for comparison between various operating modes. Results show that NOx, CO and HC emission increased in CCHP with TESS mode as compared to base case. This might be due to the fact that back pressure increased because of various additional components installed in exhaust line. At increased back pressure, the engine had to push exhaust gases with a higher pressure which involved additional mechanical work which affected intake manifold pressure and poor scavenging during exhaust. This led to an increase in fuel consumption, CO emission and exhaust temperature. The increased exhaust temperature resulted in overheating of exhaust valves and increased in-cylinder temperature, thus increasing NO_x emissions.

Results also showed that smoke and CO_2 emissions reduced in case of CCHP with TESS compared to base case. The graph of smoke emission shows that smoke emission increase rate was low in the low to intermediate load region, but smoke % rose quickly from intermediate to high load. In general, high temperature and lack of oxygen in the cylinder may cause high soot formation rates. As the load of the diesel engine increased, larger fuel injection combined with lack of oxygen in the cylinder contributed to a very quick rise in smoke emission.

4.7 Specific fuel consumption (SFC) at various modes

The SFC for CHP varied from 0.3967 kg/kWh at 0.9 kW load to 0.2305 kg/kWh at 4.4 kW (full load) compared to 0.58 kg/kWh and 0.33 kg/kWh respectively for single generation system. Hence, the reduction in SFC was in the range of 29.52 % to 32.59 %. The SFC for CHP with TESS system varied from 0.337 kg/kWh at a load of 0.9 kW to 0.212 kg/kWh at 4.4 kW load. Thus, the reduction in SFC for CHP with TESS was in the range of 35.02 % to 42.64 % as compared to single generation. In CCHP with TESS system, SFC varied from 0.3501 kg/kWh at 0.9 kW load to 0.2116 kg/kWh at 4.4 kW load. Hence, reduction in SFC for CCHP with TESS system was in the range of 33.87 % to 40.41 % as compared to single generation. Fig. 4.35 shows the comparison of specific fuel consumption for various modes of operation at different engine loads.

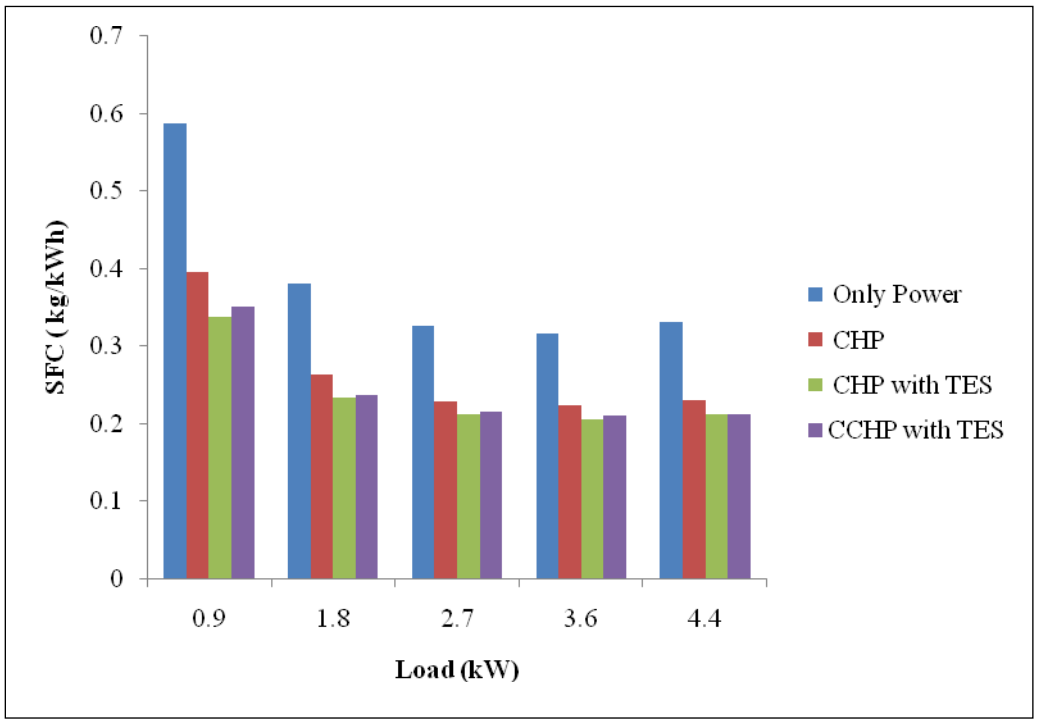

Fig. 4.35 Comparison of SFC for various modes at different engine loads

4.8 CO_2 emission in total useful output

The CO_2 emission in kg/kWh for CHP varied from 1.46 kg/kWh at 0.9 kW load to 0.6824 kg/kWh at 4.4 kW (full load) compared to 2.28 kg/kWh and 1.08 kg/kWh respective for single generation system. Hence, the reduction in CO_2 emission in kg/kWh in case of CHP was in the range of 34.88 % to 37.11 % as compared to that for single generation.

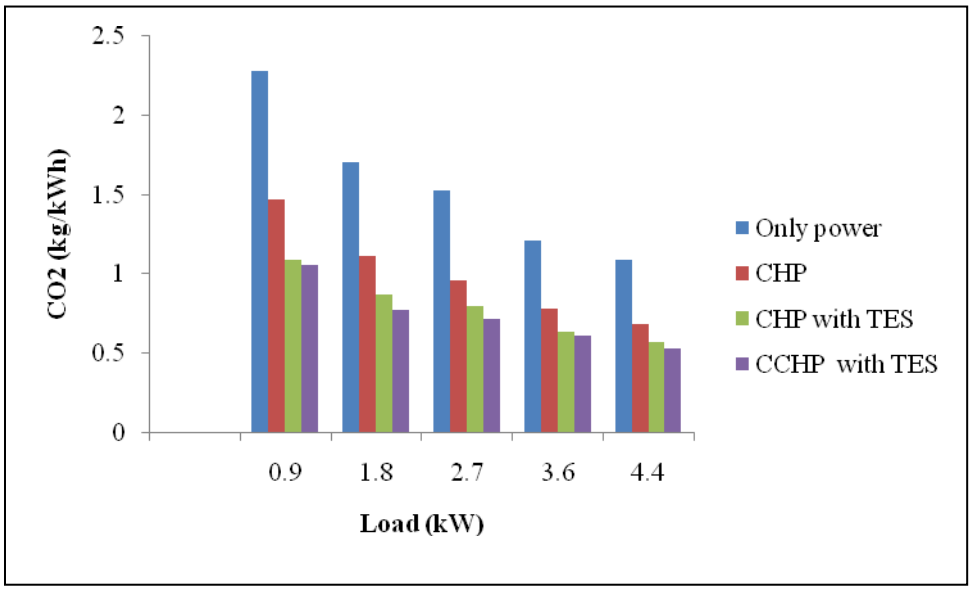

Fig. 4.36 Comparison of CO_2 emissions for various modes at different engine loads

The CO_2 emission in kg/kWh for CHP with TESS system varied from 1.09 kg/kWh at 0.9 kW load to 0.570 kg/kWh at 4.4 kW (full load). Hence, the reduction in CO_2 emission in kg/kWh in case of CHP with TESS was in the range of 47.45 % to 52.14 % as compared to single generation. The CO_2 emission in kg/kWh for CCHP with TESS system varied from 1.056 kg/kWh at 0.9 kW load to 0.5239 kg/kWh at 4.4 kW (full load). Hence, the reduction in CO_2 emission in kg/kWh in case of CCHP with TESS was in the range of 49.65 % to 54.92 % as compared to single generation. Fig. 4.36 shows the comparison of CO_2 emission in terms of useful energy output for various modes of operation at full engine load.

CHAPTER 5
MODELLING

In the present research work, performance of CI engine operated thermal energy storage integrated micro trigeneration system was predicted by a simple model. In this model, a similar diesel engine was considered for trigeneration system, as the one used for the experimental study. The equations used for calculation of performance parameters of proposed model are presented in this section.

From available literature, different models of small capacity Kirloskar engines were selected and used for plotting of swept volume (in cc) vs. power output of engine as shown in Fig. 5.1. The details of various engines are shown in Table 5.1.

Table 5.1 Variation of power with swept volume for various small Kirloskar engines

S. No.	Model	Power (kW)	Swept volume (cc)
1	FA-350	3.7	348
2	DAF-8	5.9	780
3	DAF-10	7.4	948

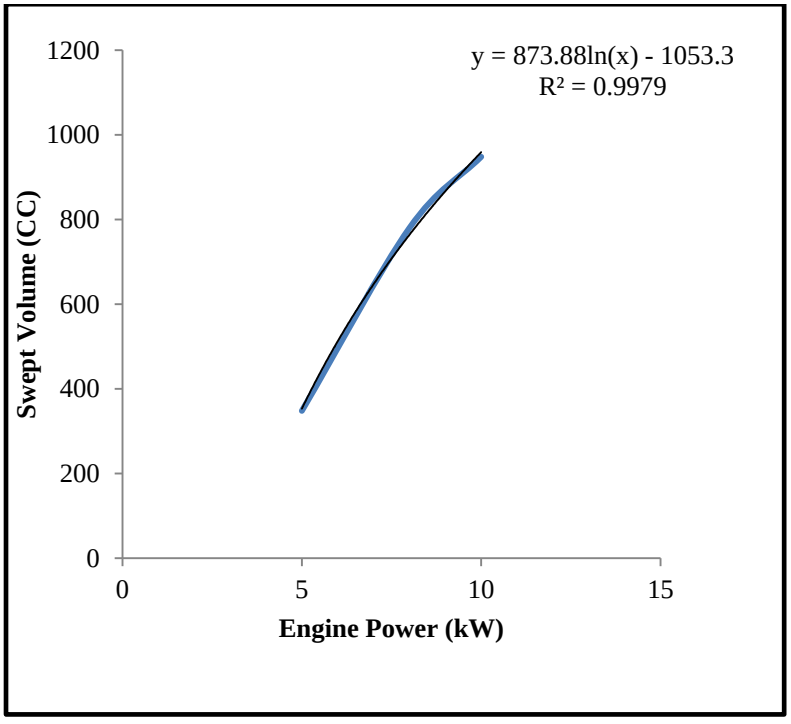

Fig. 5.1 Swept volume vs. engine power for various small Kirloskar engines

The graph shows a logarithmic variation of swept volume (y) with power of engine (x) given by the following equation (by curve fitting):

$$y = 873.88 \ln x - 1053.3$$

By using this equation swept volume of engine used for experimental work was calculated by putting the values of power for validation of above equation. A very small deviation of 1.1 % was observed between the calculated value and rated value.

Further, this equation was used for determination of mass flow rate of air (m_a) and mass flow rate (m_f) of fuel in kg/s at full load. Following parameters were assumed (a) RPM = 1500; (b) density of air = 1.2 kg/m^3 and (c) stochiometric ratio at full load is 19:1;

The value of m_a in terms of volumetric efficiency (η_v) is given by the following equation:

$$m_a = \frac{\text{Engine capacity in cc} * \text{RPM} * \text{density of air} * \text{volumetric efficiency}}{2 * 60 * 10^6} \ kg/s$$

$$m_a = \frac{(873.88 \ln x - 1053.3) * 1500 * 1.2 * \text{volumetric efficiency}}{2 * 60 * 10^6} \ kg/s$$

$$m_a = 1.5 * 10^{-5} * \eta_v * (873.88 \ln x - 1053.3) \text{ kg/s}$$

Using the stoichiometric ratio, mass flow rate of fuel is given by the following equation:

$$m_f = 1.5 * 10^{-5} * \eta_v * (873.88 \ln x - 1053.3) / 19 \text{ kg/s} \quad \text{(where } m_f = m_a / 19\text{)}$$

As total mass flow rate of exhaust gas is the sum of mass flow rate of air and that of diesel, it is given as:

$$m_{ex} = 1.5 * 10^{-5} * \eta_v * (873.88 \ln x - 1053.3) * (1+1/19) \text{ kg/s}$$

Heat available in exhaust gas is given by $Q_E = m_{ex} * C_{pex} * \Delta T$

Where, C_{pex} is specific heat of exhaust gases (1.1 kJ / kg-K) and ΔT is difference between engine exhaust temperature and ambient temperature.

$$Q_E = 1.58 * 10^{-5} * \eta_v * (873.88 \ln x - 1053.3) * \Delta T \text{ kW}$$

Amount of heat recovered in double pipe heat exchanger (DPHE) is given by:

$Q_{DPHE} = m_{ex} * C_{pex} * \Delta T * \varepsilon$ (where ε is effectiveness of double pipe heat exchanger)

$Q_{DPHE} = 1.58 * 10^{-5} * \eta_v * (873.88 \ln x - 1053.3) * \Delta T * \varepsilon$

Amount of heat stored in TESS is given by the following equation:

$Q_{TES} = [Q_E - Q_{DPHE}] * \eta_{charging}$

$Q_{TES} = 1.58 * 10^{-5} * \eta_v * (873.88 \ln x - 1053.3) * \Delta T * (1- \varepsilon) * \eta_{charging}$

Amount of heat available in generator of VA system is calculated using:

$Q_{VA} = [Q_E - Q_{DPHE} - Q_{TES}] * \varepsilon_g$ (here ε_g is effectiveness of generator)

$Q_{VA} = 1.58 * 10^{-5} * \eta_v * (873.88 \ln x - 1053.3) * \Delta T * (1- \varepsilon) * [1 - \eta_{charging}] * \varepsilon_g$

Refrigeration effect, $Q_R = COP * Q_{VA}$

$Q_R = 1.58 * 10^{-5} * \eta_v * (873.88 \ln x - 1053.3) * \Delta T * (1- \varepsilon) * [1 - \eta_{charging}] * \varepsilon_g *$ COP kW

Total useful energy output is given by:

$Q_{Total} = Q_{DPHE} + Q_{TES} + Q_R +$ B.P.

$Q_{Total} = 1.58 * 10^{-5} * \eta_v * (873.88 \ln x - 1053.3) * \Delta T * [\varepsilon + (1- \varepsilon) * \eta_{charging} + (1- \varepsilon) * (1 - \eta_{charging}) * \varepsilon_g * COP] + BP$

The efficiency of trigeneration system was calculated by the following equation:

$$\eta_{trigeneration} = \frac{\text{Total useful energy output}}{\text{Fuel input energy}}$$

$\eta_{trigeneration} = [1.58 * 10^{-5} * \eta_v * (873.88 \ln x - 1053.3) * \Delta T * \{\varepsilon + (1 - \varepsilon) * \eta_{charging} + (1 - \varepsilon) * (1 - \eta_{charging}) * \varepsilon_g * COP\}]$

$+ 4.4 / 7.89 * 10^{-7} * \eta_v * (873.88 \ln x - 1053.3) * LCV$

From the practical results, volumetric efficiency (η_v), temperature difference (ΔT), effectiveness of DPHE (ε), charging efficiency ($\eta_{charging}$), effectiveness of generator (ε_g) and COP of VA system was found to be 83 %, 500 ^{0}C, 0.6, 50 %, 0.35 and 0.11 respectively. Based on these values, using the above equations, trigeneration efficiency of modeled system was obtained.

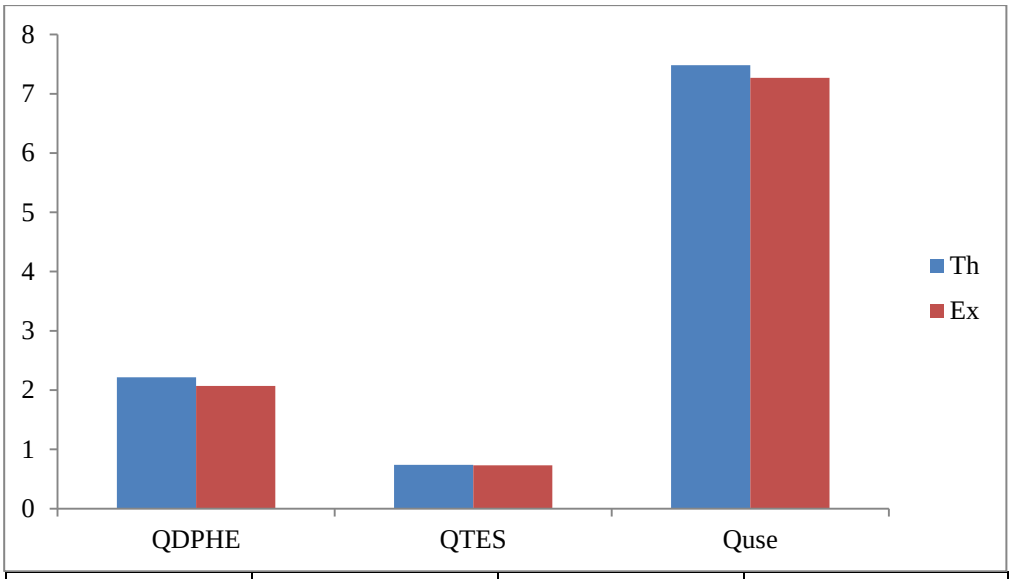

	Q_{DPHE} (kW)	Q_{TES} (kW)	Q_{Use} (kW)
Theoretical	2.21	0.738	7.48
Experimental	2.07	0.73	7.27

Fig. 5.2 Comparison of DPHE, TESS and useful energy output for theoretical & experimental results at 4.4 kW engine load

Fig. 5.2 shows the comparison of energy recovered in DPHE, energy stored in TESS, refrigeration effect and total useful energy output for theoretical & experimental results at 4.4 kW engine load.

CHAPTER 6
CONCLUSIONS AND FUTURE WORK

Thermal storage integrated micro-trigeneration system for power; heating, cooling and thermal energy storage was developed and investigated. From the results of the study, the following conclusions were drawn:

1. It was feasible to realize a thermal storage integrated micro-trigeneration system using a small stationary diesel engine. There was slight effect on performance and emission by integrating the components of trigeneration and storage to the stationary diesel engine.
2. Slight decrease in engine performance (slight decrease in BTE and slight increase in BSFC) was observed in single generation with TESS as compared to that for single generation alone. Variation in BTE and BSFC was in the range of 1.2 to 3.8 % and 1.2 to 3.9 % respectively.
3. Charging efficiency varied from 53.90 to 69.53% at different loads. Highest charging efficiency of 69.53% was obtained at load of 4.4 kW (i.e. peak load).
4. During discharging of TESS, the heat recovery efficiency was obtained 38 %.
5. Maximum energy saved in single generation with TESS mode was obtained at the peak load i.e. 4.4 kW and its value was 11.33 %.
6. Slight decrease in engine performance was observed when engine was operated in CHP mode as compared to that in single generation. Variation in BTE was in the range of 1.8 to 2.5 % and variation in BSFC was in the range of 1.8 to 2.6 %.
7. Maximum effectiveness of double pipe heat exchanger was obtained at peak load i.e. 4.4 kW and the value of effectiveness was 0.47 at a mass flow rate of 3 LPM of water.
8. Significant increase in amount of useful energy output was observed when engine was operated with CHP mode. Approximately 50% increase in useful energy output was obtained in CHP mode compared to that of single generation.
9. Maximum thermal efficiency was obtained at a load of 3.6 kW (approximately 80 % of peak load) and value of maximum efficiency in case of CHP was 36.6 %. Variation in thermal efficiency was in the range of 41 to 48 %.

10. Maximum energy saved in CHP mode was 11.09 % at 80 % of peak load i.e. at 3.6 kW.
11. The performance in CHP with TESS mode further slightly decreased as compared to the earlier mode i.e. single generation, single generation with TESS and CHP mode. Variation in BTE and BSFC was in the range of 2.35 to 5.0 % and 2.4 to 5.2 % respectively as compared to single generation.
12. Significant increase in amount of useful energy output was observed when engine was operated in CHP with TESS mode. Increase in useful energy output was in the range of 63 % to 80 % compared to that of single generation.
13. Maximum efficiency was obtained at a load of 3.6 kW and value of maximum efficiency in case of CHP with TESS was 40.06 %. Increase in energy efficiency for CHP with TESS was found to be in the range of 53 % to 74 %.
14. Maximum energy saved in CHP with TESS was obtained at a load of 3.6 kW and the value of percentage energy saved at 3.6 kW was 15.27 %.
15. In CCHP with TESS mode performance of engine decreased significantly as compared to single generation and all other modes. Variation in BTE was in the range of 3.54 to 6.37 % and variation in BSFC was in the range of 3.65 to 6.79 % as compared to single generation.
16. Significant increase in amount of useful energy output was observed when engine was operated in CCHP with TESS mode. The useful energy output for CCHP with TESS varied from 1.61 kW at 0.9 kW load to 7.27 kW at 4.4 kW load.
17. Cooling effect in VA system was obtained only at full load condition; hence, COP was obtained only at full load condition which was found to be 0.11.
18. The maximum temperature drop in the cabin of VA refrigerator was 9 ^{0}C and drop in water temperature (kept in the vessel) was 3 ^{0}C.
19. Energy stored in TESS using erythritol as storage medium had sufficient heat to maintain the temperature of refrigerator cabin for 20 minutes.
20. Energy stored in TESS using Thermia as storage medium had sufficient heat to maintain the temperature of refrigerator cabin for 50 minutes.
21. To maintain cooling in VA for longer duration during off-power mode, storage medium must be heated to higher temperature.
22. Maximum exergy saved was 5.23 % and occurred at the peak load of 4.4 kW in CCHP with TESS mode.

23. Reduction in smoke and CO_2 emissions were observed with thermal storage integrated CCHP system as compared to base case. The reduction in CO_2 emission in kg/kWh was in the range of 49.65 % to 54.92 %.
24. All other major emissions (HC, CO, NOx) increased slightly but were well within permissible rang for all the modes.
25. No adverse impacts on any parameter were found while operating in single generation with TESS mode or CHP mode or CHP with TESS mode or CCHP with TESS mode as compared to single generation system.

The experimental results obtained from the present research show that development of a micro size thermal storage integrated trigeneration system is feasible and effective to utilize the resources more efficiently.

Recommendations for future work

Some investigation objectives listed below, though not exhaustive, may be considered as future scope of work:

1. An actual representative thermal storage integrated micro-trigeneration system for a residential family using a bigger diesel engine, say up to 15 kW power can be used for further investigations, as an extension to the present work.
2. Different PCMs with higher melting point may be investigated.
3. Direct flow of hot storage medium (like Thermia) in the generator of VA system may be investigated for improvement of performance of VA system.
4. Alternative fuel operated thermal energy storage micro-trigeneration system may also be investigated including durability tests for long term operation of alternative fuel operated thermal storage integrated micro-trigeneration system.
5. Different types of prime movers, like micro-turbines, sterling engine, fuel cells, etc. could be utilized as power generating unit in the micro-trigeneration system. Further, the micro-trigeneration system may also be designed for integration with a renewable source of energy like solar or wind energy, and the investigations may be carried out.

APPENDIX A.1

Temperature and back pressure relationship

Engine Type	**Temperature**	**Maximum Back Pressure**
Diesel 2- Cycle (Naturally Aspirated)	900^0F	100 mm of Hg
Diesel 2- Cycle (Turbo)	750^0F	75 mm of Hg
Diesel 4- Cycle (Naturally Aspirated)	1000^0F	75 mm of Hg
Diesel 4- Cycle (Turbo)	900^0F	75 mm of Hg
Gasoline All types	120^0F	>100 mm of Hg

APPENDIX A.2

ERROR ANALYSIS

The values of various parameters obtained during the experiments could have errors or uncertainties due to operating conditions, environmental conditions, experimental methods adopted, calibration of equipments, accuracy and precision of equipments, human observations, test case planning, etc. Measurement errors fall into two main categories such as Systematic error and Random error. Imperfect calibration of measuring instruments (zero error), changes in environment which interfere with the measurement process and imperfect methods of observation caused the main sources of systematic error. Random error is caused by inherently unpredictable fluctuations in the readings of a measurement apparatus or in the experimenter's interpretation of the instrumental reading. In this investigation, the uncertainties were estimated from the minimum values of measured values as far as the individual measurements are concerned. To calculate the combined uncertainty of measurements a root-sum-square method was used. If a physical fundamental depends on n number of parameters, the combined uncertainties of each function was calculated by Pythagorean summation of uncertainties given by the equation.

$$z = f(x_1, x_{2,} x_{3,} x_{4,} \ldots\ldots x_n)$$

$$\sigma_z{}^2 = \left[\frac{\partial f}{\partial x_1}\right]^2 \sigma_{x_1}{}^2 + \left[\frac{\partial f}{\partial x_2}\right]^2 \sigma_{x_2}{}^2 + \left[\frac{\partial f}{\partial x_3}\right]^2 \sigma_{x_3}{}^2 + \ldots\ldots\ldots\ldots\ldots\ldots\ldots + \left[\frac{\partial f}{\partial x_n}\right]^2 \sigma_{x_n}{}^2$$

σ_z= uncertainty of the function

σ_{x_n} = uncertainty of the parameter

f= function

x_n= parameter of the measurement

n= number of variables

Uncertainty analysis for micro-trigeneration system working on diesel fuel as baseline case is presented here. The resolution of the measurements and the maximum uncertainties in the calculated results are given in table A1.

Table A.1: Percentage uncertainty in measurement of different quantities

Measured quantity	**Range of experiment**	**Resolution**	**% Uncertainty**
CO	0-10 % vol.	0.01%Vol.	±0.4 %
CO_2	0-20 % vol.	0.1%Vol.	±0.4 %
HC	0-20,000 ppm	1 ppm	±0.3 %
NO_X	0-5000 ppm	1 ppm	±0.3 %
Smoke	0-100 %	0.1 %	±0.18 %
Load	0-4400 W	100 W	±0.19 %
Fuel vol. flow	0-100 ml	±1 ml	±1 %
BTE	-	-	±1.2 %
BSFC	-	-	±1.2 %

APPENDIX A.3

ECONOMIC ANALYSIS

Cost of Erythritol (15kg)	14,000 Rs.
Cost of VA system	15,000 Rs.
Shell and Tube Heat Exchanger	25,000 Rs.
Other Piping and Modifications	5,000 Rs.
Total Cost	59,000 Rs.
If Engine is run 8 hours/day then consumption of fuel (Diesel) is	12.2 Liters
Energy saving 10 % (in terms of fuel)	1.22 Liters
Pay Back Period	1.92 Years

REFERENCES

1. U.S. Energy Information Administration, (EIA). *International Energy Outlook 2016*. Available at https://www.eia.gov/outlooks/ieo/ (accessed March 12, 2017).
2. I. E. A. India Energy Outlook. *World Energy Outlook Spec. Rep.* 1–191 (2015). Available at https://www.iea.org/publications/freepublications/publication/africa-energy-outlook (accessed March 13, 2017)
3. Bansal, N.K. BS VI fuel supply and quality up-gradation. 9th *International conference on Emission control technology for sustainable growth*. New Delhi 2016. 199-206.
4. Sugimoto, K. Diesel emission control utilizing advanced ceramic filter technologies. *SAEINDIA symposium on fuels, lubricants, emission and after-treatment devices - the road ahead.* Delhi, India, 2015.
5. Marathe, N.V. Overview – Retrofitment of heavy duty diesel vehicles. *9th International conference on emission control technology for sustainable growth.* New Delhi, India, 2016. 315.
6. Kumar, S. PCRA- An integrated energy solution provider. *SAEINDIA Symposium on Fuels, Lubricants, Emission and After-Treatment Devices - The Road Ahead.* Delhi, India, 2015.
7. Yu, Hongdong. The design, testing and analysis of a biofuel micro-trigeneration system. PhD thesis: Newcastle university, United Kingdom, 2012.
8. Klass, D. A critical assessment of renewable energy usage in the USA. *Energy Policy* **31,** 353–367 (2003).
9. Bendig, M., Maréchal, F. & Favrat, D. Defining waste heat for industrial processes. *Appl. Therm. Eng.* **61,** 134–142 (2013).
10. Junhong, L., Zhizhang, L., Jianming, G. & Zhiwei, L. Truck waste heat recovery for heating bitumen used in road maintenance. *Appl. Therm. Eng.* **23,** 409–416 (2003).
11. Wang, T., Zhang, Y., Peng, Z. & Shu, G. A review of researches on thermal exhaust heat recovery with Rankine cycle. *Renew. Sustain. Energy Rev.* **15,** 2862–2871 (2011).
12. Royale, A. & Simic, M. Research in vehicles with thermal energy recovery systems. *Procedia Comput. Sci.* **60,** 1443–1452 (2015).
13. Saidur, R. *et al.* Technologies to recover exhaust heat from internal combustion engines. *Renew. Sustain. Energy Rev.* **16,** 5649–5659 (2012).

14. Nadaf, S. & Gangavati, P. A review on waste heat recovery and utilization from diesel engines. *Int. J. Adv. Eng. Technol.* **5,** 31–39 (2014).
15. Jadhao, J. S. & Thombare, D. G. Review on Exhaust Gas Heat Recovery for I . C . Engine. *Int. J. Eng. Innov. Technol.* **2,** 93–100 (2013).
16. Khatri, K. K., Sharma, D., Soni, S. L. & Tanwar, D. Experimental investigation of CI engine operated Micro-Trigeneration system. *Appl. Therm. Eng.* **30,** 1505–1509 (2010).
17. Lin, L. *et al.* An experimental investigation of a household size trigeneration. *Appl. Therm. Eng.* **27,** 576–585 (2007).
18. Sugiartha, N., Tassou, S. A., Chaer, I. & Marriott, D. Trigeneration in food retail: An energetic, economic and environmental evaluation for a supermarket application. *Appl. Therm. Eng.* **29,** 2624–2632 (2009).
19. Onovwiona, H. I. & Ugursal, V. I. Residential cogeneration systems: Review of the current technology. *Renew. Sustain. Energy Rev.* **10,** 389–431 (2006).
20. Abusoglu, A. & Kanoglu, M. First and second law analysis of diesel engine powered cogeneration systems. *Energy Convers. Manag.* **49,** 2026–2031 (2008).
21. Abusoglu, A. & Kanoglu, M. Exergetic and thermoeconomic analyses of diesel engine powered cogeneration: Part 1 - Formulations. *Appl. Therm. Eng.* **29,** 234–241 (2009).
22. Dentice d'Accadia, M., Sasso, M., Sibilio, S. & Vanoli, L. Micro-combined heat and power in residential and light commercial applications. *Appl. Therm. Eng.* **23,** 1247–1259 (2003).
23. Simader, G.R., Krawinkler R. & Trnka, G. Micro CHP systems: state of the art. Final report: Austrain energy agency, Vienna, 2006. Available at http://ec.europa.eu/energy/intelligent/projects/sites/iee-projects/files/projects/documents/ green lodges_micro_chp_state_of_the_art.pdf (accessed December 04, 2016).
24. Dorer, V., Weber, R. & Weber, A. Performance assessment of fuel cell micro-cogeneration systems for residential buildings. *Energy Build.* **37,** 1132–1146 (2005).
25. Ozdenefe, M., Atikol, U. Assessing the applicability of trigeneration in the hotel sector. *5th IASME/WSEAS International conference on energy & environment.* University of Cambridge, UK , 2010. 299-304.
26. Tibbs, R.C. Six cycle combustion and fluid vaporization engine. United States patent 3964263. 1976. Available at http://www.google.co.in/patents/US3964263 (accessed October 09, 2016).

27. Wu, D. W. & Wang, R. Z. Combined cooling, heating and power: A review. *Prog. Energy Combust. Sci.* **32,** 459–495 (2006).
28. Khatri, K.K. Studies on straight vegetable oil – diesel blend operated trigeneration system. PhD thesis: Malaviya national institute of technology, Jaipur, India 2010.
29. Patrascu,R., Minciuc, E. Comparative analysis of different combined heat and power generation: fuel cells, gas turbine, internal combustion engine. 4th *IASME/WSEAS International conference on energy, environment and sustainable development.* Algarve, Portugal, 2008. 27-31. Available at http://www.worldses.org/books/2008/algarve/new-aspects-of-energy-environment-ecosystems.pdf (accessed March 12, 2017).
30. Bael, J.V., Peeters, E. Evaluation of the first micro combined heat and power for social housing in Belgium. *6th WSEAS International conference on power systems*. Lisbon, Portugal, 2006. 165-168. Available at http://www.wseas.us/e-library/conferences/2006lisbon/papers/517-305.pdf (accessed March 12, 2017).
31. Zarinchang, J., Yarmahmoudi, A. Optimization of Stirling engine heat exchangers selected papers from the WSEAS Conference Santander. Cantabria, Spain, 2008, 143-150. Available at http://www.wseas.us/e-library/ conferences/ 2008/spain/ selected/ selected17.pdf (accessed March 19, 2017)
32. ACEEE. *Residential micro CHP using stirling engine, emerging technology & practices.* American Counsil for an energy efficient economy, 2004.
33. Zhao, X., Fu, L., Li, F. & Liu, H. Design and operation of a tri-generation system for a station in China. *Energy Convers. Manag.* **80,** 391–397 (2014).
34. Sonar, D., Soni, S. L. & Sharma, D. Micro-trigeneration for energy sustainability: Technologies, tools and trends. *Appl. Therm. Eng.* **71,** 790–796 (2014)
35. Pandiyarajan, V., Chinna Pandian, M., Malan, E., Velraj, R. & Seeniraj, R. V. Experimental investigation on heat recovery from diesel engine exhaust using finned shell and tube heat exchanger and thermal storage system. *Appl. Energy* **88,** 77–87 (2011).
36. Pandiyarajan, V., Chinnappandian, M., Raghavan, V. & Velraj, R. Second law analysis of a diesel engine waste heat recovery with a combined sensible and latent heat storage system. *Energy Policy* **39,** 6011–6020 (2011).
37. Medrano, M. *et al.* Experimental evaluation of commercial heat exchangers for use as PCM thermal storage systems. *Appl. Energy* **86,** 2047–2055 (2009).

38. Nath, R. Encapsulation of high temperature phase change materials for thermal energy storage. Master of Science thesis: College of engineering, Florida 2012.
39. Sharma S.D and Sagara K. Latent heat storage materials and systems: A review. *Int. J. Green Energy* **2,** 1–56 (2005).
40. Atear, O.E. Storage of thermal energy, in energy storage systems, *Encyclopedia of life support system*. Developed under the auspices of the UNESCO. Eolss, Oxford, UK 2006.
41. Sciuto, G. Innovative latent heat thermal storage elements design based on nanotechnologies. PhD thesis: University of Trieste, Italy, 2012.
42. Wu, D. W. & Wang, R. Z. Combined cooling, heating and power: A review. *Prog. Energy Combust. Sci.* **32,** 459–495 (2006).
43. Liu, M., Shi, Y. & Fang, F. 234–241: A survey. *Renew. Sustain. Energy Rev.* **35,** 1–22 (2014).
44. Goyal, R. Development of CI engine operated micro trigeneration system for power, heating and space cooling. PhD thesis: Malaviya national institute of technology, Jaipur, India 2010.
45. Sonar, D. Experimental studies and simulation on alternative fuel operated micro-trigeneration system for residential applications. PhD thesis: Malaviya national institute of technology, Jaipur, India 2016.
46. Jradi, M. & Riffat, S. Tri-generation systems: Energy policies, prime movers, cooling technologies, configurations and operation strategies. *Renew. Sustain. Energy Rev.* **32,** 396–415 (2014).
47. Maghanki, M. M., Ghobadian, B., Najafi, G. & Galogah, R. J. Micro combined heat and power (MCHP) technologies and applications. *Renew. Sustain. Energy Rev.* **28,** 510–524 (2013).
48. Temir, G. & Bilge, D. Thermoeconomic analysis of a trigeneration system. *Appl. Therm. Eng.* **24,** 2689–2699 (2004).
49. Godefroy, J., Boukhanouf, R. & Riffat, S. Design, testing and mathematical modelling of a small-scale CHP and cooling system (small CHP-ejector trigeneration). *Appl. Therm. Eng.* **27,** 68–77 (2007).
50. Manzela, A. A., Hanriot, S. M., Cabezas-Gómez, L. & Sodré, J. R. Using engine exhaust gas as energy source for an absorption refrigeration system. *Appl. Energy* **87,** 1141–1148 (2010).

51. Kong, X. Q., Wang, R. Z. & Huang, X. H. Energy efficiency and economic feasibility of CCHP driven by stirling engine. *Energy Convers. Manag.* **45,** 1433–1442 (2004).
52. Thombare, D. G. & Verma, S. K. Technological development in the Stirling cycle engines. *Renew. Sustain. Energy Rev.* **12,** 1–38 (2008).
53. Sternlicht, B. The stirling engine: prime mover of the 21st century. *Endeavour* **8,** 21–28 (1984).
54. Kongtragool, B. & Wongwises, S. A review of solar-powered Stirling engines and low temperature differential Stirling engines. *Renew. Sustain. Energy Rev.* **7,** 131–154 (2003).
55. Kuhn, V., Klemeš, J. & Bulatov, I. MicroCHP: Overview of selected technologies, products and field test results. *Appl. Therm. Eng.* **28,** 2039–2048 (2008).
56. Cockroft, J. & Kelly, N. A comparative assessment of future heat and power sources for the UK domestic sector. *Energy Convers. Manag.* **47,** 2349–2360 (2006).
57. Pilavachi, P. Mini-and micro-gas turbines for combined heat and power. *Appl. Therm. Eng.* **22,** 2003–2014 (2002).
58. Alanne, K. & Saari, A. Sustainable small-scale CHP technologies for buildings: The basis for multi-perspective decision-making. *Renew. Sustain. Energy Rev.* **8,** 401–431 (2004).
59. El-Khattam, W. & Salama, M. M. A. Distributed generation technologies, definitions and benefits. *Electr. Power Syst. Res.* **71,** 119–128 (2004).
60. Masepohl, T. On site power systems for laboratories. *The National Renewable Energy Laboratory* (2003) Available at www.nrel.gov/docs/fy04osti/33978.pdf (accessed April 14, 2017)
61. A joint project of the Gas Research Institute (GRI) and the National Renewable Energy Laboratory (NREL), prepared for office of energy efficiency and renewable energy (2003). Available at www.nrel.gov/docs/fy04osti/34783.pdf (accessed April 14, 2017)
62. *The European association for promotion of cogeneration.* December 02, 2001. www.cogen.org (accessed July 24, 2012)
63. Srikhirin, P., Aphornratana, S. & Chungpaibulpatana, S. A review of absorption refrigeration technologies. *Renew. Sustain. Energy Rev.* **5,** 343–372 (2000).
64. Duparchy, A., Leduc, P., Bourhis, G. & Ternel, C. Heat recovery for next generation of hybrid vehicles: Simulation and design of a Rankine cycle system. *World Electr. Veh. J.* **3,** 440–456 (2009).

65. Vaja, I. & Gambarotta, A. Internal Combustion Engine (ICE) bottoming with Organic Rankine Cycles (ORCs). *Energy* **35,** 1084–1093 (2010).
66. Rowe, D. M. Thermoelectric waste heat recovery as a renewable energy source. *Int. J. Innov. Energy Syst. Power* **1,** 13–23 (2006).
67. www.grimsby.ac.uk/documents/defra/tech-ejector.pdf (accessed December 14, 2016).
68. Riffat, S. B. & Ma, X. Thermoelectrics: A review of present and potential applications. *Appl. Therm. Eng.* **23,** 913–935 (2003).
69. Ziher, D. & Poredos, A. Economics of a trigeneration system in a hospital. *Appl. Therm. Eng.* **26,** 680–687 (2006).
70. Bassols, J., Kuckelkorn, B., Langreck, J., Schneider, R. & Veelken, H. Trigeneration in the food industry. *Appl. Therm. Eng.* **22,** 595–602 (2002).
71. Biezma, M. V. & San Cristóbal, J. R. Investment criteria for the selection of cogeneration plants - A state of the art review. *Appl. Therm. Eng.* **26,** 583–588 (2006).
72. Arteconi, A., Brandoni, C. & Polonara, F. Distributed generation and trigeneration: Energy saving opportunities in Italian supermarket sector. *Appl. Therm. Eng.* **29,** 1735–1743 (2009).
73. Cardona, E. & Piacentino, A. A methodology for sizing a trigeneration plant in mediterranean areas. *Appl. Therm. Eng.* **23,** 1665–1680 (2003).
74. Ebrahimi, M. & Keshavarz, A. Prime mover selection for a residential micro-CCHP by using two multi-criteria decision-making methods. *Energy Build.* **55,** 322–331 (2012).
75. Basrawi, F., Yamada, T. & Obara, S. Theoretical analysis of performance of a micro gas turbine co/trigeneration system for residential buildings in a tropical region. *Energy Build.* **67,** 108–117 (2013).
76. Deng, J. *et al.* Exergy cost analysis of a micro-trigeneration system based on the structural theory of thermoeconomics. *Energy* **33,** 1417–1426 (2008).
77. Wu, J. Y., Wang, J. L., Li, S. & Wang, R. Z. Experimental and simulative investigation of a micro-CCHP (micro combined cooling, heating and power) system with thermal management controller. *Energy* **68,** 444–453 (2014).
78. Huangfu, Y., Wu, J. Y., Wang, R. Z., Kong, X. Q. & Wei, B. H. Evaluation and analysis of novel micro-scale combined cooling, heating and power (MCCHP) system. *Energy Convers. Manag.* **48,** 1703–1709 (2007).
79. Kong, X. Q. *et al.* Experimental investigation of a micro-combined cooling, heating and power system driven by a gas engine. *Int. J. Refrig.* **28,** 977–987 (2005).

80. Angrisani, G., Roselli, C. & Sasso, M. Distributed microtrigeneration systems. *Prog. Energy Combust. Sci.* **38,** 502–521 (2012).
81. Wang, Y. *et al.* An investigation of a household size trigeneration running with hydrogen. *Appl. Energy* **88,** 2176–2182 (2011).
82. Wang, Y., Huang, Y., Roskilly, A. P., Ding, Y. & Hewitt, N. Trigeneration running with raw jatropha oil. *Fuel Process. Technol.* **91,** 348–353 (2010).
83. Badami, M. & Portoraro, A. Performance analysis of an innovative small-scale trigeneration plant with liquid desiccant cooling system. *Energy Build.* **41,** 1195–1204 (2009).
84. Cacua, A. K., Olmos-villalba, L. & Herrera, B. Experimental evaluation of a diesel-biogas dual fuel engine operated on micro-trigeneration system for power, drying and cooling. *Appl. Therm. Eng.* (2016). doi:10.1016/j.applthermaleng.2016.02.067
85. Ciampi, G., Rosato, A., Scorpio, M. & Sibilio, S. Experimental analysis of a micro-trigeneration system composed of a micro-cogenerator coupled with an electric chiller. *Appl. Therm. Eng.* **73,** 1309–1322 (2014).
86. Fong, K. F. & Lee, C. K. Performance analysis of internal-combustion-engine primed trigeneration systems for use in high-rise office buildings in Hong Kong. *Appl. Energy* **160,** 793–801 (2015).
87. Zhang, H., Baeyens, J., Cáceres, G., Degrève, J. & Lv, Y. Thermal energy storage: Recent developments and practical aspects. *Prog. Energy Combust. Sci.* **53,** 1–40 (2016).
88. Stritih, U. An experimental study of enhanced heat transfer in rectangular PCM thermal storage. *Int. J. Heat Mass Transf.* **47,** 2841–2847 (2004).
89. Nallusamy, N., Sampath, S. & Velraj, R. Experimental investigation on a combined sensible and latent heat storage system integrated with constant/varying (solar) heat sources. *Renew. Energy* **32,** 1206–1227 (2007).
90. Regin, A. F., Solanki, S. C. & Saini, J. S. Heat transfer characteristics of thermal energy storage system using PCM capsules: A review. *Renew. Sustain. Energy Rev.* **12,** 2438–2451 (2008).
91. Butala, V. & Stritih, U. Experimental investigation of PCM cold storage. *Energy Build.* **41,** 354–359 (2009).
92. Agyenim, F., Hewitt, N., Eames, P. & Smyth, M. A review of materials, heat transfer and phase change problem formulation for latent heat thermal energy storage systems (LHTESS). *Renew. Sustain. Energy Rev.* **14,** 615–628 (2010).

93. Iten, M. & Liu, S. A work procedure of utilising PCMs as thermal storage systems based on air-TES systems. *Energy Convers. Manag.* **77,** 608–627 (2014).
94. Dubovsky, V., Ziskind, G. & Letan, R. Analytical model of a PCM-air heat exchanger. *Appl. Therm. Eng.* **31,** 3453–3462 (2011).
95. Tay, N. H. S., Belusko, M. & Bruno, F. Designing a PCM storage system using the effectiveness-number of transfer units method in low energy cooling of buildings. *Energy Build.* **50,** 234–242 (2012).
96. Tay, N. H. S., Belusko, M. & Bruno, F. Experimental investigation of tubes in a phase change thermal energy storage system. *Appl. Energy* **90,** 288–297 (2012).
97. Mosaffa, A. H., Infante Ferreira, C. A., Talati, F. & Rosen, M. A. Thermal performance of a multiple PCM thermal storage unit for free cooling. *Energy Convers. Manag.* **67,** 1–7 (2013).
98. Kozak, Y., Abramzon, B. & Ziskind, G. Experimental and numerical investigation of a hybrid PCM-air heat sink. *Appl. Therm. Eng.* **59,** 142–152 (2013).
99. Majid, A. M. A., Nasir, M. & Waluyo, J. Energy Procedia Operation and Performance of a Thermal Energy Storage System: A Case Study of Campus Cooling using Co-generation Plant. *Energy Procedia* **14,** 1280–1285 (2012)
100. Li, Y., Wang, X., Li, D. & Ding, Y. A trigeneration system based on compressed air and thermal energy storage. *Appl. Energy* **99,** 316–323 (2012).
101. Tao, Y.-B., Li, M.-J., He, Y. & Tao, W. Effects of parameters on performance of high temperature molten salt latent heat storage unit. *Appl. Therm. Eng.* **72,** 48–55 (2014).
102. Nomura, T., Tsubota, M., Oya, T., Okinaka, N. & Akiyama, T. Heat release performance of direct-contact heat exchanger with erythritol as phase change material. *Appl. Therm. Eng.* **61,** 28–35 (2013).
103. Operating manual of AVL DITEST, AVL, Austria. AVL DiGas 4000 light.
104. Operating manual of AVL 437 smoke meter.
105. Rakicka, M., Biegalska, A., Rymowicz, W., Miron, A. & Dobrowolski. Bioresource Technology A two-stage fermentation process of erythritol production by yeast Y. lipolytica from molasses and glycerol. *Bioresour. Technol.* **198,** 445–455 (2015).
106. Edwards, B. J. E. Design and rating shell and tube heat exchangers. Available at http://www.chemstations.com/content/documents/Technical_Articles/shell.pdf
107. Donaldson. Retrieved from *Donaldson-filters.com*: http://www.donaldson-filters.com/products.html (accessed December 14, 2016).
108. R.W.Serth. *Process heat transfer principles and applications.* USA: Elsevier, 2007.

PUBLICATIONS

Papers published in international journals

1. Johar, D.K., Sharma, D., Soni, S.L., Gupta, P. K. & Goyal, R. Experimental investigation on latent heat thermal energy storage system for stationary C . I . engine exhaust. *Appl. Therm. Eng.* **104,** 64–73 (2016). **(Elsevier, SCI, IF 3.356)**
2. Johar, D.K., Sharma, D., Soni, S.L., Gupta, P. K. & Goyal, R. Experimental investigation and exergy analysis on thermal storage integrated micro-cogeneration system. *Energy Convers. Manag.* **131,** 127–134 (2017). **(Elsevier, SCI, IF 5.589)**
3. Johar, D.K, Sharma, D., Soni, S.L., Goyal, R. & Gupta, P. K. Experimental investigation of thermal storage integrated micro trigeneration system. *Energy Convers. Manag.* **146,** 87–95 (2017). **(Elsevier, SCI, IF 5.589)**

Publications as co-author

Papers published / accepted in international journals

1. Gupta, P.K., Sharma, D., Soni,S.L., Goyal,R., Johar, D.K. Experimental investigation of impact of diesel particulate filter on smoke and NOx emissions of a Euro-I compression ignition engine with active and off-board regeneration. *Clean Technologies and Environmental Policy* **19**, 883-895 (2017). doi:10.1007/s10098-016-1279-8 **(Springer, SCI, Impact Factor 1.934)**

2. Gupta, P.K., Sharma, D., Soni,S.L., Goyal,R., Johar, D.K. Experimental investigation and optimization of Exhaust Gas Recirculation on a Euro-1 variable speed CI engine. *Environmental Progress & Sustainable Energy*, **Manuscript number EP-16-307.R3** (Accepted, In Production) **(Wiley, SCI, Impact Factor 1.631)**

3. Goyal, R., Sharma, D. Soni, S.L., Gupta, P.K., Johar, D.K. Experimental Investigation of CI Engine Operated Micro-Cogeneration System for Power and Space Cooling. *Energy Conversion and Management*, **89**, 63–70 (2015). DOI: http://dx.doi.org/10.1016/j.enconman.2014.09.028 **(Elsevier, SCI, IF 5.589)**
4. Goyal, R., Sharma, D. Soni, S.L., Gupta, P.K., Johar, D.K., Sonar, D. Performance and emission analysis of CI engine operated micro trigeneration system for power,

heating and space cooling. *Applied Thermal Engineering* **75**, 817–825 (2015). DOI: http://dx.doi.org/10.1016/j.applthermaleng.2014.10.026 **(Elsevier, SCI, IF 3.356)**

Papers presented/published in international conferences:

1. Dheeraj K Johar, Satyanarayan Patel, Pradeep K Gupta, Dilip Sharma, Shyam Lal Soni and Rahul Goyal, 'Energy and Exergy Analysis of Pebble Bed Heat Storage System', Proceedings of 13th International Conference on Sustainable Energy Technologies (SET2014), Geneva, Switzerland, 25–28 August 2014, ID: E30027, pp 125.
2. Dheeraj Kishor Johar, Pradeep K Gupta, Vinod Singh Yadav and Dilip Sharma, 'Design, Development & Performance Investigation of CI engine Waste Heat Operated Cooker', Proceedings of The 3rd International Conference on Microgeneration and Related Technologies, Naples, Italy, 15-17 April 2013, ID: 104, ISBN: 978890848902.
3. Satyanarayan Patel, Dheeraj Kishor Johar, Dilip Sharma and Pradeep K Gupta, 'Experimental Investigation of Pebble Bed Heat Recovery and Storage System for Compression Ignition Engine Exhaust', Proceedings of The 3rd International Conference on Microgeneration and Related Technologies, Naples, Italy, 15-17 April 2013, ID: 320, ISBN: 978890848902.
4. Rahul Goyal, Dheeraj Kishor Johar, Pradeep K Gupta, Dilip Sharma, S.L.Soni, 'An experimental investigation and exergy analysis of compression ignition engine operated cooker', Proceedings of 5th International Conference on 'Advances in Engineering and Technology' (AET-17), Singapore, 27-30 March 2017, Paper ID: EAP317001, pp 88-93, ISBN: 978-81-933894-0-9.
5. Rahul Goyal, Dilip Sharma, S.L.Soni, Pradeep Kumar Gupta, Dheeraj Johar, 'Experimental Optimization of CI Engine Operated Micro-Trigeneration System for Power, Heating and Space Cooling', In: Rodrigues, L. ed., Sustainable Energy for a Resilient Future: Proceedings of the 14th International Conference on Sustainable Energy Technologies, 25-27 August 2015, Nottingham, UK. University of Nottingham: Architecture, Energy & Environment Research Group. Volume II, pp 27-35. ISBN: 9780853583141

Applied Thermal Engineering 104 (2016) 64–73

Contents lists available at ScienceDirect

Applied Thermal Engineering

journal homepage: www.elsevier.com/locate/apthermeng

Research Paper

Experimental investigation on latent heat thermal energy storage system for stationary C.I. engine exhaust

Dheeraj Kishor Johar [a,*], Dilip Sharma [a], Shyam Lal Soni [a], Pradeep K. Gupta [a], Rahul Goyal [b]

[a] Malaviya National Institute of Technology, J.L.N. Marg, Jaipur, Rajasthan 302017, India
[b] Manipal University Jaipur, Rajasthan 303007, India

HIGHLIGHTS

- Thermal energy storage system is integrated with stationary CI engine.
- Erythritol is used as phase change material.
- Maximum 69.53% charging efficiency is obtained.
- Percentage energy saved is 11.33%.

ARTICLE INFO

Article history:
Received 28 February 2016
Revised 5 May 2016
Accepted 9 May 2016
Available online 10 May 2016

Keywords:
Waste heat recovery
Energy storage
Latent heat storage
Charging efficiency

ABSTRACT

Increasing gap between demand and supply of energy has resulted in raised prices of conventional energy sources, and concern for clean environment has led to increase in use of renewable energy and focus on increased energy efficiency. In context of increased energy efficiency, energy storage and waste heat recovery play an important role as these systems improve overall efficiency of systems. In this study, a latent heat thermal energy storage system (LHTESS) for stationary C.I. engine exhaust heat was developed and integrated with engine. A shell and tube type heat exchanger having 346 mm diameter and 420 mm height with 45 numbers of tubes with 18 mm diameter was developed to store thermal energy, in which Erythritol ($C_4H_{10}O_4$) was used as a phase change material. The engine performance and the thermal energy storage system performance parameters such as amount of heat stored, and charging efficiency were evaluated. Slight decrease in the engine performance was observed when latent heat thermal energy storage system was integrated to engine but amount of energy which could be recovered was significant. At a load of 4.4 kW the maximum charging efficiency, recovery efficiency and percentage energy saved was 69.53%, 38% and 11.33% respectively.

1. Introduction

About 30% of the heat of combustion is carried out by exhaust gas from an internal combustion engine. The energy available in the exit stream of many energy conversion devices goes as waste; if not utilized properly. To achieve an optimal solution for the current energy crisis, the world needs to focus more on (a) renewable sources of energy or (b) look for recycling/appropriate utilization of energy being wasted [1]. Waste heat (as a by-product) from the prime mover is recovered and used to (a) drive thermally activated components such as vapor absorption system or adsorption chiller or desiccant dehumidifier and (b) to produce hot water, steam, warm air or other heated fluid through the use of heat exchanger [2,3]. The major technical constraint that prevents successful implementation of waste heat recovery is its intermittent and time mismatched demand and availability [4–6]. Thermal energy storage (TES) technology plays an important role to overcome this problem by way of rationale use of energy as it allows excess thermal energy to be stored for later use [7]. Thermal energy storage transfers heat to storage media during the charging period, and releases it at a later stage during the discharging step [8]. A lot of work has been carried out in the field of thermal energy storage. Iten and Liu [9] presented a review on procedure to design an effective short term thermal energy storage (TES) system using phase change materials. Stritih [10] experimentally studied heat-transfer characteristics of a latent-heat storage unit with a finned surface in terms of the solidification and melting processes by comparing them with those of a heat-storage unit with a plain

* Corresponding author at: Department of Mechanical Engineering, Malaviya National Institute of Technology, J.L.N. Marg, Jaipur, Rajasthan 302017, India.
E-mail address: johar.dheeraj@gmail.com (D.K. Johar).

http://dx.doi.org/10.1016/j.applthermaleng.2016.05.060
1359-4311/

Energy Conversion and Management 131 (2017) 127–134

Contents lists available at ScienceDirect

Energy Conversion and Management

journal homepage: www.elsevier.com/locate/enconman

Experimental investigation and exergy analysis on thermal storage integrated micro-cogeneration system

Dheeraj Kishor Johar [a,*], Dilip Sharma [a], Shyam Lal Soni [a], Pradeep K. Gupta [a], Rahul Goyal [b]

[a] Malaviya National Institute of Technology, Jaipur, Rajasthan, India
[b] Manipal University, Jaipur, Rajasthan, India

ARTICLE INFO

Article history:
Received 20 May 2016
Received in revised form 13 October 2016
Accepted 31 October 2016
Available online 14 November 2016

Keywords:
Waste heat recovery
Energy storage
Latent heat storage
Cogeneration

ABSTRACT

This paper describes the performance of thermal storage integrated micro-cogeneration system based on single cylinder diesel engine. In addition to electricity generated from genset, waste heat from hot exhaust of diesel engine was used to heat water in a double pipe heat exchanger of 67.70 cm length with inside tube diameter of 3.81 cm and outside tube diameter of 5.08 cm. Additionally, a latent heat thermal energy storage system was also integrated with this cogeneration system. A shell and tube type heat exchanger of 346 mm diameter and 420 mm height with 45 tubes of 18 mm diameter each was designed and fabricated, to store thermal energy, in which Erythritol ($C_4H_{10}O_4$) was used as phase changing material. The test results show that micro capacity (4.4 kW), stationary, single cylinder, diesel engine can be successfully utilized to simultaneously produce power as well as heating, and to also store thermal energy. Slight decrease in engine performance was observed when double pipe heat exchanger and latent heat thermal energy storage system was integrated with engine but the amount of energy which could be recovered was significant. Maximum percentage of energy saved was obtained at a load of 3.6 kW and was 15.2%.

1. Introduction

The energy available in the exit stream of many energy conversion devices goes waste; if not utilized properly. To achieve an optimal solution for the current energy crisis, the world needs to focus more on (a) renewable sources of energy, or (b) look for recycling/appropriate utilization of energy being wasted [1]. Waste heat (as a by-product) from the prime mover is recovered and used to (a) drive thermally activated components such as vapor absorption refrigeration system or adsorption chiller or desiccant dehumidifier and (b) produce hot water, steam, warm air or other heated fluids through the use of heat exchangers [2,3]. Energy storage and waste heat recovery play an important role to improve overall efficiency of systems [4]. Co-generation has emerged as a fast growing technique to increase efficiency and reduce overall emissions. Co-generation is defined as simultaneous production of power and heat [5–7]. These systems utilize the waste heat produced during power generation and allow more efficient fuel consumption [8]. In cogeneration systems, the efficiency of energy conversion increases to over 80% as compared to an average of 30–35% for conventional fossil fuel fired electricity generation systems [7]. The major technical constraint that prevents successful implementation of waste heat recovery is its intermittent and time mismatched demand and availability [9–11]. Thermal energy storage (TES) technology plays an important role to overcome this problem by way of rational use of energy as it allows excess thermal energy to be stored for later use [12]. Thermal energy storage transfers heat to storage media during the charging period, and releases it at a later stage during the discharging step [13].

A lot of work has been carried out in the field of thermal energy storage and cogeneration systems. Iten and Liu presented a review on procedure to design an effective short term TES system using phase change materials [14]. Takahiro Nomura et al. described heat release performance of a direct contact heat exchanger using erythritol as phase changing material (PCM) [15]. Hugues and Asfaw, through mathematical and experimental results, suggested that running absorption chillers from recovered heat is thermodynamically feasible and could significantly enhance system performance [16]. Hatami et al. presented numerical study of finned type heat exchangers for internal combustion engines' exhaust waste heat recovery [17]. Cakirv et al. concluded that cogeneration systems contribute to sustainable use of energy directly or indirectly in various ways with different applications [18]. Hatami et al. presented a review on different heat exchangers' designs for increasing the

* Corresponding author at: Department of Mechanical Engineering, Malaviya National Institute of Technology, JLN Marg, Jaipur, Rajasthan 302017, India.
E-mail address: johar.dheeraj@gmail.com (D.K. Johar).

http://dx.doi.org/10.1016/j.enconman.2016.10.075
0196-8904/

Energy Conversion and Management 146 (2017) 87–95

Contents lists available at ScienceDirect

Energy Conversion and Management

journal homepage: www.elsevier.com/locate/enconman

Experimental investigation of thermal storage integrated micro trigeneration system

Dheeraj Kishor Johar [a,*], Dilip Sharma [a], Shyam Lal Soni [a], Rahul Goyal [b], Pradeep K. Gupta [a]

[a] MNIT Jaipur, J.L.N. Marg, Jaipur, Rajasthan 302017, India
[b] VGU, Jaipur, Rajasthan 302017, India

ARTICLE INFO

Article history:
Received 18 December 2016
Received in revised form 23 March 2017
Accepted 13 April 2017
Available online 18 May 2017

Keywords:
Trigeneration
Combined heating and power
Energy storage
Latent heat storage

ABSTRACT

In this study a 4.4 kW stationary compression ignition engine is coupled with a double pipe heat exchanger, vapour absorption refrigeration system and thermal energy storage system to achieve Trigeneration i.e. power, heating and cooling. A shell and tube type heat exchanger filled with erythritol is used to store thermal energy of engine exhaust. Various combinations of thermal energy storage system integrated micro-trigeneration were investigated and results related to performance and emissions are reported in this paper. The test results show that micro capacity (4.4 kW) stationary single cylinder diesel engine can be successfully modified to simultaneously produce power, heating and cooling and also store thermal energy.

1. Introduction

Increasing demand of energy has raised the prices of conventional energy sources, and environmental awareness has led to increase in use of renewable energy sources and focus on increased energy efficiency. In context of increased energy efficiency, thermal energy storage and waste heat recovery play an important role as these systems improve overall efficiency of various systems [1,2]. The energy available in the exit stream of many energy conversion devices goes waste; if not utilized properly [3,4]. Among several options available for waste heat recovery, micro-cogeneration and micro-trigeneration are emerging as the fast growing techniques to increase energy efficiency and reduce overall emissions in domestic and small-scale applications [5,6]. Micro-cogeneration (MCHP, Micro Combined Heat and Power Generation), is the combined production of electric power (lower than 50 kW) and thermal power. Micro-trigeneration (MCCHP, Micro Combined Cooling, Heat and Power Generation), is a combined cooling, heating and power generation system that consists basically of a module generating electricity (lower than 50 kW) and heat that, depending on the demand, is used either to satisfy domestic hot water requirement and/or space heating or for cooling purposes, or for both [7]. The major technical constraint that prevents successful implementation of waste heat recovery is its intermittent and time mismatched demand and availability [8,9]. Thermal energy storage (TES) technology plays an important role to overcome this problem by way of rational use of energy as it allows excess thermal energy to be stored for later use [10].

A lot of work has been carried out in the field of thermal energy storage, cogeneration and trigeneration systems. Godefroy et al. [11] presented design and analysis of possible trigeneration systems based on a gas engine mini-CHP unit (5.5 kW) and an ejector cooling cycle and analyzed that an overall efficiency around 50% could be achieved with systems designed for applications with simultaneous requirement for heating and cooling. Huangfu et al. [12] introduced a micro-scale combined cooling, heating and power (MCCHP) system which mainly consisted of a reciprocating internal combustion LPG and natural gas engine/generator, an adsorption chiller and heat recovery devices. With an analysis it was concluded that for high efficiency and good regulation performance, the system had to operate with electricity output greater than 50% of peak load. From the exergy point of view, the electricity efficiency of the gas engine/generator should be enhanced for an improved MCCHP system. Cakir et al. [13] studied the importance of cogeneration systems in sustainable energy. Majid et al. [14] presented a study on operation and performance of thermal energy storage system installed at a cogeneration plant for campus cooling. Iten and Liu [15] presented a review on procedure to design an effective short term thermal energy storage (TES) system using phase change materials. Nomura et al. [16] described heat release performance of a direct contact heat exchanger using erythritol as a PCM. Hatami et al. [17] presented a review of different

* Corresponding author at: Department of Mechanical Engineering, Malaviya National Institute of Technology, J.L.N. Marg, Jaipur, Rajasthan 302017, India.
E-mail address: johar.dheeraj@gmail.com (D.K. Johar).

http://dx.doi.org/10.1016/j.enconman.2017.04.106
0196-8904/